Predicting Muscle Activations in a Forward-Inverse Dynamics Framework Using Stability-Inspired Optimization and an In Vivo-Based 6DoF Knee Joint

Brigitte Potvin, B.SC., B.A.Sc.

Thesis submitted to the Faculty of Graduate and Postdoctoral Studies

in partial fulfillment of the requirements for the degree of

MASTER OF APPLIED SCIENCE

in Biomedical Engineering

Ottawa-Carleton Institute for Biomedical Engineering
University of Ottawa
Ottawa, Canada

May 2016

Abstract

Modeling and simulations are useful tools to help understand knee function and injuries. As there are more muscles in the human knee joint than equations of motion, optimization protocols are required to solve a problem. The purpose of this thesis was to improve the biofidelity of these simulations by adding in vivo constraints derived from experimental intra-cortical pin data and stability-inspired objective functions within an OpenSim-Matlab forward-inverse dynamics simulation framework on lower limb muscle activation predictions.

Results of this project suggest that constraining the model knee joint’s ranges of motion with pin data had a significant impact on lower limb kinematics, especially in rotational degrees of freedom. This affected muscle activation predictions and knee joint loading when compared to unconstrained kinematics. Furthermore, changing the objective will change muscle activation predictions although minimization of muscle activation as an objective remains more accurate than the stability inspired functions, at least for gait.

La modélisation et les simulations *in-silico* sont des outils importants pour approfondir notre compréhension de la fonction du genou et ses blessures. Puisqu’il y a plus de muscles autour du genou humain que d’équations de mouvement, des procédures d’optimisation sont requises pour résoudre le système. Le but de cette thèse était d’explorer l’effet de changer l’objectif de cette optimisation à des fonctions inspirées par la stabilité du genou par l’entremise d’un cadre de simulation de dynamique directe et inverse utilisant MatLab et OpenSim ainsi qu'un model musculo-squelétaire contraint cinématiquement par des données expérimentales dérivées de vis intra-corticales, sur les prédictions d’activation musculaire de la jambe.

Les résultats de ce projet suggèrent que les contraintes de mouvement imposées sur le genou modélisé ont démontré des effets importants sur la cinématique de la jambe et conséquemment sur les prédictions d'activation musculaire et le chargement du genou. La fonction objective de l'optimisation change aussi les prédictions d’activations musculaires, bien que la fonction minimisant la consommation énergétique soit la plus juste, du moins pour la marche.

Acknowledgments

There are many people I would like to thank that have supported me in the past and have continued to do so in various ways during this whole process that has been my post-secondary and post-graduate education.

This project would not have been possible without the invaluable help, expertise and simulation scripts from Dr. Mohammad S. Shourijeh. Thanks are also extended to Kenneth Smale for collecting the gait data used in this thesis, even though it meant participating in his study at a cost of what felt like 10 000 squats resulting in very sore quadriceps!

None of this would have even taken place without the guidance and support from my supervisor Dr. Daniel Benoit, who hired me as a COOP student for a few summers then took me on as a Master's student, giving me an amazing opportunity to learn about biomechanics technology and all that could be done in his lab and how they could be applied in real life. I have learned so much more in this lab than I could have simply out of textbooks!

Thanks are also offered to Dr. Davide Spinello in his role as co-supervisor during my graduate studies. Your perspective and knowledge on the subject of this research project was definitely an asset on the engineering side of things.

Of course, I must underline the financial help from the Ontario Ministry of Training, Colleges and Universities for the Ontario Graduate Scholarship (OGS) and from the National Science and Engineering Research Council for the CGS-M scholarship.

I would also like to thank all of my colleagues, friends and family for encouraging me and supporting me in pursuing my education despite my occasional complaints and grumbling. Eleven years of university would not have been feasible without you!

Statement of Contributions

The results of this work have come together with the help and collaboration from various individuals as stated in the previous section. Their main contributions are detailed below:

Dr. Mohammad S. Shourijeh developed the main simulation framework scripts used for musculoskeletal simulations used in this project. I modified his scripts to incorporate bone pin range of motion constraints as well as adapt my chosen musculoskeletal model and objective functions to this framework. Dr. Shourijeh was an important source of knowledge about musculoskeletal modeling and simulations as well as a source of advice and helpful troubleshooting throughout this research project.

Kenneth B. Smale, a PhD candidate in Human Kinetics, collected the gait trials used as inputs into the simulation software. He was also a source of advice in statistical methods as well as in editing the various elements of this thesis.

Dr. Davide Spinello, as co-supervisor, offered useful advice into concepts of mathematical stability and control theories that helped to guide the focus of this research project.

Dr. Daniel Benoit, as principal supervisor, contributed valuable advice in developing the research questions, methods and overall concepts covered in this work, as well as collecting the in vivo bone pin data used herein and editing the thesis and papers.

Table of Contents

List of Tables

List of Figures

Chapter 1

Chapter 2

Chapter 3

Journal Manuscript 1

Journal Manuscript 2

Journal Manuscript 3

Appendices

Nomenclature

ACL: Anterior cruciate ligament

ANOVA: Analysis of Variance

Amax: Maximization of muscle activation

Amin: Minimization of muscle activation

BFEM: Biceps femoris

DoF: Degree of freedom

EMG: Electromyography

GLTMED: Gluteus medius

GLTMAX: Gluteus maximus

GRF: Ground reaction forces

IK: Inverse Kinematics

Jmax: Maximization of knee joint compression forces

LGAS: Lateral gastrocnemius

MGAS: Medial gastrocnemius

OA: Osteoarthritis

RFEM: Rectus femoris

RRA: Residual reduction algorithm

Smin: Minimization of knee joint shear forces

SO: Static Optimization

SOL: Soleus

SPM: Statistical Parametric Mapping

STA: Soft tissue artifact

STEN: Semitendinosus

Tmin: Minimization of torque error objective function

TA: Tibialis anterior

TFL: Tensor fascia latae

VLAT: Vastus lateralis

VMED: Vastus medialis

Chapter 1-Literature Review

1.1 A General Introduction to Musculoskeletal Modeling and Simulations

Musculoskeletal disorders such as osteoarthritis, ligament injuries and neuromuscular disorders are costly to the health care system, consuming billions of dollars each year and play an important role in the quality of life of affected people (Fregly et al., 2011; Jacobs et al., 2008; Mansouri & Reinbolt, 2012; Roux et al., 2005). Understanding how these disorders develop and how to best treat them is a difficult task as many variables can be involved in the process.

Following diagnosis of a joint pathology or neuromuscular disorder, treatment plans are devised to help patients recover or to maximize functionality over time. However, determining the ideal treatment procedure is sometimes subjective and based on the medical professional's observations and past experience (Delp et al., 1990; Fregly et al., 2011). There is also uncertainty in knowing what may be expected after a treatment or surgery, as research has not conclusively discovered how muscles, ligaments and other external forces all contribute to healthy joint function (Komistek, Kane, Mahfouz, Ochoa, & Dennis, 2005; Lloyd & Buchanan, 2001; Shelburne, Torry, & Pandy, 2006; Winby, Lloyd, Besier, & Kirk, 2009). The exact way in which muscles contribute to human movement and joint stability is not yet fully understood as it is difficult and risky to make direct measurements on muscle fibers inside a live subject (Buchanan & Shreeve, 1996; Delp et al., 2007; Erdemir, McLean, Herzog, & Van Den Bogert, 2007; Hicks, Uchida, Seth, Rajagopal, & Delp, 2015; Kim et al., 2009; Reinbolt, Seth, & Delp, 2011). Recently, some individuals have been surgically outfitted with specialized knee joint implants which can measure contact forces (Bergmann et al., 2014; Heinlein et al., 2009), but this is not a common occurrence and requires extremely invasive procedures (Data from such individuals can be found online at *orthoload.com,* or from the Grand Knee Challenge at *simtk.org* - last visited December 2015).

Because of the challenges posed by difficult measurement acquisition, musculoskeletal modeling and computer simulations have become increasingly attractive tools to better understand joint function and to address musculoskeletal joint disorders (Delp et al., 1990; Fregly et al., 2011; Hicks et al., 2015; Kinney, Besier, D'Lima, & Fregly, 2013; Komistek et al., 2005; Reinbolt et al., 2005). These tools can provide insights into what goes on within a joint to determine the potential influences of various parameters on the joint function, loading patterns and the magnitude of muscle forces developed in a given condition (Cadova, 2013). They are also potentially very useful clinical tools to objectively and quantifiably determine the best course of action to take without putting patients at risk through trial and error surgeries (Delp et al., 1990; Fregly et al., 2011; Hicks et al., 2015; Kinney et al., 2013; Komistek et al., 2005; Mansouri & Reinbolt, 2012; Reinbolt et al., 2005). As well, risk factors associated with developing joint pathologies such as osteoarthritis due to changes in joint contact forces or in muscle activation patterns could also be identified. Preventative measures could then be put into place to correct or minimize the potential problem (Besier, Fredericson, Gold, Beaupre, & Delp, 2009).

Musculoskeletal models and their simulation protocols can not only be used clinically, but can help researchers in their respective investigations. These simulations allow for testing large numbers of scenarios (injury simulations, muscle function changes or various disease conditions) while manipulating various parameters to determine how outputs differ and with what magnitude, without the need to recruit specific populations that might fit a given set of criteria to study (Fregly et al., 2011; Reinbolt et al., 2011). Neuromuscular research can benefit from modeling and simulation software as developing similar in-vivo or in-vitro protocols would prove to be challenging and likely costly (Pandy, 2001; Van Den Bogert, Gerritsen, & Cole, 1998). Furthermore, models can also be used in concrete applications in the design of prosthetics or any device that may interact with a person, in order to optimize designs and identify potential problems before building costly physical prototypes (Fregly et al., 2011; Kocmond, Delp, & Stern, 1995).

Work in the field of musculoskeletal model development has been growing since the 1970s (Morrison, 1970; Seireg & Arvikar, 1975), and with the advent of more powerful computers, increasingly complex simulations can now be performed (Fregly et al., 2011). Although important advances have been seen in the last decades, current models are not yet accurate enough, involve many assumptions and simplifications, and have not been sufficiently validated to be reliably applied in clinical settings (Kinney et al., 2013). Musculoskeletal modeling software packages such as AnyBody (AnyBody Technology, Denmark) and OpenSim (Simtk.org, Simbios, National NIH Center for Biomedical Computing, USA) have been further developed in recent years to improve the ease and efficiency of creating and visualizing models as well as running simulations (Cadova, 2013; Wibawa et al., 2013). OpenSim in particular, is an open access package, where researchers can share their models and scripts with others, thus allowing reproduction and validation of their work and promoting a collaborative effort in addressing the challenges that musculoskeletal models and simulation frameworks face today (Delp et al., 2007).

1.2 Building a Musculoskeletal Model

Building a computer musculoskeletal model requires knowledge of anatomy, physiology and mechanical properties of all the elements of the body or joint of interest, as well as how all these elements interact together. Simpler models, perhaps omitting certain joint structures or muscles, assuming linearity, considering reduced numbers of degrees of freedom or lumping multiple body segments into single masses, will require less computation time to obtain solutions. However, this comes at the expense of bio-fidelity and limits the applicability of models' predictions. However, depending on the study, simplifying assumptions may be acceptable (Pandy, 2001; Shelburne et al., 2006) .

Musculoskeletal models are typically composed of two main parts, an anatomical model that defines bone, muscle and joint geometries, and a mathematical model that estimates forces and moments produced by muscles and/or ligaments based on mechanical representations of these tissues. As illustrated in Figure 1, these models are incorporated into simulation frameworks and associated to kinematic data (i.e. motion capture marker trajectories), kinetic data and/or experimental electromyography (EMG)-derived muscle activation patterns to predict muscle activations, muscle forces or joint loading (Buchanan, Lloyd, Manal, & Besier, 2004; Cao, Inoue, Liu, & Shibata, 2013; Winter, 2004).

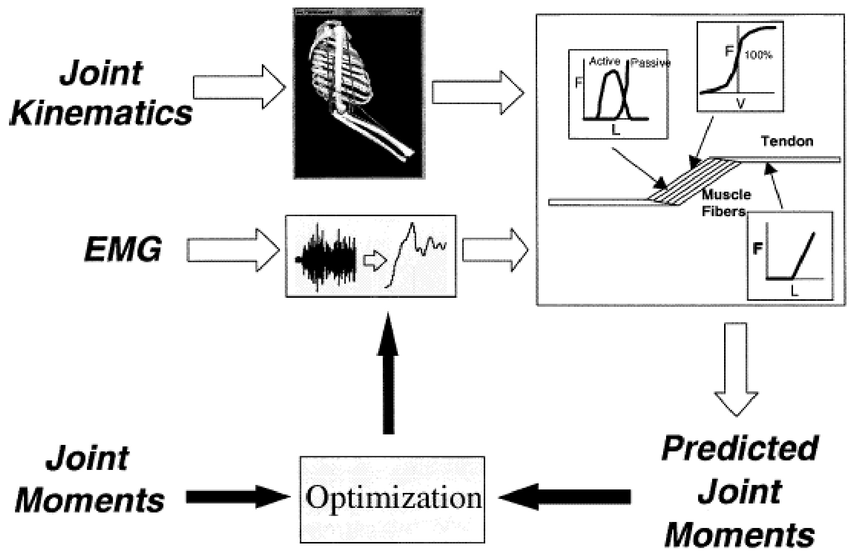

Figure 1 : General schema of a musculoskeletal modeling and simulations. Joint kinematics are combined with an anatomical model and a muscle mechanics model to obtain predicted joint moments. EMG can be incorporated into the framework as well. Optimization protocols compare predicted joint moments with real ones to predict muscle activations. The simulation runs until adequate optimization is achieved. (Buchanan et al., 2004)

1.2.1 Musculoskeletal Models: Anatomical and Geometrical Representation of Tissues

Improved imaging and computer graphics technologies over the years have allowed for better visualization of musculoskeletal structures within a body and how they move together between joints and segments (Baratta et al., 1988; Delp et al., 1990; Pandy, 2001). However, computer simulation results' accuracy depends on the model that generated them, and there are multiple challenges to consider when creating or working with these anatomical models.

Many measurements of tissue dimensions, orientation, attachment locations and geometry are still obtained from cadaveric studies (Brand et al., 1982; Delp et al., 1990; Pandy, 2001; Shelburne et al., 2006; Yamaguchi & Zajac, 1989). Cadavers are typically the remains of older people, at various levels of muscle atrophy, making it difficult to scale these to healthy young populations. Although muscle attachment locations remain the same, some muscle groups seem to atrophy more quickly as well, which could affect musculoskeletal geometry measurements and muscle lines of action (Buchanan, Lloyd, Manal, & Besier, 2005; Buchanan & Shreeve, 1996). More advanced imaging technologies could be of use here in recreating subject specific limb and joint elements *in-silico*.

Geometrical simplifications of shapes and positions of bodies are also often used to represent structures within joints, using elliptical shapes to represent the femoral condyles or representing muscles attachment locations as specific points on bones rather than spread over larger surfaces for example (Delp et al., 1990; Pandy, 2001). The path that muscles travel during a contraction, wrapping around surfaces or pulling in a particular direction will change depending on the position of the limb. This means that moment arms created by muscle attachment points and the direction of tension will change over time as well. Some models assume these remain constant for the sake of simplicity (Buchanan et al., 2004; McLean & Van Den Bogert, 2003). Bone shapes and muscle dimensions and orientations are difficult to obtain in a live specimen and are often based on textbook averages (Buchanan et al., 2004). Correctly defining the geometry of a musculoskeletal model is of crucial importance as it has been shown that changing the length of a body or insertion point of a muscle will impact the final output of the model (Delp et al., 1990).

To further simplify musculoskeletal models, some studies focus on a single joint rather than a whole body system. However, many muscles involved in one joint are also implicated in a second joint, such as muscles crossing both the knee and hip joint (biceps femoris or rectus femoris for example) or the knee and ankle joint (gastrocnemius for example). These biarticular muscles increase the complexity of models as kinematic and kinetic calculations must consider larger systems rather than focus on only the joint of interest. Many other variables associated with these dual function muscles are sometimes omitted and the results will therefore reflect this (Buchanan et al., 2004; Buchanan & Shreeve, 1996; Kim et al., 2009). On the other hand, considering the extra joints may help define constraints on muscle force estimations, as a whole system must be stabilized rather than only a single joint (Fregly et al., 2011).

The range of motion of a musculoskeletal model is defined by giving joints certain degrees of freedom to constrain motion possibilities. Although quite a few models define the knee joint as a simple hinge or reduced DoF joint between the tibia and femur for example (Anderson & Pandy, 2001; Arnold, Ward, Lieber, & Delp, 2010; Delp et al., 1990; Modenese, Phillips, & Bull, 2011; Sasaki & Neptune, 2010; Xu, Bloswick, & Merryweather, 2014), the reality is that these bones can actually move in 6DoFs in relation to one another (Benoit et al., 2006, 2007; Marieb, 1998). Using only a hinge joint for example, simplifies the model considerably but also significantly changes the results of the simulations (Komistek et al., 2005; McLean & Van Den Bogert, 2003). It has been noted that differences between experimental marker trajectories and the ones adapted into a scaled anatomical model will differ due to the lack of motion flexibility of the model coming from the lack of DoFs at certain joints (Kuo, 1995).

1.2.2 Musculoskeletal Models: Mechanical Representation of Tissues

There are many material properties and parameters that must be defined within a musculoskeletal mechanical model to be able to simulate it, such as tissue stiffness and strength as well as muscle contraction dynamics (length, force and velocity relationships) for example. When working with different populations such as older adults or those with injuries or joint pathologies, these parameters may need to be adjusted within musculoskeletal models (Thelen, 2003).

1.2.2.1 Mechanical Representation of Muscles: The Hill-Type Muscle Model

In the case of muscles, the most commonly used model is the macro-scale Hill-type model, while some studies utilize the micro-scale cross-bridge theory model as well (Buchanan et al., 2004; Millard & Delp, 2012; Van Den Bogert et al., 1998). Some models incorporating tissue properties in their calculations can also use continuum mechanics to define geometric deformations constraints and help predict the non-linear behaviours of complex biological tissues (Epstein & Herzog, 2003).

The Hill-type model represents muscles in 3 main components followed by another elastic element to represent the behaviour of tendons as illustrated in Figure 2 (Hill, 1938; Pandy, 2001; Pandy, Zajac, Sim, & Levine, 1990). The muscle is made up of a contractile element (CE) linked to a series elastic element (SEE). In parallel to this is the parallel elastic element (PEE). Typically, these elastic components are non-linear in order to be more physiologically representative. The contractile element is the active component of the muscle and represents the actin-myosin complex generating a contraction when the muscle is activated. As the exact processes are not yet fully understood, this element is often a “black box” with inputs and outputs defined by experimentally determined relationships between force production and length as well as force-velocity relations (Van Den Bogert et al., 1998). The series elastic element relates to the elasticity of the myofilaments of the muscle tissue and tendon elasticity. The parallel component refers to the connective tissue surrounding the contractile component of the muscle.

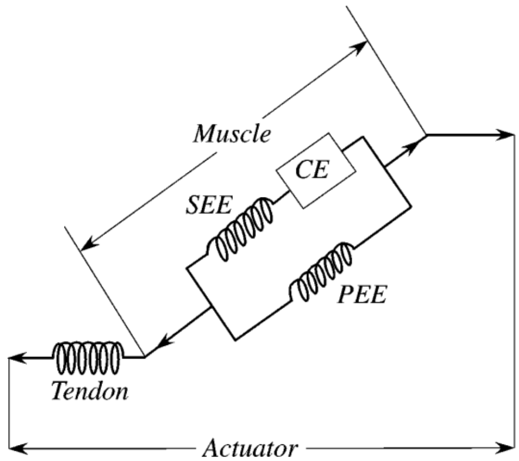

Figure 2: Hill-model of muscle tissue. CE: contractile element or active actin/myosin complex. SEE: Series elastic element or elasticity of myofilaments, PEE: Parallel elastic element or elasticity of surrounding connective tissue. (Pandy, 2001; Pandy et al., 1990)

The Hill-type model can be affected by complex factors including activation dynamics or neural excitation of muscle tissue, time history behaviour of muscle activity, fatigue and muscle tissue yielding during lengthening phases (Van Den Bogert et al., 1998). Muscle forces determined with the Hill model are a function of the muscles' peak isometric forces, their corresponding optimal fiber length and pennation angle, tendon slack length, and muscle activation dynamics (Manal & Buchanan, 2003; Pandy, 2001).

1.2.2.2 Mechanical Representation of Muscles: Converting EMG to Muscle Activation

Muscle excitation can be detected as electrical signals recorded through electrodes placed on the skin surface or within muscles with the use of needles (electromyography data - EMG) before actual force production begins. This can be explained by the biochemical processes and electrical properties of muscle fibers. When a muscle contracts and begins to develop force, the tendon linking the muscle to the bone begins to stretch and carry a load as well, providing force to move body segments (Marieb, 1998).

Experimental EMG recordings are converted to measures of muscle activations and then to muscle force through the Hill model. Many experimental factors can affect EMG signals, such as amplifier gain, the type of electrode used, placement of the electrode on the muscle, soft tissue impeding the signal, and general external noise (De Luca, 1997). Stimulation frequency, muscle fiber type (fast and slow twitch) and muscle fiber recruitment patterns will also have an effect on the onset of muscle force production and its magnitude after muscle excitation (Baratta et al., 1988; Buchanan et al., 2004; Pandy, 2001). In modeling, the conversion between muscle excitation and actual muscle activation can be optimized to fit individual subjects rather than relying on pre-determined mathematical relationships (Hof & Van den Berg, 1981; Manal & Buchanan, 2003).

1.3 Simulation Frameworks for Predicting Muscle Activations and Joint Loading: Inverse and Forward Dynamics

A musculoskeletal model alone without kinematic, kinetic or external disturbance inputs has limited applications. A simulation framework is often required to associate a model with this type of data and from there calculate and/or predict variables of interest such as joint angles, segment velocities and acceleration, joint reaction forces and moments, muscle activation profiles, muscle forces or joint contact forces for example.

In order to estimate muscle activations and forces as well as joint loading during an activity, two main methods can be used, namely inverse or forward dynamics. In some cases, a combination of both may be used to compare and validate predictions or to optimize results (Cao et al., 2013). An example of this is shown in Figure 3.

1.3.1 Inverse Dynamics

Inverse dynamics is a non-invasive method used to calculate segment kinetics and joint moments and forces. It requires the measurement of ground reaction forces (GRF) and body kinematics over the course of a specific movement typically collected with motion capture camera systems and force plates or with smaller sensors such as accelerometers and gyroscopes (Cao et al., 2013; Pandy, 2001; Winter, 2004). When using inverse dynamics, it is very important to have proper marker placement on bony landmarks, and to consider soft tissue artifact (STA) effects, especially during ballistic movements like at heel strike during gait for example (Benoit et al., 2006; Buchanan et al., 2005; Cappozzo, Catani, Leardini, A., Benedetti, & Della Croce, 1996; Corazza et al., 2006; Szczerbik & Kalinowska, 2011). Errors in kinematic data resulting from such issues will be translated to joint force and moment calculations and subsequent analysis. To solve this issue, different methods have been used to introduce anatomical, kinematic or geometrical constraints in musculoskeletal models to limit STA (Andersen, Benoit, Damsgaard, Ramsey, & Rasmussen, 2010; Duprey, Cheze, & Dumas, 2010; Gasparutto, Sancisi, Jacquelin, Parenti-Castelli, & Dumas, 2015; Leardini, Chiari, Della Croce, & Cappozzo, 2005) however in many cases this may in fact increase the error (Andersen et al., 2010).

Once joint reaction forces and moments are determined, optimization protocols are defined to predict likely combinations of muscle forces and thus activations and excitations using a Hill type model, as there are typically more muscles to consider than there are equations of motion to solve them. The choice of optimization is an important step in finding a reasonable solution that fits both muscle physiology and the constraints of the tested condition (Lloyd & Buchanan, 1996).

1.3.2 Forward Dynamics

Forward dynamics measures neural signals (from EMG data) to identify and normalize muscle activations that are then converted to muscle forces. This conversion is typically based on muscle activation dynamics, the use of musculoskeletal geometry for moment arm calculation and a Hill-type muscle model. Once muscle force estimates are made, joint moments can be estimated followed by joint kinematics (Buchanan et al., 2005). A disadvantage of this method however, is that small errors in joint moments become amplified through multiple integrations in determining segment positions (Buchanan et al., 2004).

Forward dynamics is a more computationally demanding process as it must solve an entire trial at once rather than by individual frame as is the case of inverse dynamics (Pandy, 2001). EMG recording methods and theory are well discussed in biomechanics literature in general (De Luca, 1997; Frigo & Crenna, 2009; Stashuk, 2001; Staudenmann, 2007) and care should be taken when collecting this type of data. Using EMG measurements can be limiting as generally only large superficial muscles can be monitored when trying to record data non-invasively although deeper muscles can be measured with intra-muscular needle electrodes (Cao et al., 2013; De Luca, 1997; Sartori, Farina, & Lloyd, 2014). Additionally, noise in EMG signals from skin preparation, soft tissue thickness and movement or from interference from other muscles due to non-ideal electrode placement will affect the quality of the signal and may skew muscle activation measurements in the model. Despite these limitations, EMG data provides the only objective, measurable estimate of subject-specific muscle activity patterns, as recorded experimentally from the muscles of interest.

1.3.3 A Forward-Inverse Dynamics Simulation Framework

Both forward and inverse dynamics methods have advantages and disadvantages, therefore hybrid models using a combination of forward and inverse dynamics to predict biomechanical variables can be used to solve a system or to cross-validate the solutions as shown in Figures 3 and 4 (Buchanan et al., 2004, 2005; Sartori et al., 2014). The hybrid approach is advantageous in predicting abnormal patterns in individuals with muscular disorders for example, as well as can run optimization sequences with EMG data to guide the simulation in finding a more realistic solution for unmonitored muscles, without being too computationally costly (Higginson, Ramsay, & Buchanan, 2012).

A hybrid-style simulation method was used in this thesis to create a system capable of predicting muscle activations and joint loading (shown in Figure 4).(Shourijeh, Smale, Potvin, & Benoit, 2016) In simple terms, this method first calculates torques at the knee through inverse dynamics. Subsequently, the first steps of forward dynamics (up to calculating joint torques) are run to find a muscle activation solution that matches knee joint torques calculated in the inverse dynamics step. Instead of using EMG data as a starting point for the forward dynamics element, the framework uses the kinematics of the trial in question to prescribe the motion of the model and uses the muscle moment arms calculated in the inverse dynamics step. Muscle forces and therefore activations and excitations are determined in such a way as to minimize the difference in calculated knee joint torque values between the inverse and forward dynamics elements.

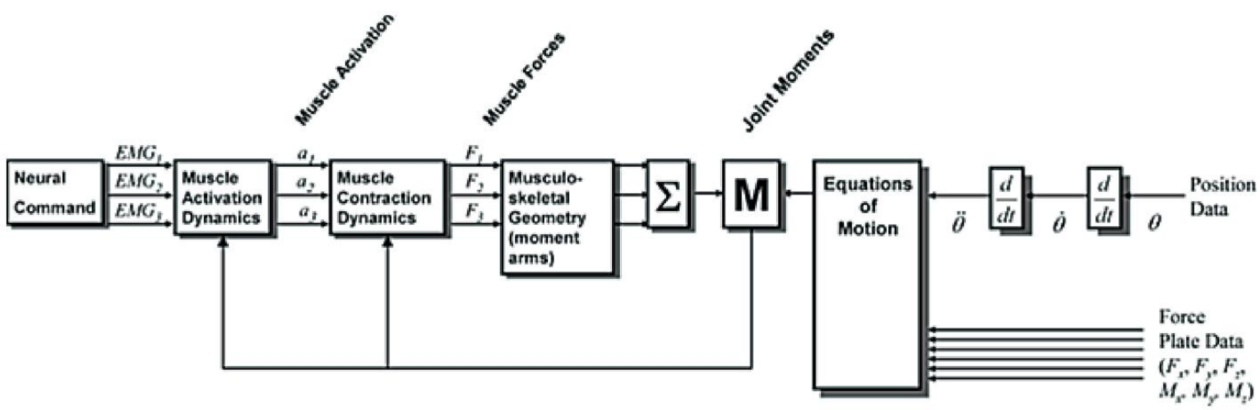

Figure 3: Typical hybrid forward-inverse dynamics simulation setup. Forward dynamics begins on the left and predict joint motions from muscle excitation (EMG_i) to muscle activations (a_i) to muscle forces (F_i) while inverse dynamics starts on the right of the figure and predicts joint moments based on joint kinematics (ϴ) and its derived segment velocities and accelerations, combined with ground reaction forces and moments ($F_{x,y,z}$ and $M_{x,y,z}$). Both systems work together to find a common joint moment solution (Buchanan et al., 2005).

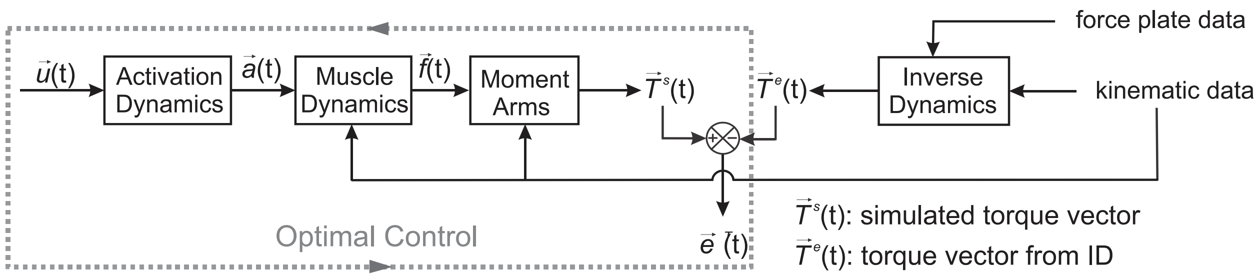

Figure 4: Forward-inverse dynamics simulation framework minimizing joint torque prediction error $\boldsymbol{e(t)}$. Other variables are defined as follows: $\boldsymbol{u(t)}$: muscle excitation, $\boldsymbol{a(t)}$: muscle activation, $\boldsymbol{f(t)}$:tendon-muscle forces, $\boldsymbol{T^s}$:simulated torque vector, $\boldsymbol{T^e}$:torque vector from inverse dynamics (ID). Adapted from (Shourijeh & Benoit, 2015; Shourijeh & McPhee, 2014).

1.4 Simulation Frameworks for Predicting Muscle Activations and Joint Loading: Optimization Methods and Objective Functions

1.4.1 Static and Dynamic Optimization

The way in which muscles contribute to movement and joint stability is complex and is not yet fully understood. In addition, as there are many muscles to consider and too few equations resulting from the inverse dynamics or too few muscle EMG measured for forward dynamics processes, optimization methods in simulations are employed with different objective functions to distribute the joint loads among these muscles (Buchanan & Shreeve, 1996). Studies have shown that muscle activation and force predictions are sensitive to optimization method selection (Herzog, 1992; Sanford, Williams, Zucker-Levin, & Mihalko, 2013). Choosing appropriate optimization protocols and objective functions to predict muscle activation and force generation in an under-defined system is difficult, especially when there are only a few constraints to narrow the possibility of solutions (Buchanan et al., 2004).

There are two main ways in which to optimize a system solution: static optimization and dynamic optimization.

1.4.1.1 Static Optimization

Static optimization is a computationally efficient method as it solves the muscle activation problem for each individual time frame of a motion capture trial. It uses inverse dynamics, relying on motion capture data, to predict ideal muscle activity patterns and corresponding joint contact loads and can consider multiple muscles. One of the challenges with this approach is that there are many muscle force combinations that result in the same net joint loads. Such methods may use EMG data to validate their results by comparing experimental muscle activity over time to simulated muscle forces (Cao et al., 2013; Kim et al., 2009; Lloyd & Buchanan, 1996).

1.4.1.2 Dynamic Optimization

Dynamic optimization on the other hand, relies on forward dynamics and uses muscle activity to predict muscle forces and joint loading. EMG driven simulation frameworks for example, rely on dynamic optimization to estimate muscle forces involved in joint motion and stability, using measured EMG data and activation dynamics from a selection of muscles crossing the joint of interest and forward dynamics principles. This method accounts for different strategies used in recruiting muscles to stabilize and move joints as well as considers muscle dysfunctions where activation patterns may not be the same between subjects (Besier et al., 2009; Winby, Gerus, Kirk, & Lloyd, 2013). However, this method is computationally more costly as it solves its equations for an entire motion trial at once rather than by individual time frame as in the static optimization case (Anderson & Pandy, 2001; Pandy, 2001). It is also dependant on many biological tissue properties that are not entirely understood.

In some cases, both static and dynamic optimization methods are used to cross-validate results and potentially improve accuracy (Buchanan et al., 2005; Fregly et al., 2011). Deciding which method to use depends on the purpose of the study, the available data and the time frame required to run simulations (Pandy, 2001).

1.4.2 Objective Functions

To optimize a system's solution, an objective function (or cost function) must be defined. There is a variety of cost functions that have been used in recent models in an attempt to obtain realistic results at the knee joint such as minimizing total muscle force, muscle activation, muscle stress, fatigue of muscles and metabolic energy expenditure over a given distance (Anderson & Pandy, 2001; Cao et al., 2013; Kim et al., 2009; Lloyd & Buchanan, 1996; Winby et al., 2009). These all have their limitations however, as it is not yet known exactly how the human body's musculoskeletal system is controlled (Walter et al., 2013).

The validity of many cost functions has been questioned as results of predicted muscle activity from simulations do not always match well with measured muscle activity (Erdemir et al., 2007; Herzog, 1987, 1992, 1992; Winby et al., 2009). It has also been argued that although these cost functions may seem reasonable for certain movements, such as minimizing muscle activity to increase efficiency of normal pace walking, in other situations, this cost function may not be optimal, such as in the case of trying to reach maximum jump height or high speed sprinting, where efficiency is no longer the main objective of the task (Kim et al., 2009). Another example found that although people tend to walk on flat ground at a speed minimizing energetic costs, in the case of downhill walking, individuals changed their gait pattern to increase stability at the cost of some energy expenditure efficiency (Hunter, Hendrix, & Dean, 2010). Studies have also shown that for the same activities, different people will use different muscle activation strategies for various reasons such as the task at hand, muscular disorders or previous training experiences (Besier et al., 2009; Buchanan & Lloyd, 1995; Menegaldo & Oliveira, 2011; Sartori et al., 2014).

In some simulation systems, mathematical cost functions (those that are not physiologically based) can also be included, such as the minimization of torque calculations in the hybrid-style forward-inverse dynamics (FID) simulation framework described in Figure 4. Using only a mathematical objective is insufficient within musculoskeletal simulation frameworks as they can result in multiple solutions that are not necessarily physiologically possible. Multiple cost functions can therefore be combined with different weighting factors to obtain desired results (Cleather & Bull, 2011).

1.4.3 Defining Stability as an Objective Function

The term *stability* has been used in multiple biomechanical and musculoskeletal studies, but has not been standardized in its definition and can depend on the field of study or simply the authors' own linguistic preferences. This variety of definitions becomes a challenge when trying to reproduce clinical or research studies involving musculoskeletal or joint stability (Hasan, 2005; Senavongse et al., 2003). It also complicates defining an optimization objective function in musculoskeletal modeling based on principles of stability, as in the case of this thesis.

In biomechanics and neuromuscular control, there have been numerous studies looking at how different structural elements of a joint, muscle activation patterns and loading of the knee (weight bearing or not) may help to stabilize or alter the stability and loading patterns of a joint (Flaxman, Speirs, & Benoit, 2012; Giesl & Wagner, 2007; Smith, Flaxman, Speirs, & Benoit, 2012).

Bones within a joint are sometimes shaped in a way to limit the range of possible movements, such as the hip joint for example that is shaped as a ball and socket. In the case of the knee joint, however, bone shapes do not offer much constraint. Passive ligaments provide some support in stabilizing joints but are not always enough. Muscle activity comes in to provide the active neuromuscular control of joints (Giesl & Wagner, 2007; Smith et al., 2012; Solomonow & Krogsgaard, 2001).

If we take the knee joint as an example, some studies found particular muscle groups helped maintain knee joint stability in the frontal plane and supported varus/valgus moments in situations stressing the ACL ligament (Lloyd & Buchanan, 2001; Shelburne et al., 2006; Solomonow et al., 1987; Winby et al., 2009). It was also suggested that higher muscle activity could help joint stability by increasing joint stiffness, thus increasing compression between articulating surfaces (Riemann & Lephart, 2002).

Co-contraction, a term describing the simultaneous activation of antagonistic muscles, has also been shown to play an important role in supporting varus/valgus and flexion/extension moments of the knee to enhance stability, as well as increase joint stiffness, potentially protecting the surrounding soft tissues from large or sudden impacts. (Ambegaonkar et al., 2011; Doorenbosch & Harlaar, 2003; Lloyd & Buchanan, 1996; Maitland, Ajemian, & Suter, 1997; Milner, 2002; Schipplein & Andriacchi, 1991; Schmitt & Rudolph, 2008; Senavongse et al., 2003; Smith et al., 2012; Solomonow et al., 1987; Sturnieks, Besier, & Lloyd, 2011).

However, other studies have hypothesized that increased co-activation of muscles to improve stability in people with knee joint pathologies could increase joint contact loading and therefore may lead to damage of the articular surfaces if these loads were to go beyond physiologically acceptable levels (Lloyd & Buchanan, 1996; Winby et al., 2009). Co-contraction is also a strategy that would be more metabolically costly than only activating a minimum of muscles to achieve a desired limb motion (Milner, 2002).

Another method of defining joint stability is using classic mechanical control theory definitions of a system's ability to achieve a fixed point after a perturbation (Bergmark, 1989; Rugh, 1996). Control theory describing feedback and feed-forward controls can be used in neuromuscular systems to describe how nerves, muscles, ligaments and other soft tissues work together with sensory systems to continuously monitor the state of a body and modify signals to maintain or regain stability (Riemann & Lephart, 2002; Williams, Chmielewski, Rudolph, Buchanan, & Snyder-Mackler, 2001).

The ability of a system to return to an equilibrium state can be described using constraints and boundaries for given parameters or implementing penalty functions assigned to a system if it attempts to move outside of allowed conditions (Moengin, 2010, 2011; Murphy, 1974). For example, Lyapunov stability theory refers to the points that minimize a given non-negative function (Lyapunov function) as the basin of attraction, where a system will eventually converge (Derouin & Potvin, 2005; Giesl & Wagner, 2007). This definition has been used in biomechanical studies to describe whole body stability in various populations, to describe static joint stability strategies or to analyze EMG signal reception in powered assistive devices (Giesl & Wagner, 2007; Bisi, Riva, & Stagni, 2014; Wagner, Giesl, & Blickhan, 2007; Kwon, Kim, & Kim, 2014). A concrete example comes from (Giesl & Wagner, 2007), where they explained that the basin of attraction is a range of joint positions where no additional muscle activity is required to keep the joint stable. If a disturbance causes the components of a joint to move outside of this basin, changed muscle activation is seen to bring the joint back into a stable equilibrium.

In musculoskeletal modeling, studies have used principles of mechanical control theories to describe muscle contributions in joint stabilization using equilibrium (static with constant muscle activations and joint position) states (Derouin & Potvin, 2005; Giesl, Meisel, Scheurle, & Wagner, 2004; Pel, Spoor, Pool-Goudzwaard, Hoek Van Dijke, & Snijders, 2008; Wagner et al., 2007).

1.5 Validation Methods for Musculoskeletal Models and Simulation Frameworks

Validation of models, simulation frameworks and their outputs is a crucial step in the development of their future applications (Manal & Buchanan, 2013; Vanheule et al., 2013; Wibawa et al., 2013). The final practical application of the model and its required accuracy will help to define what should be included and what can be omitted for simplification purposes (Petrella et al., 2013).

Current musculoskeletal models are not yet sufficiently validated to be used in evidence based clinical decision making, and will require better estimations of geometrical and material properties of the musculoskeletal system that will then be used within simulation frameworks to predict muscle activity and joint contact loading. However, it must be kept in mind that optimization protocols only guess how the neuromuscular system controls muscle activations.

In order to validate results of joint contact loads and muscle forces and activations determined by models and compare them to real life conditions, accurate experimental data are required. The Knee Grand Challenge, for example, has been a source of valuable knee joint information, collecting motion, EMG and force data using instrumented knee prostheses for a variety of motions over the past few years (Delp et al., 2007; Fregly et al., 2011; Kinney et al., 2013; Knowlton, Wimmer, & Lundberg, 2012). Many studies also validate their results by comparing muscle activation predictions to experimental EMG data if using inverse dynamics, or by comparing predicted motion to experimental kinematics data if using forward dynamics(Buchanan & Shreeve, 1996; Collins, 1995; Crowninshield & Brand, 1981; Glitsch & Baumann, 1997; Seireg & Arvikar, 1975).

1.6 Musculoskeletal Modeling and Simulation Framework Tools

1.6.1 OpenSim and Other Modeling Platforms

In recent years, different systems have been developed to facilitate the creation and visualization of musculoskeletal models as well as the development of simulation frameworks. Some of these have been more mechanical/engineering based where their applications are not limited to musculoskeletal studies, for example SD/FAST (PTC, USA), Autolev (OnLine Dynamics Inc. USA), MatLab (The MathWorks, USA), Ansys (Ansys Inc., USA), and others more biomechanically focused, for example Visual 3D (C-Motion, USA), SIMM (Musculographics Inc./Motion Analysis Corp., USA), AnyBody (AnyBody Technologies, Denmark) and OpenSim (Simtk.org, Simbios, National NIH Center for Biomedical Computing, USA) (Delp et al., 2007; Mansouri & Reinbolt, 2012; Pandy, 2001).

OpenSim 3.2 was chosen for this thesis for a few reasons. OpenSim is an open-source modeling and simulation platform, meaning that it is freely available to download and any interested person can use materials posted in the OpenSim repository at *simtk.org*, or post their own models for others to use. Source code is accessible to view and edit, and therefore it is easier to understand, modify and/or verify how models and processes are defined, unlike in other systems such as SIMM (MusculoGraphics Inc, USA), Visual3D (C-Motion Research Biomechanics, USA) and AnyBody (Delp et al., 2007; Mansouri & Reinbolt, 2012). This open access feature allows easier collaboration between research groups around the world in the development of musculoskeletal modeling and simulation (Delp et al., 2007). OpenSim uses inverse dynamics and static optimization in its simulation functions (Delp et al., 2007), and this is what this thesis's work is built upon.

1.6.2 Examples of Existing Musculoskeletal Models in the OpenSim Repository

There are many models available from the OpenSim repository with varying levels of complexity in terms of number of muscles, ligaments and degrees of freedom involved both in full body models or focused on particular joints or limbs. A few examples of full or lower limb models used for musculoskeletal modeling and muscle activation predictions are presented below. Many more are available at *simtk.org*.

Table 1: Selected examples of musculoskeletal models available in the OpenSim repository simtk.org

Model Based on Work From:	Description	No. of Actuators (Muscles Segments)	No. of DoFs at the Hip, Knee and Ankle
(Hamner, Seth, & Delp, 2010)	Full body	92	12 (Hip:3, knee:1, ankle: 1)
(Modenese et al., 2011)	Unilateral lower body	163	5 (Hip:3, knee:1, ankle:1)
(Delp et al., 1990)	Lower body	43/leg	Hip:3, knee:1, ankle:1
(Delp et al., 1990)	Torso+Lower body	92 (43/leg+obliques)	23 (Hip:3, knee:1, ankle:1)
(Xu et al., 2014)	Torso+Lower body	56 (25/leg+obliques)	29 (Hip:3, knee:4, ankle:1)

A modified version of the Xu et al. model was used in this thesis as it was based on previous work by Delp et al. 1990, and included key features such as multiple DoFs at the knee as well as had some muscle simplifications which would make simulations more computationally economical.

1.7 Motivation, Research Questions and Study Goals

The previous sections gave an overview of the components and function of musculoskeletal models and their related simulation frameworks. It was also noted that current models and simulation protocols, although promising, are not currently accurate enough or validated enough in predicting knee joint contact loading and solving for the multiple muscle forces involved in knee joint control (Fregly et al., 2011; Higginson et al., 2012; Manal & Buchanan, 2013; Vanheule et al., 2013; Wibawa et al., 2013). It is therefore the goal of this thesis to explore how musculoskeletal simulations could be improved. Two key areas of possible improvements to musculoskeletal models and simulation frameworks were identified in the literature, in particular considering the knee joint.

Objective 1: As stated in section *1.3.1 Inverse Dynamics*, obtaining accurate kinematic data is crucial in obtaining valid simulation results. In vivo evidence from a study by (Benoit et al., 2006) using marker equipped bone pins inserted into participants' femurs and tibias, showed that the knee moves in six degrees of freedom although only flexion/extension is well tracked by skin mounted markers. It was also shown that these degrees of freedom are, on an individual level, not obviously prescribed from the knee flexion angle as is the case in many musculoskeletal models (Benoit et al., 2006, 2007). Defining and evaluating an optimal range of motion for the knee joint based on the best available information of knee kinematics without requiring extensive and invasive measurement techniques is warranted. Therefore, our first research question becomes "Will adding range of motion limits, rather than using function prescriptions or skin mounted markers, to non-principal DoF movement in the knee affect model kinematics and joint torques predicted during gait?".

Objective 2: As described in section *1.4.3 Defining Stability as an Objective Function*, given the evidence that co-contraction exists and is not coherent with a physiological response to minimize energy/activation, defining and evaluating an optimization function based on joint stability is warranted. Put in question form, we ask "Will changing the optimization objective within a simulation framework to different definitions of joint stability applied to the lower limb affect muscle activation prediction results during gait?".

Objective 3: Based on the results from Objective 1 and 2, we will answer the question "Will changing both the simulation objective and incorporating in-vivo derived kinematic constraints improve muscle activation predictions?"

This research therefore serves to further the understanding of how the musculoskeletal system may work in-vivo and the strategies that it utilizes to preserve its integrity. If the muscle activation profiles are found to be improved with one of these stability based cost functions as well as the addition of experimental bone pin kinematic constraints and consequently potentially improving joint contact loading predictions, the model and simulation protocol could be used by other students and researchers to get an idea of joint contact loading and muscle activity during various activities in different populations and perhaps study how they relate to different muscle recruitment strategies and joint pathologies.

The next chapter outlines how these questions were addressed experimentally. Subsequently, in chapter 3, results and related discussion points are presented in the form of three journal manuscripts. The first manuscript details how incorporating in-vivo bone pin data derived range of motion constraints affected lower limb kinematics and kinetics of a musculoskeletal model over a gait trial. The second manuscript describes how changing the objective function within a simulation framework impacted muscle activation predictions. And lastly, the third manuscript presents the combined effect of kinematic changes induced by the bone pin knee joint constraints as well as changing the objective function of the simulation's optimization protocol.

Chapter 2 –Overall Methodology

This project consisted of two main parts. The first involves the extension of an existing musculoskeletal model to add additional degrees of freedom at the knee. Gait kinematics were then calculated using versions of this model with DoFs defined either with a combination of function prescribed DoFs or skin mounted marker trajectories, or with the addition of bone pin derived range of motion constraints from Benoit et al.'s study (Benoit et al., 2006). Inverse kinematics and dynamics were calculated for gait trials from 5 healthy young adult male subjects to see the effect on bone pin constraints on resulting model motion and joint torques. The model conditions tested were with:

1- (4DoF) A 4DoF knee model with 2 prescribed DoFs (distraction/compression and anterior/posterior translations) without bone pin range of motion constraints.

2- (5DoF) A 5DoF knee musculoskeletal model with 1 prescribed DoF (distraction/compression) without bone pin range of motion constraints.

3- (5DoFb) A 5 DoF knee model with 1 prescribed DoF (distraction/compression), and 4 of the remaining 5 DoFs (excluding flexion/extension) constrained by bone pin ranges of motion.

4- (6DoFb) A 6 DoF knee model with no prescribed DoFs and 5 DoFs (excluding flexion/extension) constrained by bone pin ranges of motion.

Results, which are presented in the first of three manuscripts in Chapter 3: *"Effect of Adding In-Vivo Based Kinematic Knee Joint constraints on Inverse Kinematics and Dynamics Results in Musculoskeletal Modeling using OpenSim*, were analyzed to determine if there were significant differences in kinematics and joint torques between the conditions.

In the second part of this thesis project, kinematic and torque results from the part 1 were used as inputs into the FID simulation framework described briefly in Chapter 1, *section 1.3.3 A Forward-Inverse Dynamics Simulation Framework* and is defined in more detail in (Shourijeh & Benoit, 2015; Shourijeh et al., 2016). Muscle activations about the hip, knee and ankle joints were predicted using 4 different optimization objective functions inspired by concepts of joint stability: minimum and maximum sum of muscle activations squared, as well as minimum shear and maximum compressive knee joint contact loading.

Results from these simulations were compared to experimental EMG data recorded during the motion trials to see if predictions were improved by 1) changing the objective function of the optimization protocol (refer to the second manuscript of Chapter 3: *"Musculoskeletal Knee Joint Stability Inspired Optimization of Forward-Inverse Dynamics Simulations to Predict Muscle Activations"* and 2) adding kinematic constraints. Correlations and visual observations are used to characterize these elements (refer to the third manuscript of Chapter 3: *"Using an In-Vivo Based Knee Kinematic Model in a Forward-Inverse Musculoskeletal Modeling Framework Alters Predicted Knee Joint Forces"*).

2.1 Musculoskeletal Model

A musculoskeletal model created by Xu et al. (Xu et al., 2014) and based on (Delp et al., 1990) which is available at *simtk.org* was used for this research project and includes 56 muscles (25 per leg and abdominal muscles), 8 knee ligaments and 29 DoFs, as shown in Figure 5. This model includes 4 non-prescribed DoF knee joint that follow skin mounted marker trajectories (rotations and medio/lateral translation) and the remaining two are prescribed as functions of the flexion/extension angle. The model also includes the patella to better visualize and control the moment arms created by the patellar tendon and quadriceps muscles (Xu, 2013; Xu et al., 2014).

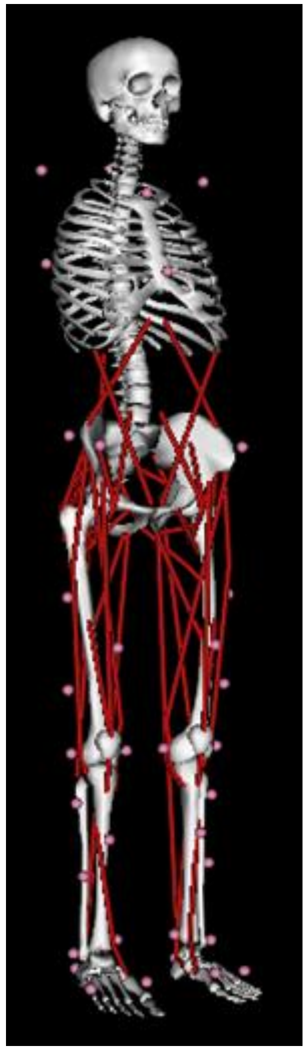

Figure 5: Xu et al's (Xu et al., 2014) musculoskeletal models outfitted with the University of Ottawa HMBL cluster marker set.

The Xu model contained multiple knee ligament bundles to study the deformation and forces applied to them during various motions. However it was found during preliminary tests that these ligaments made the model very stiff and prevented successful kinematics determinations. As ligament deformation and force evaluations are not principal components of this research project, the ligaments were removed from the musculoskeletal model, and successful analyses were then obtained.

2.1.1 Changing the Model's Patella Definition

In some OpenSim lower limb musculoskeletal models, the patella segment's motion (if present) or leg extensor muscle attachment location points are described in terms of the flexion/extension angle of the knee with relation to the tibia's position and orientation, for example in the case of the Gait2392, Gait2354 models, available on simtk.org (Delp et al., 1990; Yamaguchi & Zajac, 1989) as well as Xu's model (Xu et al., 2014). Although the patella is connected to the tibia by the patellar ligament, the motion of the patella tracks the distal end of the femur in the trochlear groove in a healthy joint (Marieb, 1998). When anterior/posterior and distal/proximal DoFs are prescribed by functions in the model, the patella tracks the end of the femur adequately. However, when these DoFs are no longer strictly prescribed, the patella's motion deviates from its intended path, an extreme example of which is shown in Figure 6. How the patella's position is defined will have an impact on both knee joint alignment and on the moment arm of muscles surrounding the joint (Coughlin, Incavo, Churchill, & Beynnon, 2003; Yamaguchi & Zajac, 1989). Because of this, the musculoskeletal model script developed by Xu et al. (Xu et al., 2014) was modified so that the prescribed tibio-patellar joint became the femoro-patellar joint, where motion of the patella was defined in terms of the flexion/extension angle and the position of the femur as is more anatomically realistic. This was done using the motion of the patella from the original model and the work done by Yamaguchi and Zajac (Yamaguchi & Zajac, 1989) and Coughlin et al. (Coughlin et al., 2003) to guide the new trajectories. Excerpts from the original and modified model scripts for the patella can be found in Appendices A1.

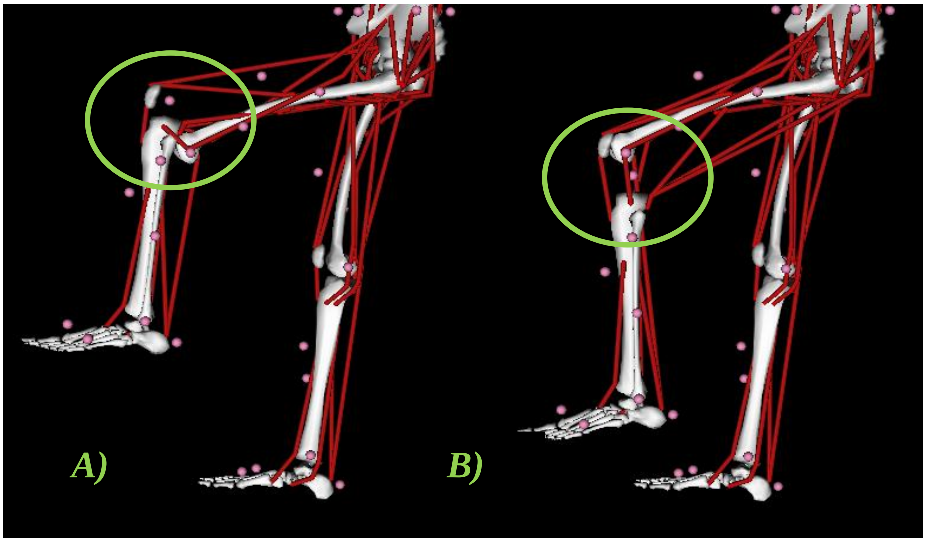

Figure 6: A) Patella position definition in terms of the tibia can be physiologically unrealistic in models with 6 DoFs. B) Patella definition in terms of the distal femur is more anatomically relevant.

2.1.2 Changing the Muscle Model from Thelen to Millard

As the Xu model was initially developed when the most current Hill-type muscle model was the one developed for OpenSim based on Thelen's (Thelen, 2003) and Winters's muscle model (Winters, 1995) , the model script used the "Thelen2003Muscle" model to describe the various muscles and their mechanical representations. This was the gold standard built into OpenSim for running static optimization protocols to determine muscle forces. Since then, a slightly modified version of the Thelen model developed by Millard et al. (Millard, Uchida, Seth, & Delp, 2013) has been implemented in the new OpenSim update and is found under the name "Millard2012EquilibriumMuscle" in model scripting files. The Millard model determines force exerted by a muscle based on its normalized activation level, muscle length, maximal isometric force, non-linear muscle force-length and force-velocity curves as well as tendon length and the tissue's pennation angle. The main differences between the Millard2012EquilibriuMuscle model and the Thelen2003Muscle model are the additions of constraints to prevent the muscle model from using unrealistically short muscle lengths as well as prevents muscles from being fully deactivated. Further details on the model and differences between the two can be found on the OpenSim website (*http://simtk-confluence.standford.edu*, last visited April 2016). To update the Xu model used in this thesis, the muscle model in the musculoskeletal model script was changed from the “Thelen2003Muscle” model to that of the “Millard2012EquilibriumMuscle” muscle model.

2.1.3 Releasing Prescribed Degrees of Freedom

The original Xu model has 2 prescribed DoFs (anterior/posterior and distraction/compression translations), and 4 others that were free to move within a broadly and loosely constrained range of motion. In order to implement the bone pin derived range of motion constraints on a 5 and 6DoF knee model, the two prescribed DoFs were released of their function prescribed motions by changing the model script in the section defining the tibial body, under the custom joint spatial transform section in the OpenSim model file (Body (tibia) → Joint → CustomJoint → SpatialTransform).

In the following section of the model script, (Body (tibia) → Joint → CustomJoint → CoordinateSet), it is possible to set ranges of motion for each degree of freedom of a joint and either enforce them strictly by setting them as “clamped” where the model may not adjust its calculations to beyond this range, or leaving them as general guidelines only (not “clamped”) from which the model may deviate if necessary. This feature was used to define the bone pin derived ranges of motion and to constrain the model to appropriate values. Scripts of the original 4 DoF knee model with 2 prescribed DoFs as well as an example of the 6 DoF knee model with clamped ranges of motion can be found in Appendices A2.

For each time step of inverse kinematics process, the allowed ranges of motion for the relevant DoFs were determined and updated in the model script to constrain the kinematics to the new bone pin defined range of motion envelopes. Each single frame of resulting inverse kinematics was then assembled into one motion file that was applied to the scaled musculoskeletal model to make it move.

2.2 Bone Pin Data Processing

As was described in an earlier section, motion data from walking, hops and cut trials were recorded using marker clusters mounted on pins that were directly inserted into participants' femur and tibia as shown in Figure 7. A detailed description of how this data was collected and processed is available from (Benoit et al., 2006).

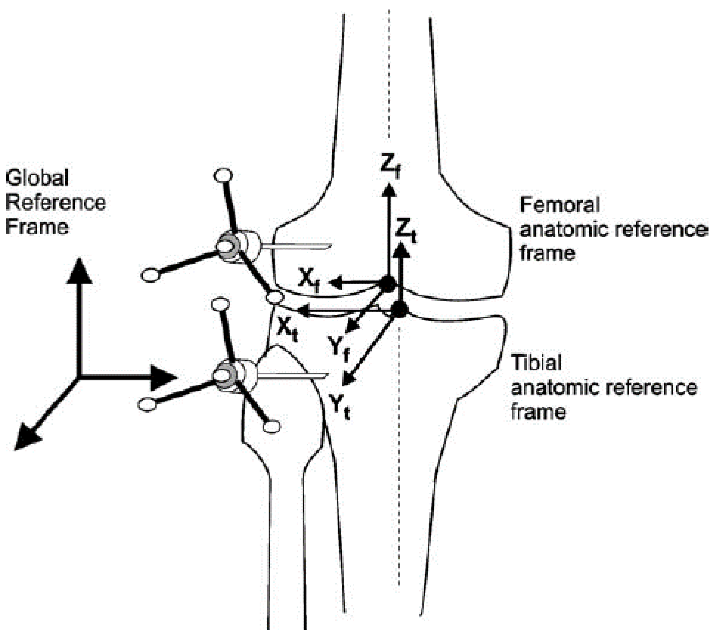

Figure 7: General illustration of bone pin marker cluster placements and anatomical reference frames in the study by Benoit et al. 2006

Rotations and translations at the knee joint were obtained from each of these trials (3 to 5 repeated trials of each motion for 6 participants) from this study (Benoit et al., 2006).

Determination of allowed ranges of motion for each DoF in the inverse kinematics calculation is as follows:

For each individual subject and for each of the three motions separately, the mean values (from the 3-5 repeated trials) over the time normalized trials were calculated for each DoF. The 95% confidence interval (CI) surrounding these means was also calculated. In some trials, the first and last few data points were skewed as a result of the subject stepping into and out of the capture volume during data collection. To reduce this effect, the first and last 10 points (out of 100 interpolated data points) were trimmed.

For each type of motion, the means for each subject just obtained were then averaged between subjects and the corresponding average CI range was also calculated.

As shown in Figure 8, these means +/- CI for each DoF were then plotted in terms of flexion/extension angle of the knee for gait, hop and cut motions separately. An envelope of the maximum and minimum values over the range of flexion/extension angles was then determined. It was then assumed that at a fully upright position (0^o flexion), the rotations and translations are also at a zeroed point. This was confirmed by visually checking the model in its upright position. If the positions were not zeroed, the bones did not align well. Therefore the range of motion envelopes were shifted to accommodate this. These ranges of values in terms of flexion angle were used to determine allowed ranges of motion constraints for the knee joint translations and rotations in the Xu model.

The bone pin derived ranges of flexion/extension angles went from 0 (fully extended) to 45 degrees of flexion. As some of the simulation trials required values exceeding this interval, the range of motion envelopes were extended based on the range of motion values and patterns near each extreme. Figure 8 shows the bone pin derived range of motion envelopes in terms of knee flexion angle and the gait, hop and cutting kinematics from which they were calculated.

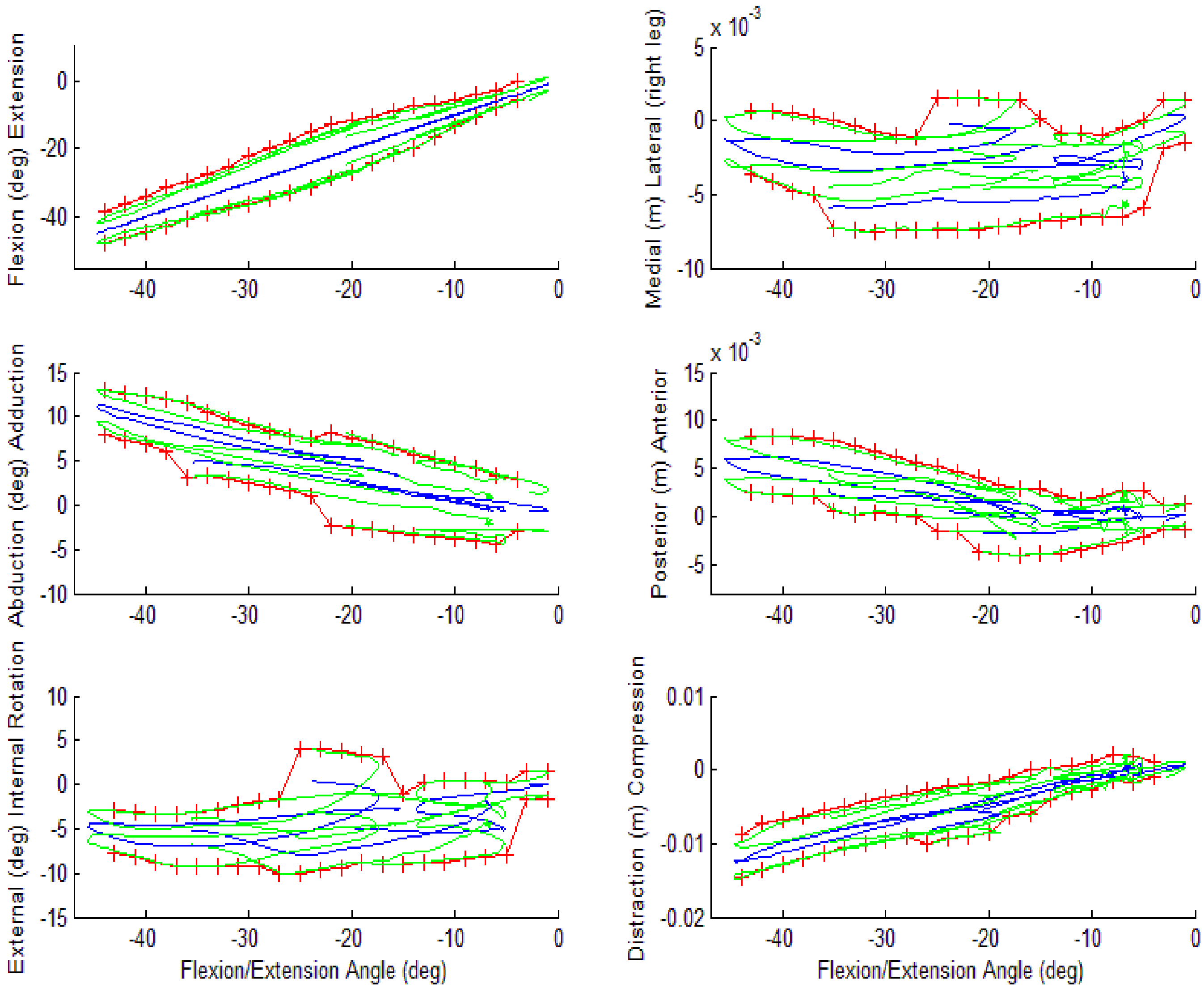

Figure 8: Allowed ranges of motion for each DoF at the knee joint. The black solid lines show average values for each motion type (gait, hop or cut). Grey lines show confidence intervals for each motion type. The black solid line with + symbols show the maximum and minimum envelopes. Flexion, abduction, and external rotations as well as medial, posterior and distraction translations are shown with negative values. Their corresponding opposite motions are positive values.

The anatomical reference frame definitions used in the bone pin study by (Benoit et al. 2006) are not exactly the same as those in the (Xu et al., 2014) OpenSim model. The bone pin study defined the coordinate systems of the femur and tibia using radiographs of the subjects' knee joints. The femur's point of origin was chosen as the deepest point of the inter-condylar groove. The vertical axis (Z) follows a parallel line starting at the origin and following the long axis of the femur. The anterior/posterior axis (Y) is the cross-product between the Z axis and the line between the medial and lateral edges of the condyles. Finally, the X axis is defined as the cross-product between the Z and Y axes pointing laterally.

The tibia is similarly defined, but with a point of origin at the highest point of the medial inter-condylar eminence. The Z axis passes through the point of origin and points parallel to the long axis of the tibia, the Y axis is the cross-product of the Z axis and the line formed between the medial and lateral edges of the tibial plateau, and the X axis is defined by the cross-product of the Z and Y axes. The resulting anatomical reference frames can be seen in Figure 7 (Benoit et al., 2006).

In the case of the Xu model, the femoral and tibial coordinate systems are described as follows: The origin point of the tibia is located at the midpoint between the lateral and medial femoral condyles, at the knee joint center. The origin of the femoral system is at the center of the femoral head. The tibia and femur have axes pointing in the same directions, where the vertical axis Y is perpendicular to the transverse plane that passes through the origin point of the tibia. The Z-axis points laterally lying on the same transverse plane. The X-axis points anteriorly and is the result of the cross-product between the Z and Y axes (Xu et al., 2014). An illustration of this is shown in Figure 9. The knee joint's DoFs are defined with the tibia's position in relation to the femur.

To minimize the effect of different coordinate systems, the bone pin derived envelopes were centered at zero flexion (full extension) within the model so that both bone pin data and model coordinate systems had a matching reference point. Even with slight differences in definitions, the bone pin derived rotation and translation ranges of motion can still provide a reasonable physiological range in which the Xu model may move.

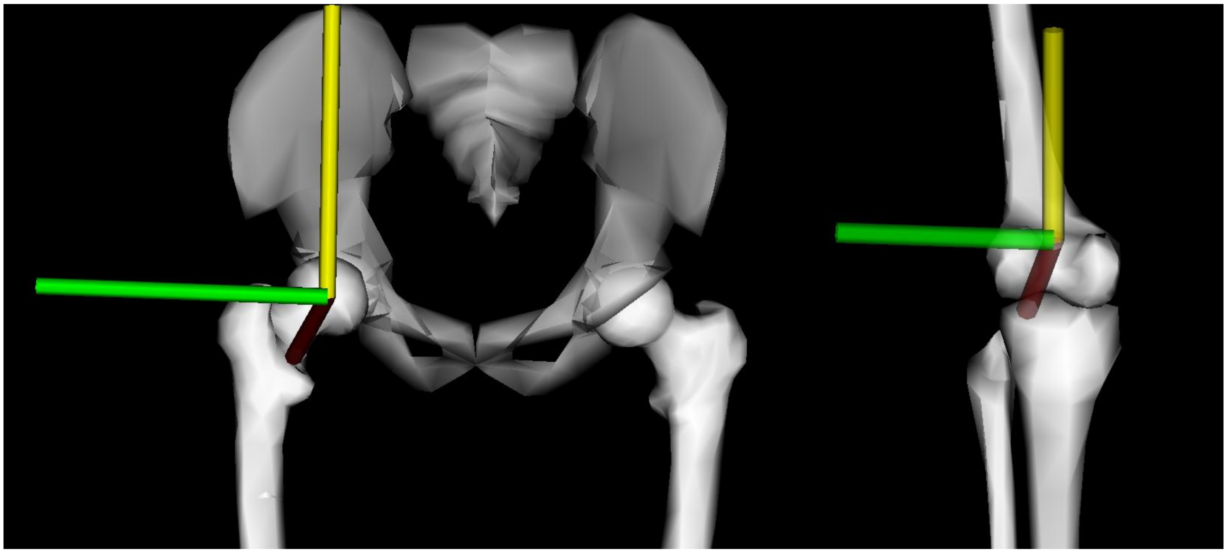

Figure 9: Visual representation in OpenSim of the femoral and tibial anatomical reference frames of the Xu et al. (2014) model.

2.3 The Simulation Framework

Calculation and simulation protocols applied to the models in this project come from a FID framework developed within our research team by Dr. Mohammad S. Shourijeh (Shourijeh et al., 2016). As was briefly explained in Chapter 1 section 1.3.3, this FID method, illustrated in Figure 4 and repeated here (Figure 10) for clarity will be used to run muscle activation simulations on gait data.

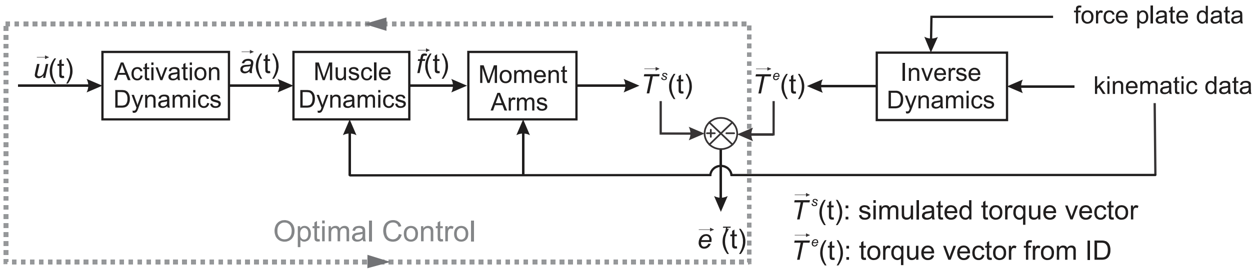

Figure 10: Forward-inverse dynamics simulation framework minimizing joint torque prediction error $e(t)$. Other variables are defined as follows: $u(t)$: muscle excitation, $a(t)$: muscle activation, $f(t)$: tendon-muscle forces, T^s: simulated torque vector, T^e: torque vector from inverse dynamics (ID). Adapted from (Shourijeh & Benoit, 2015; Shourijeh & McPhee, 2014).

The FID method first calculates knee joint torques by inverse dynamics (right hand side of Figure 10 up to "torque vector from ID") then runs the first steps of forward dynamics with prescribed motion (starting on the left at "Muscle Dynamics") to estimate muscle activations and forces that yield knee joint torques (simulated torque vector) as close to those described by the inverse dynamics method. This is done by running an optimization sequence that minimizes a given cost function (objective function) which will test iterations of muscle activation combinations to see if the joint torque difference can be minimized (illustrated by the Optimal Control box in Figure 10). This cost function can be composed of multiple elements, mathematical (non-physiological) cost functions such as minimizing torque error between forward and inverse dynamics as shown in Figure 10, and can include physiological cost functions as well, such as minimization of muscle activation. As noted in section 1.4.2 Objective Functions, this is not necessarily a realistic physiological condition to include in a simulation and we will explore how changing this cost function alters final simulation outputs. Although experimental EMG data will not be used directly within the simulation, we will use the data to validate the muscle activity prediction results.

2.3.1 Part 1 of the Forward-Inverse Dynamics Framework Method: Inverse Kinematics, Dynamics and Static Optimization

The first step in determining knee joint torques using inverse dynamics (right hand part of the FID framework in Figure 10) involves loading and scaling the musculoskeletal model to fit the individual's measurements. A static motion capture trial is loaded into OpenSim and the model is dimensionally scaled by comparing positions of experimental markers and the model's virtual markers that are defined at approximate locations on the model's body as well as uses height and weight values given as additional anthropometric data. Each segment's inertial properties are adjusted and muscle attachment points are scaled to the new segment lengths. Maximum muscle forces remain the same as the generic model unless otherwise updated (which was not the case in this thesis). The model is saved in its scaled form.

The following steps calculate inverse kinematics and inverse dynamics through predefined functions in OpenSim. A motion trial in *.C3D format is defined and opened through MatLab and trajectory and force plate data from that file are split into file formats that can be read by OpenSim - MOT, GRC and TRC files - through specialized MatLab C3D reading functions.

To incorporate the bone pin range of motion constraints for the simulation conditions using them, an initial joint angle is required to start the process. The first time step is run without constraints to obtain this initial joint flexion angle value and to determine allowed ranges of motion based on the data from Figure 8 in the 2nd time step for the relevant DoFs requiring constraints. For the 3rd time step, knee flexion angle from the 2nd time step is used and so on over the course of the trial. Although this creates a minor time shift in flexion angles, from one time step to the next the angle change remains small as gait data is mostly smooth and does not have sharp angle changes as might be seen in cutting motions for example. Inverse kinematics are calculated through OpenSim 3.2's built in function by first attempting to minimize the error of fit between experimental marker placement and how the model is able to move, and then calculates joint and segment positions from there. Details on this method can be found at *http://simtk-confluence.stanford.edu:8080/display/OpenSim/How+Inverse+Kinematics+Works* (last visited December 2015) and is also copied for convenience in Appendices A3. Each time step's inverse kinematics results were then assembled into a single continuous sequence to create a motion file from dominant heel strike to next dominant heel strike from which the inverse dynamics calculations are then performed.

Because there are errors and assumptions in the model and noise in collected data, calculated forces for the segments of the leg do not coincide exactly with $mass * acceleration$ $(F = ma)$ as defined in Newton's law ("How RRA Works - OpenSim Documentation - Confluence," 2013). As such, once inverse kinematics and dynamics are determined, some users recommend running a residual reduction algorithm (RRA). The equation becomes $F + F_{residual} = ma$. The RRA function in OpenSim will optimize the model to minimize the residual force values as much as possible so that kinematics and dynamics are followed as well as the laws of physics. This process was run for multiple trials and was found to produce unreliable results, where in some cases, instead of showing stable gait data, the model collapsed into a non-admissible state as a result of RRA adjustments as shown in Figure 11. Because of this, only torque data from inverse dynamics were used instead of RRA adjusted torque values.

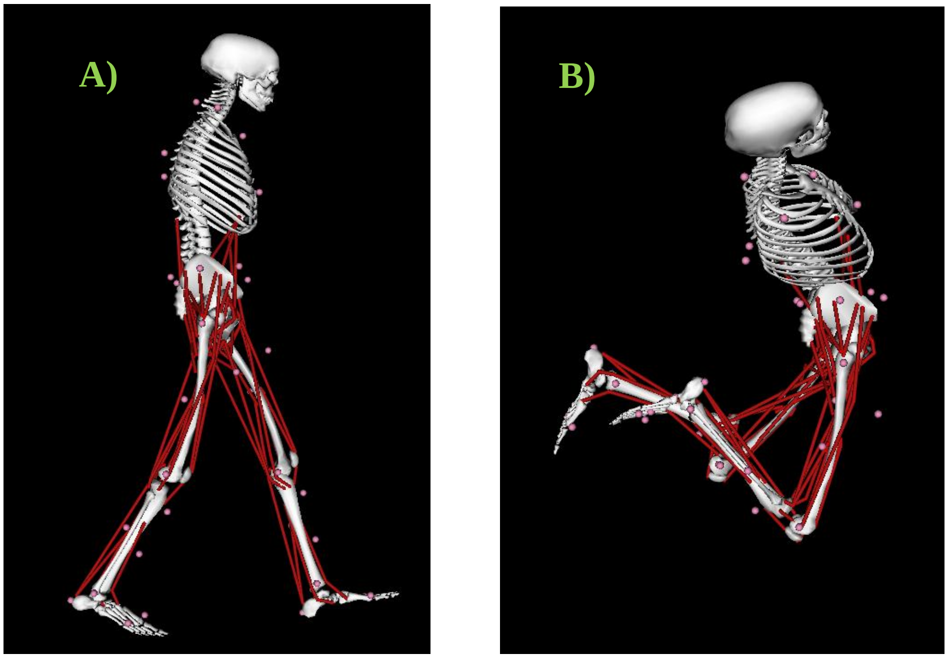

Figure 11: Kinematic results for one subject at the same time frame from running A) Inverse kinematics only and B) running RRA adjustments after inverse kinematics to minimize residual errors. Combined with bone pin derived constraints, RRA gave inadmissible results.

As an additional step that is not required to get final FID simulation muscle activation results, conventional static optimization simulations were run using the OpenSim Static Optimization tool that minimizes the sum of muscle activations squared. Results of this static optimization were compared to the other final FID framework simulation results.

All results (scaled model file, muscle moment arms, kinematics and knee joint torques) were saved for analysis and for use as inputs into the forward part of the FID simulation protocol.

2.3.2 Part 2 of the Forward-Inverse Dynamics Simulation Method: Forward Dynamics and Changing the Objective Function in Optimization

To run the forward dynamics part of the FID simulation framework, the scaled model was given a set of motions to follow from the inverse kinematics results as is illustrated in Figure 10. As well, the moment arm of each muscle was retrieved through OpenSim from the scaled model and inverse kinematics results for each time step and each DoF of the model. These moment arms were combined with predicted muscle forces derived from activation values to determine knee joint torques.

An initial guess for muscle activation predictions used the results of the OpenSim static optimization tool as a starting guess for the combination of muscle activations likely to fulfill the optimization criteria of minimizing the difference between joint torques calculated by inverse dynamics and predicted by forward dynamics. Optimization functions to find a solution used a combination of optimization functions from the MatLab Optimization and Global Optimization toolboxes (MatLab 2013a, The MathWorks, US). More specifically, using the functions *fmincon* (find minimum of constrained nonlinear multivariable function), *GA* (find minimum of function using a genetic algorithm) and *fminsearchbnd* (find minimum constrained multivariable function using derivative-free method) Results of muscle activations were saved to be analyzed afterwards. Optimization was done on 50 evenly spaced time points over the course of the gait cycle defined from dominant leg heel strike to the following dominant leg heel strike.

Simulations were repeated with four different objective functions in the optimization protocol as described in the next section.

2.3.2.1 Defining Cost Functions to Optimize Stability of the Knee

Details of the FID framework can be found in (Shourijeh & Benoit, 2015; Shourijeh et al., 2016). The basic mathematical (non-physiological) objective function of the FID framework's optimization minimizes the absolute value of torque error (*TE*) divided by absolute values of torque determined from inverse dynamics (*ID_Torques*), and rejects combinations of values where muscle activations (*a*) are above 1 or below 0 (beyond 0 to 100% maximum activation effort). The simulation attempts to obtain the solution with the smallest value of the mathematical objective function J_{Tmin}.

$$J_{Tmin} = \min\left(\Sigma(|TE|/|ID\_Torques|)\right) \quad \text{(Eq1)}$$

Only the sagittal (flexion) plane of the hip, knee and ankle DoFs and their relevant muscle lines of actions and activations were optimized to minimize torque error, as the muscle activation combinations from the other DoFs showed difficulties in recreating required torque conditions due to reduced amount of muscles in the model able to create abduction or rotation torques.

This cost function can be changed to include a physiological component as well. The more common cost function of minimizing muscle activation (Eq2: J_{Amin} where a_i represents muscle activation) required to achieve a given position is defined by minimizing the sum of squared muscle activations.

$$J_{Amin} = |min\Sigma(a_i)^2| \quad \text{(Eq2)}$$

Different weighting factors can be selected to put more importance on the purely mathematical or the physiological conditions as necessary. Simulations were run with this physiological cost function as a starting point. More tests were run using other possible cost functions based on improving stability of the joint considering the various explanations of stability outlined in Chapter 1, section 1.4.3. In each case, the mathematical cost function of minimizing torque error and rejecting solutions with normalized muscle activations outside of the physiologically possible range of 0 to 1 (0-100% maximal effort) were kept as part of the whole objective function.

One of the new physiological cost functions was simply the opposite of the first one, a function to maximize muscle activation (J_{Amax}):

$$J_{Amax} = |max\Sigma(a_i)^2| \tag{Eq3}$$

As the optimization coding of the FID simulation framework seeks the global minimum of the combination of mathematical and physiological cost functions, this equation becomes:

$$J_{Amax} = |\min \frac{1}{\Sigma(a_i)^2}| \tag{Eq4}$$

This cost function option could help tighten and therefore increase stiffness of the joint, thus improve stability according to one of the definitions of stability.

With a similar reasoning, two other cost functions based on stability definitions were to maximize joint compression (J_{Jmax}) where F_{compr} is axial compression force, and minimize joint shear loading (J_{Smin}) where F_{shear} is the resultant shear force. Maximizing compression could increase joint stiffness and thus stability. Minimizing shear loading could promote co-contraction of muscles to cancel out opposite forces, as well as protect ligaments from excessive stress and strain. These objective functions were respectively defined using joint contact loads as criteria as:

$$J_{Jmax} = |min \frac{1}{\Sigma(F_{compr})}| \quad \text{(Eq5)} \qquad J_{Smin} = |min\Sigma(F_{shear})| \quad \text{(Eq6)}$$

These cost functions were tested on gait trials of the 5 subjects used in the first part of the FID simulation framework and applied to 2 of the model conditions described previously:

1- (4DoF) A 4DoF knee model with 2 prescribed DoFs (distraction/compression and anterior/posterior translations) without bone pin range of motion constraints

2- (5DoFb) A 5 DoF knee model with one prescribed DoFs (distal/proximal translation) and 4 DoFs (excluding flexion/extension) constrained by bone pin ranges of motion.

In this way, the effect of adding kinematic constraints to final muscle activation results could be observed. This second model condition was chosen as OpenSim was unable to calculate joint forces when all DoFs were released as a 6DoF knee model. As well, since the bone-pin constrained distal/proximal translation DoF was quite similar to the prescribed function, it was deemed an acceptable compromise.

The physiological cost functions described for the simulations were defined and incorporated with the torque error minimization to outline the total cost function to be minimized in the forward part of the FID simulation. As the weighing factors for both the torque error minimization and physiological cost functions can be modified, simulations were run in a way to equally distribute the weight of the physiological cost function with that of the minimization of torque error.

2.4 Experimental Motion Trials

Level ground gait trials were recorded over the last 2 years from 5 young healthy male adults (mean age, weight and height 24±1.9yr, 80.8±9.1kg and 177.3±8.1cm respectively) walking with a self-selected pace. The protocol for collecting the data was approved by the University of Ottawa Ethics Review Board.

The data uses a Plug-In Gait marker set (Vicon Motion Systems, UK), illustrated in Figure 5, modified to include 3-marker clusters on the thigh and shank along with other bony landmarks on the body. Passive reflective marker trajectories were sampled at 200 Hz using the Vicon Nexus 1.8.3 motion capture system (Vicon Motion Systems ltd, UK) and force plate data from a Bertec platform (Bertec, USA) was sampled at 1000Hz. Marker trajectories and force plate data were filtered with a 4^{th} order dual pass Butterworth filter with a cutoff frequency of 10Hz.

Muscle EMG was collected at 1000Hz with a Delsys Bagnoli 16 EMG system (Delsys, USA) electrodes on the dominant leg for 12 muscles: gluteus maximus (GLTMAX), gluteus medius (GLTMED), tensor fascia latae (TFL), rectus femoris (RFEM), vastus medials (VMED), vastus lateralis (VLAT), biceps femoris (BFEM), semitendinosus (STEN), tibialis anterior (TA), medial gastrocnemius (MGAS), lateral gastrocnemius (LGAS) and the soleus (SOL).

Electromyography data from each motion trial was full wave rectified and filtered with a 4^{th} order dual pass Butterworth filter with cutoff frequency of 8Hz to obtain a linear envelope of muscle activity. Maximum voluntary isometric contraction (MVIC) trials were collected on a Biodex dynamometer (Biodex, USA) instrument. MVIC EMG data collected from these trials were also filtered in the same way. Maximum EMG values were recorded from each muscle over all MVIC trials and are the values used to normalize the motion trial EMG data. Simulations were run for one gait cycle between dominant heel strike and the following dominant heel strike. Therefore normalized EMG trials were trimmed to these event times for better comparisons.

The data used to constrain the range of allowable kinematic translations and rotations come from (Benoit et al., 2006). As the bone pin data was collected only on healthy male adults, the FID simulations will only be run on the male participants (5 of the 10 collected participants). Running simulations to compare results in different populations, those affected by fatigue, osteoarthritis or ACL injuries for example, may be done using a similar methodology in future projects. However, additional bone pin data collections may be required to have information that reflects the studied population.

2.5 Statistical Analysis

2.5.1 Statistical Analysis of Inverse Kinematics and Inverse Dynamics Result with and without Bone Pin Range of Motion Constraints

Mean and standard deviations for resulting hip, knee and ankle joint kinematics and knee joint dynamics were plotted and compared between each of the four testing conditions both visually and with one-way ANOVA testing using statistical parametric mapping (SPM) to find significant ($p<0.05$) differences between conditions over the entire duration of the gait trials. Post-hoc tests on significant results were conducted using Bonferroni corrected two-tailed t-tests to reduce the effect of running multiple comparisons in the ANOVA test and to conservatively find which condition comparisons showed significant differences.

In the literature, studies with similar styles of data often calculate means and standard deviations to see changes over time during motion trials for example, followed by one or two way ANOVA tests (Behm, Anderson, & Curnew, 2002; Besier et al., 2009; Vanrenterghem, Venables, Pataky, & Robinson, 2012). However, this type of testing can only analyze particular time points in the whole series of data, usually selected as peaks or key events in the graphs and not over a time period as is important in the case of trial kinematics and dynamics (Pataky, 2012; Serrien, Blondeel, Clijsen, Goossens, & Baeyens, 2014; Vanrenterghem et al., 2012). SPM testing, typically used for 3D neuro-imaging procedures, has recently been adapted to processing other one-dimensional data sets such as marker trajectories or ground reaction forces that vary over time. This type of testing allows calculations of means and standard deviations over the course of a trial but also to calculate other statistical tests such as the one-way ANOVA over an entire trial and identify which parts show significance (Pataky, 2012; Pataky, Robinson, & Vanrenterghem, 2013). A research group has developed scripts to run SPM statistical tests for MatLab and Python, and these codes are freely available from www.spm1d.org (Pataky, 2012). SPM testing has been used in other biomechanical studies such as (De Ridder, Willems, Vanrenterghem, Robinson, & Roosen, 2014; Serrien et al., 2014; Vanrenterghem et al., 2012) for example. More details on how the process works can be found in (Friston, Holmes, Worsley, Frith, & Frackowiak, 1995; Pataky, 2010, 2012; Pataky et al., 2013). In addition to statistical testing, kinematics and torque values were also compared to data found in the literature to identify similarities.

Results and their discussion can be found in the first manuscript in Chapter 3: *"Effect of Adding In-Vivo Based Kinematic Knee Joint constraints on Inverse Kinematics and Dynamics Results in Musculoskeletal Modeling using OpenSim"*, Potvin B.M, Shourijeh M.S., Smale K.B., Benoit D.L.

2.5.2 Statistical Analysis of the Effect of Changing the Objective Function in Forward Dynamics Optimization within the FID framework with and without Bone Pin Constraints

To see if the new cost functions used in the forward dynamics part of the FID framework enabled the model simulations to predict muscle activity more accurately, muscle activation results were compared to processed experimental EMG data. Results can be found in the second and third manuscripts presented in Chapter 3: *"Musculoskeletal Knee Joint Stability Inspired Optimization of Forward-Inverse Dynamics Simulations to Predict Muscle Activations"*, Potvin B.M, Shourijeh M.S., Smale K.B., Spinello D., Benoit D.L.

and *"Using an In-Vivo Based Knee Kinematic Model in a Forward-Inverse Musculoskeletal Modeling Framework Alters Predicted Knee Joint Forces"*, Potvin B.M, Shourijeh M.S., Smale K.B., Spinello, D., Benoit D.L.

Visual observations as well as statistical correlations tests and root mean square error (RMSE) calculations were used to compare experimental and predicted muscle activation patterns. There was some delay between EMG peaks and muscle activation results due to the typical electrochemical delay seen between muscle excitation and production of force. Therefore, EMG data was shifted up to a maximum of 150ms to match muscle activation curves using the cross-correlation function *xcorr* built into Matlab statistical testing scripts.

Correlation results from the simulations revealed if changing the cost function had a significant impact on simulation outputs and which of the objective functions provided the most accurate predictions in terms of curve pattern. RMSE analysis gave insights into how close the estimations were to EMG data in terms of magnitude. Predicted muscle activity patterns were also compared to EMG data from the literature and to simulation results obtained by other studies.

SPM scripts were used to graphically represent the across subject means and standard deviations of muscle activation predictions as well as joint contact loading over the course of the gait cycle for each simulation condition.

Chapter 3 – Journal Manuscripts

Results from each part of the methodology described previously will be presented in the following manuscripts. Note that these have not been published in journals as of the date of submission of this thesis but are presented in this way to underline the different stages and objectives of this thesis.

1)

"Effect of Adding In-Vivo Based Kinematic Knee Joint constraints on Inverse Kinematics and Dynamics Results in Musculoskeletal Modeling using OpenSim"

Potvin B.M, Shourijeh M.S., Smale K.B., Benoit D.L.

2)

"Musculoskeletal Knee Joint Stability Inspired Optimization of Forward-Inverse Dynamics Simulations to Predict Muscle Activations"

Potvin B.M, Shourijeh M.S., Smale K.B., Spinello D., Benoit D.L.

3)

"Using an In-Vivo Based Knee Kinematic Model in a Forward-Inverse Musculoskeletal Modeling Framework Alters Predicted Knee Joint Forces"

Potvin B.M, Shourijeh M.S., Smale K.B., Spinello, D., Benoit D.L.

Effect of Adding *In-Vivo* Based Kinematic Knee Joint Constraints on Inverse Kinematics and Dynamics Results in Musculoskeletal Modeling Using OpenSim

Brigitte M. Potvin,
University of Ottawa, School of Biomedical Engineering

Dr. Mohammad S. Shourijeh
University of Ottawa, School of Rehabilitation Sciences

Kenneth B. Smale
University of Ottawa, School of Human Kinetics

Dr. Daniel L. Benoit
University of Ottawa, School of Human Kinetics and Rehabilitation

ABSTRACT

Musculoskeletal modeling and simulations have vast potential in clinical and research fields, but face various challenges in representing the complexities of the human body such as soft tissue artifact created by applying skin mounted marker motion data to models in simulations. To address this, we developed joint constraints on five of the six degree of freedom of the knee joint based on *in vivo* tibio-femoral joint motions recorded during walking, hoping and cutting from subjects instrumented with intra-cortical pins inserted into their tibia and femur. A musculoskeletal model developed in OpenSim simulation software was constrained to these boundaries and inverse kinematics and dynamics were then resolved. Statistical parametric mapping of simulation showed significant differences ($p<0.05$) in kinematics between bone pin constrained and unconstrained model conditions, notably in knee translations, while hip, knee and ankle flexion/extension angles showed minimal differences between model conditions. Changes in hip, knee and ankle moments were also noted.

The goal of most musculoskeletal modeling studies is to represent physiological events. We have developed and evaluated a kinematically constrained knee joint based on in vivo tibio-femoral motions which resulted in more physiologically realistic translation and rotation movements. Given that soft tissue artifact induces significant kinematic error and studies have also indicated that current modeling approaches used to reduce this error may in fact exacerbate this error, our in vivo based constraints represent a simple method to provide more realistic kinematics for the remaining degrees of freedom within musculoskeletal models.

KEY WORDS

Musculoskeletal modeling, kinematics, soft tissue artifact, knee joint, bone pins

BACKGROUND

Musculoskeletal modeling and computer simulations are very useful clinical and research tools to objectively address musculoskeletal disorders and their costly effect on the health care system(Delp et al., 1990; Fregly et al., 2011; Kinney, Besier, D'Lima, & Fregly, 2013; Komistek, Kane, Mahfouz, Ochoa, & Dennis, 2005; Reinbolt et al., 2005). The knee joint is a complex load bearing joint and moves in 6 degrees of freedom (DoF): 3 rotations - flexion/extension, abduction/adduction, internal/external rotation, and 3 translations - anterior/posterior, lateral/medial and distal/proximal. Yet, it is often simplified into a reduced DoF joint in musculoskeletal modeling and simulations (Anderson & Pandy, 2001; Arnold, Ward, Lieber, & Delp, 2010; Delp et al., 1990; Modenese, Phillips, & Bull, 2011; Sasaki & Neptune, 2010; Xu, Bloswick, & Merryweather, 2014), limiting its physiological realism. The remaining degrees of freedom are typically neglected or defined as functions of the flexion/extension angle of the knee based on cadaveric studies and geometric modeling of the femur, tibia and patella (Coughlin, Incavo, Churchill, & Beynnon, 2003; Delp et al., 1990; Yamaguchi & Zajac, 1989). A musculoskeletal model developed by Xu et al. defines the knee more flexibly as a 4 free DoFs joint with the remaining two (anterior/posterior and distal/proximal translations) prescribed as functions of the knee flexion angle (Xu et al., 2014). However, accurate kinematics are required to correctly define model motion.

Typically, reflective skin mounted markers tracked by motion capture systems are used to track experimental body kinematics (position of bones relative to each other and to the environment) during various activities and are applied to musculoskeletal models (Benoit et al., 2006; Worsley, Stokes, & Taylor, 2011). Soft tissue artifact (STA), the movement of markers caused by skin deformation and not actual bone motion, has a large effect on determining body kinematics (Benoit et al., 2006; Gao & Zheng, 2008; Gasparutto, Sancisi, Jacquelin, Parenti-Castelli, & Dumas, 2015; Li, Zheng, Tashman, & Zhang, 2012; Reinschmidt, Van Den Bogert, Nigg, Lundberg, & Murphy, 1997). Benoit et al.'s work (Benoit et al., 2006) compared knee joint skeletal segment movement in healthy adult males using skin mounted markers as well as rigidly linked marker clusters directly implanted into the femur and tibia with bone pins. Skin markers were found to be heavily affected by STA in all but the larger motion of flexion/extension, where the error in relation to the magnitude of movement was small (Benoit et al., 2006, 2007). Errors of up to 13.1^{o} in rotations (observed in abduction/adduction) and up to 16.1mm in translations (observed in anterior/posterior translation) were identified (Benoit et al., 2006). This error is a function of marker cluster translation and rotation, rather than cluster deformation (inter-marker motions)(Benoit, Damsgaard, & Andersen, 2015) and while modeling the error is possible (Andersen, Damsgaard, Rasmussen, Ramsey, & Benoit, 2012) it is not yet feasible without subject specific data obtained in vivo to generate the model.

To solve this issue, different methods have been used to introduce anatomical, kinematic or geometrical constraints in musculoskeletal models to limit STA (Andersen, Benoit, Damsgaard, Ramsey, & Rasmussen, 2010; Duprey, Cheze, & Dumas, 2010; Gasparutto et al., 2015; Leardini, Chiari, Della Croce, & Cappozzo, 2005) however in many cases this may in fact increase the error (Andersen et al., 2010).

In order to improve the biofidelity of musculoskeletal models of the lower limb, we have developed a model of knee joint motion constrained for each non-principal DoF using the in-vivo bone pin data from Benoit et al.'s study(Benoit et al., 2006). Knee motions were compared during gait between skin marker derived kinematics and those of a model whose knee joint ranges of motion were constrained within the physiological range measured in vivo. It is hypothesized that implementing realistic yet somewhat flexible ranges of motion may yield kinematic and kinetic results more reflective of in-vivo bone motions as well as allow subject variability and additional model flexibility.

METHODOLOGY

Musculoskeletal Model Definition and Modification

OpenSim (OpenSim 3.2, simtk.org, Simbios, National NIH Center for Biomedical Computing, USA), an open-source modeling and simulation platform, and MatLab 2013a (The Mathworks, US) were used to scale the musculoskeletal models described below and calculate joint kinematics and kinetics.

A modified version of Xu et al.’s musculoskeletal model was used for its multi-DoF knee joint. It includes 56 muscles 29 DoFs overall (Xu, 2013; Xu et al., 2014). The knee joint, defined using the tibia's position in relation to the femur segment, has 4 DoFs with loose constraints: flexion/extension from -120 to 10^{o}, internal/external rotation (-45 and 30^{o}), abduction/adduction (+/-15^{o}), and medial/lateral translation (+/-2cm). The other DoFs are functions of the flexion/extension angle (Xu et al., 2014; Yamaguchi & Zajac, 1989). The model was modified to have more knee DoFs for this study. The patella’s definition was modified to follow the femur's position and orientation rather than the tibia's using the current Xu model and studies by Yamaguchi et al. and Coughlin et al. as references(Coughlin et al., 2003; Xu et al., 2014; Yamaguchi & Zajac, 1989). In the original 4DoF model, this trajectory is not changed in either case. However, when the two remaining prescribed DoFs were released, this change proved to be more relevant.

<u>Development of Bone-Pin-Data-Based Model of Knee Kinematic Constraints</u>

Bone pin data from Benoit et al. 2006 were processed for 3 to 5 motion capture trials each of walking, hopping and cutting motions from each of the 6 healthy young adult male participants (Benoit et al., 2006). Rotations and translations at the knee joint were obtained from transformations of marker cluster positions mounted on bone pins inserted into the lateral aspect of the femur and tibia into the knee's local coordinate system (Benoit et al., 2006, 2007). This data was then processed to create boundary envelopes for each non-principal DoF plotted against knee flexion angle to be used as the allowed ranges of motion for the model's constrained knee DoFs. As only flexion/extension of the knee is tracked reliably with skin mounted markers, experimental motion capture data can be used as an input to identify corresponding ranges of motion for the other DoFs.

For each individual participant and each of the three types of motions, the mean and 95% confidence interval (CI) of the 3-5 time normalized trials were obtained for each rotation and translation. The first and last 10 frames (of 100) were trimmed due to skewed kinematics as a result of some of the participant stepping into and out of the capture volume during data collection.

The calculated means and CIs for each participant were averaged between all participants for each motion type. Each final DoF average +/- CI was plotted in terms of flexion/extension angle for gait, hop and cut motions. An envelope of the maximum and minimum values over the range of flexion/extension angle was then obtained. The envelopes were shifted to be at zero position at full leg extension (0^{o} flexion; Figure 1.1). Kinematic constraints beyond bone pin experimental data were estimated by extending the envelope by hand following the curve shapes.

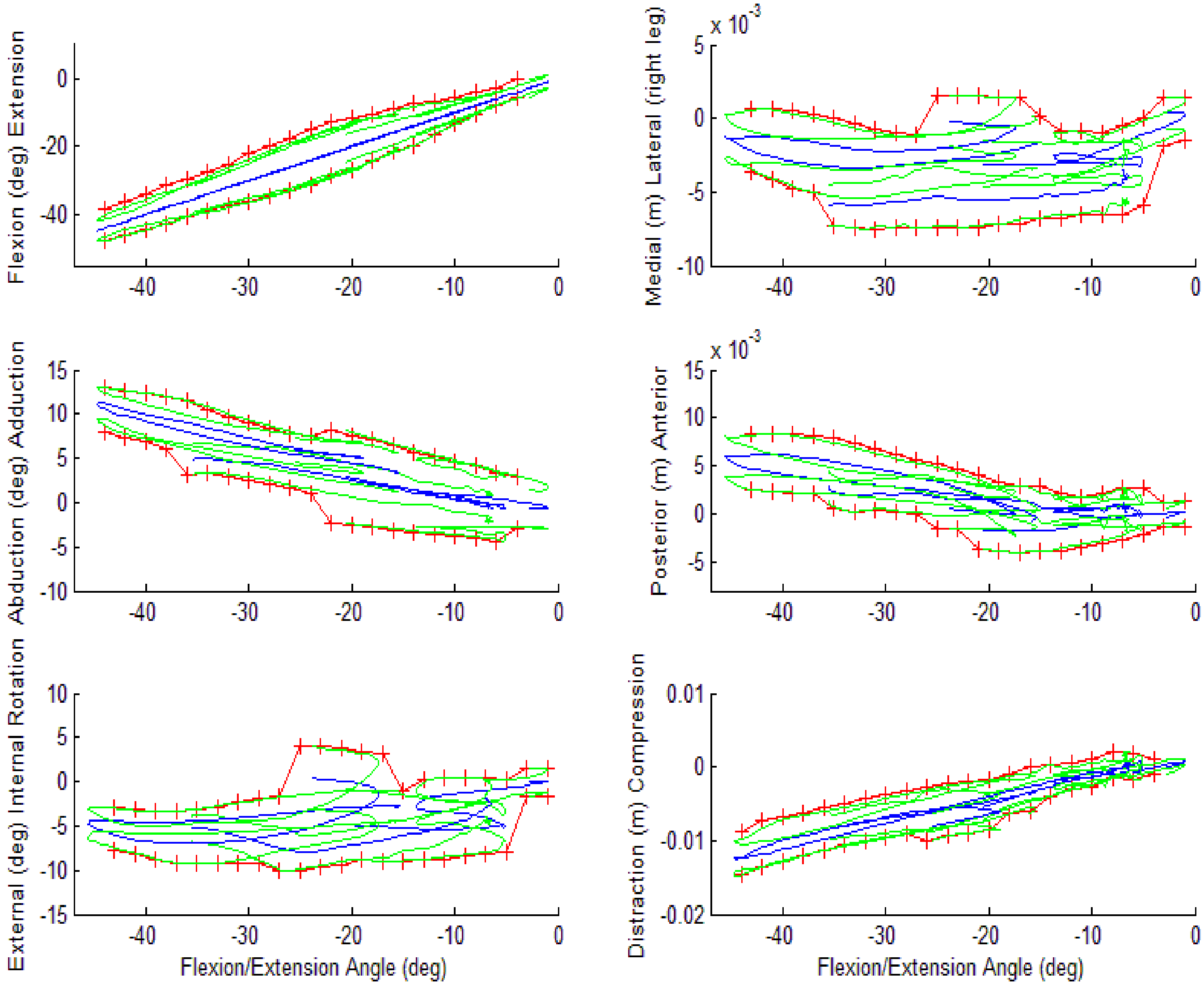

Figure 1.1: Allowed ranges of motion for each DoF at the knee joint (tibia w.r.t femur). Solid blue lines show average values for each motion type (gait, hop or cut) for the 6 subject in Benoit et al. 2006's study. Green lines show 95% confidence intervals for each motion type. Red solid line with + symbols show the final maximum and minimum motion envelopes. Flexion, abduction, and external rotations as well as medial, posterior and distraction translations are noted with negative values.

<u>Data Collection</u>

Three gait trials at a self-selected pace each from 5 healthy young adult males with no significant history of lower limb injuries (mean age, weight and height 24±1.9yr, 80.8±9.1kg and

177.3±8.1cm respectively) were collected and time normalized between two consecutive right heel strikes using a 10-camera motion capture system (Nexus 1.8.3, Vicon Motion Systems ltd, UK). Fifty-two passive reflective markers were placed on subjects using a combined Plug-in-Gait and cluster model (Figure 5). Marker trajectories were sampled at 200 Hz while kinetics were sampled at 1000Hz (Bertec, USA). Motion and force data were filtered with a 4th order zero lag Butterworth filter with a cut-off frequency of 10Hz and exported in .c3d format for post-processing. The data collection protocol was approved by the University of Ottawa Ethics Review Board and informed consent was provided by all subjects.

Scaling and Inverse Kinematics

The musculoskeletal model was dimensionally scaled using static motion trials, the subject's height and his weight. OpenSim 3.2 functions calculated inverse kinematics and dynamics using the following four model definition conditions to describe knee joint kinematics:

1. A 4DoF knee model with 2 prescribed DoFs (distal/proximal and anterior/posterior translations) without bone pin range of motion constraints ("*4DoF"*).
2. A 5DoF knee musculoskeletal model with 1 prescribed DoF (distal/proximal translation) without bone pin range of motion constraints ("*5DoF"*).
3. A 5 DoF knee model with 1 prescribed DoF (distal/proximal translation), where 4 of the unprescribed DoFs (excluding flexion/extension) were constrained by bone pin ranges of motion ("*5DoFb"*).
4. A 6 DoF knee model with no prescribed DoFs and 5 DoFs (excluding flexion/extension) constrained by bone pin ranges of motion ("*6DoFb"*).

In the bone pin constrained model conditions, at each time point during inverse kinematics calculations, the allowed ranges of motion for the relevant DoFs were determined from Figure 1.1 based on knee flexion angles and updated within the model's script.

Statistical Analysis

All trials were time normalized from right heel strike to right heel strike and the resulting kinematics (joint angles and translations) and kinetics (joint moments and forces) of the hip, knee and ankle joint of each subject's three trials were then ensemble averaged. Means and standard deviations across subjects were then calculated to have four curves (mean and standard deviation) for each DoF representing each model condition for graphical representation.

One-way ANOVA tests using statistical parametric mapping (SPM) (Pataky, 2010, 2012; Pataky, Varenterghem, & Robinson, 2015) over the duration of the gait trials were run to compare each model condition as the repeated measure. Where significant differences were found, post-hoc comparisons were carried out by doing multiple two-tailed t-tests using a Bonferroni corrected critical p-value to identify which conditions were significantly different from each other and at which time points during the gait cycle.

RESULTS

Kinematic results of the model conditions without bone pin constraints vary widely, especially in medial/lateral and posterior/anterior translation as well as internal/external rotation (see Figure 1.2 for a representative subject). For example, the medial lateral translations estimated with the 4 and 5DoF models fall consistently outside the constrained range from 60-18 degree of knee flexion. As well, in the "4DoF" model condition, 2 of the DoFs are prescribed (anterior/posterior translation and distal/proximal translation) when only distal/proximal translations are prescribed in the "5DoF" and "5DoFb" model conditions. These prescribed motions fall close to the bone pin boundaries and show similar trends in relation to knee flexion angle (anterior/posterior translation and distal/proximal translation).

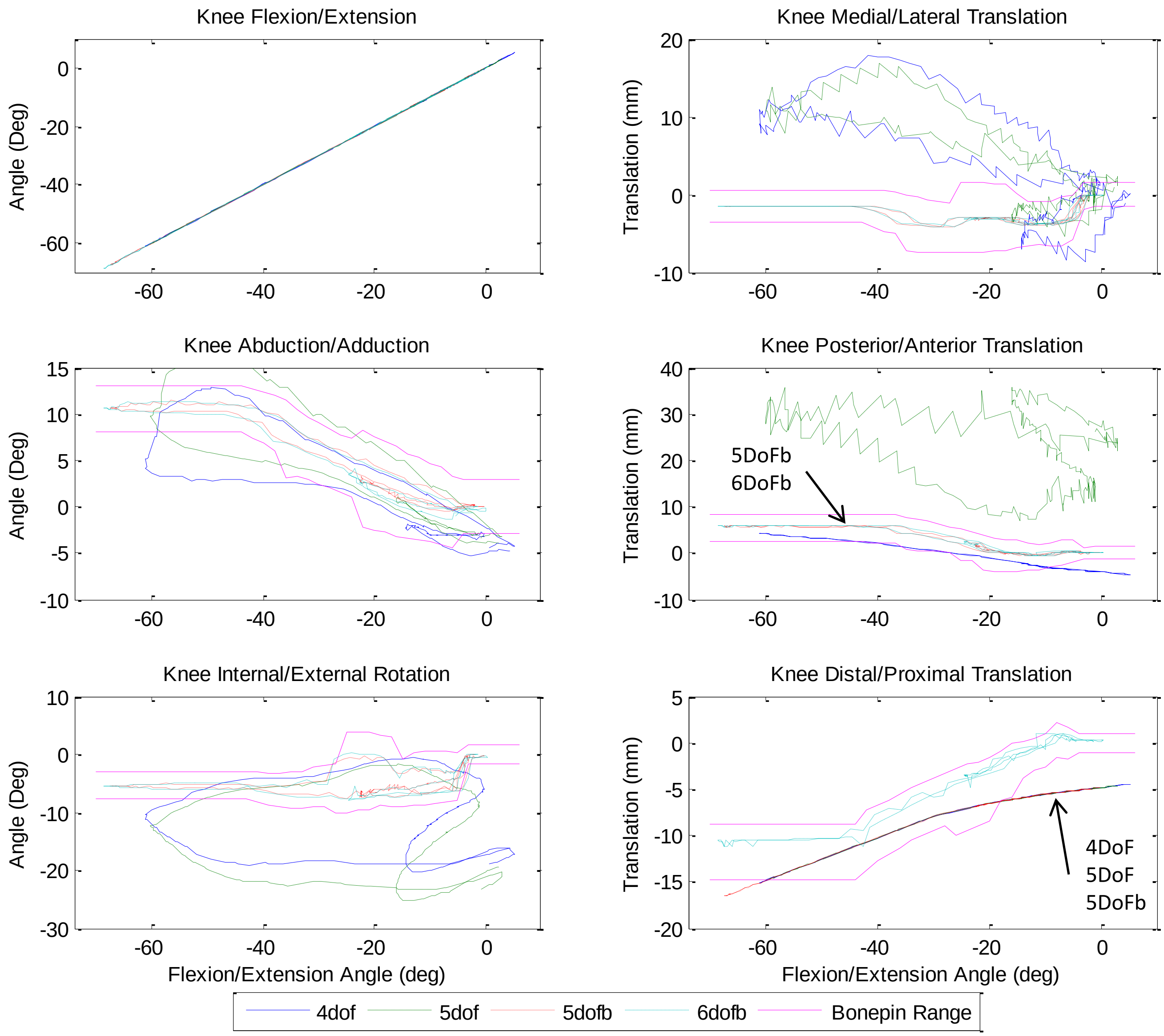

Figure 1.2: Knee joint kinematics of one gait trial from a typical subject in terms of joint flexion/extension angle. Solid blue line is for the 4 DoFs with 2 prescribed. Dashed green line shows the 5 free DoF with 1 prescribed DoF model. Dotted red line shows 5 DoF model with 1 free and 4 constrained by bone pin ranges, and 1 prescribed. Dashed turquoise line shows 6Dof model with 1 free DoF and 5 constrained by bone pin ranges. Magenta solid lines show bone pin ranges for each DoF. For posterior/anterior translation, the 4DoF model is prescribed. For distal/proximal translation, models with 4 and 5DoFs are prescribed and therefore show a smooth line.

ANOVA tests from the SPM analysis indicate significant differences ($p<0.05$) in kinematics at certain time instances for most DoFs as illustrated in Figure 1.3. Significant differences between model conditions were most notable at the knee joint where bone pin constraints were introduced. Knee anterior/posterior translations determined by skin mounted markers (5DoF) varied widely from those resulting from the use of bone pin constraints as well as prescribed motion functions. Knee rotations and medial/lateral translations were also visibly and statistically very different when using skin markers (4DoF and 5DoF) compared to bone pin constrained motions (5DoFb and 6DoFb). Hip and ankle kinematics were affected by the addition of bone pin derived changes at the knee joint but to a lesser extent. These results suggest skin markers are not reliable in determining actual knee joint motion and that the addition of in-vivo experimental bone pin constraints to kinematics calculations may be a way to improve physiological realism of musculoskeletal models.

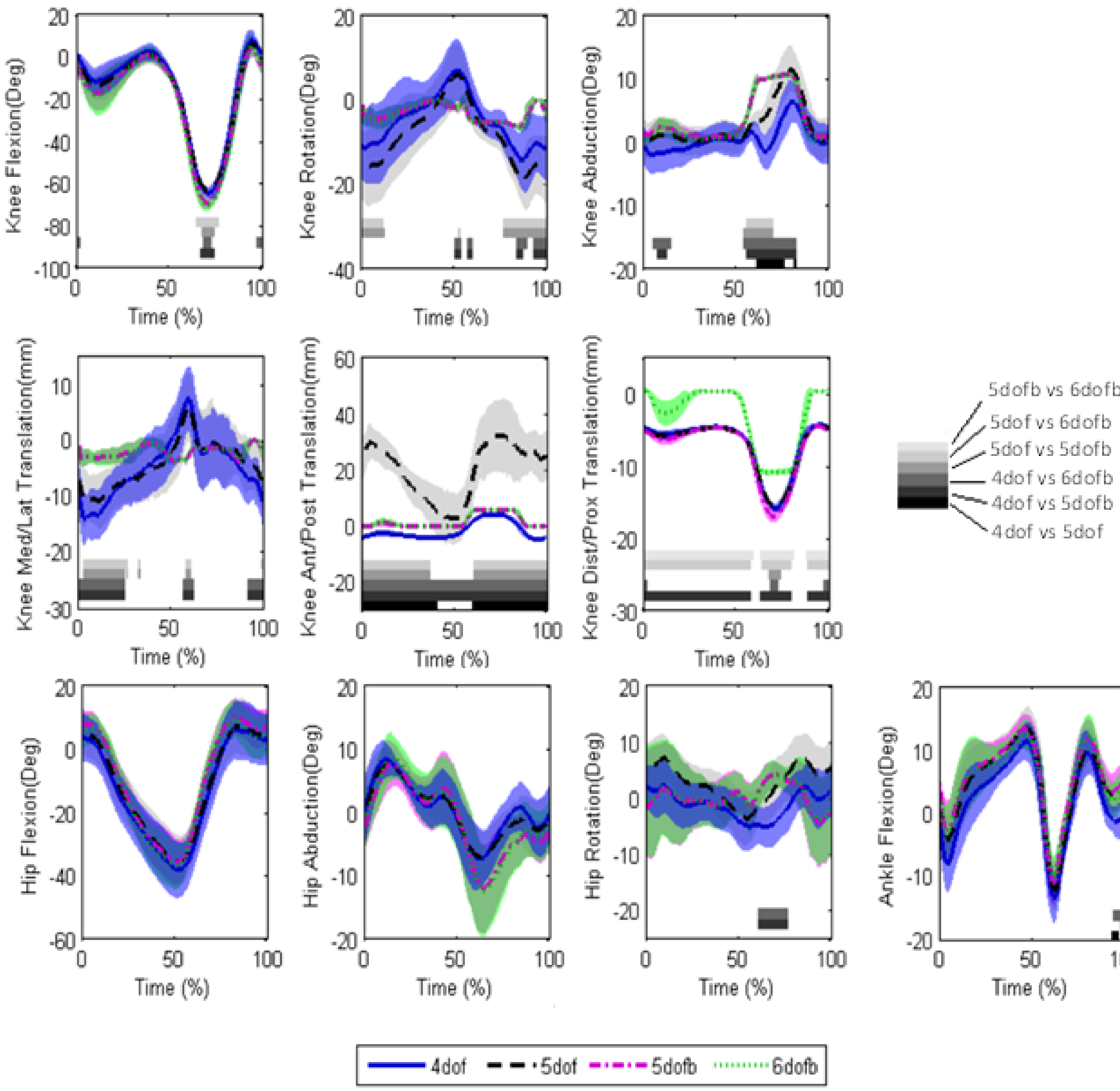

Figure 1.3: Hip, knee and ankle joint kinematics means over all trials and all subjects with a standard deviation cloud for each of the four model conditions for one stride. Blue solid line is for the 4 free DoFs with 2 prescribed. Dashed black line shows the 5 free DoF with 1 prescribed DoF model. Dash-dot pink line shows 5 DoF model with 1 free and 4 constrained by bone pin ranges, and 1 prescribed. Dotted green line shows 6Dof model with 1 free DoF and 5 constrained by bone pin ranges. For posterior/anterior translation, the 4DoF model is prescribed. For distal/proximal translation, models with 4 and 5DoFs are prescribed and therefore show smooth lines. Shaded rectangles on the x-axis show incidences of significant difference results between at least 2 model conditions ($p<0.05$) after one-way ANOVA and SPM-Bonferroni correction.

Important changes in the ranges of motion of the knee joint were observed with the addition of bone pin derived constraints compared to those determined from skin mounted markers. This is especially notable for the internal/external rotation (5DoFb - 6.1^o and 6DoFb - 6.5^o versus 4DoF - 21.2^o and 5DoF - 24.7^o), medial/lateral translation (5DoFb and 6DoFb - both 0.4cm versus 4DoF - 2.1cm and 5DoF - 1.7cm) as well as anterior/posterior translation (5DoFb and 6DoFb both at 0.6cm versus 5DoF - 3.1cm). Prescribing motion also had an impact compared to skin marker derived range of motion for knee anterior/posterior translation (4DoF - 0.9cm versus 5DoF 3.1cm) (Table 1.1).

Table 1.1: Mean amplitude of motion for all lower limb DoFs between model conditions.

	4 DoF	**5 DoF**	**5 DoFb**	**6DoFb**
Hip Flexion(^{o})	44.0	42.6	45.9	46.4
Hip Abduction(^{o})	15.5	14.6	19.5	21.1
Hip Internal/External Rotation(^{o})	7.4	10.6	8.6	8.2
Knee Flexion(^{o})	72.5	69.8	73.0	75.1
Knee Internal/External Rotation(^{o})	21.2	24.7	6.1	6.5
Knee Abduction(^{o})	8.4	11.4	10.0	10.2
Knee Anterior/Posterior Translation(cm)	0.9	3.1	0.6	0.6
Knee Distal/Proximal Translation(cm)	1.2	1,1	1,2	1,1
Knee Medial/Lateral Translation(cm)	2,1	1,7	0.4	0.4
Ankle Flexion(^{o})	24.7	25.6	24.5	22.8

Joint reaction moments and forces for each of the DoFs of the hip, knee and ankle joints are shown in Figure 1.4. Results showed few significant differences ($p<0.05$) although some were observed for knee internal/external rotation and knee abduction/adduction. Hip abduction was also affected.

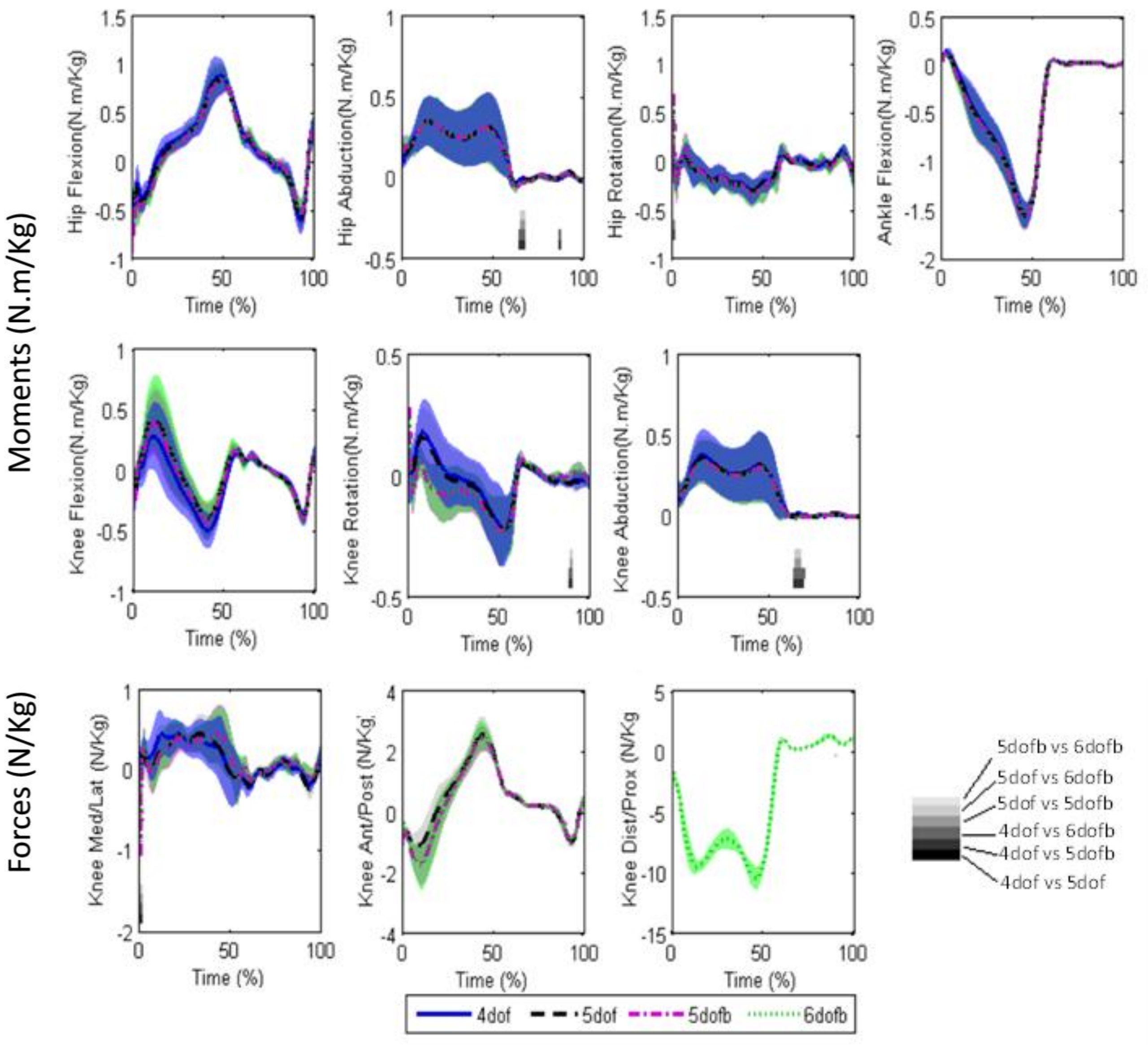

Figure 1.4: Bodyweight normalized hip, knee and ankle joint torques (Nm/Kg) or forces (N/Kg) means over all trials and all subjects with a standard deviation cloud for each of the four model conditions from right heel strike to next right heel strike. Solid blue line is for the 4 free DoFs with 2 prescribed. Dashed black line shows the 5 free DoF with 1 prescribed DoF model. Dash-dot pink line shows 5 DoF model with 1 free and 4 constrained by bone pin ranges, and 1 prescribed. Dotted green line shows 6Dof model with 1 free DoF and 5 constrained by bone pin ranges. Forces for prescribed motions are not plotted (anterior/posterior and distal/proximal translation forces). Shaded rectangles on the x-axis show incidences of significant difference results between at least 2 model conditions ($p<0.05$) after one-way ANOVA and SPM-Bonferroni correction.

DISCUSSION

This study used the in vivo bone-pin derived tibio-femoral motions of six healthy male participants (Benoit et al., 2006) to create physiological experimentally based knee joint bone motion boundaries. These boundaries were applied within a musculoskeletal modeling framework (OpenSim) to guide musculoskeletal model scaling and inverse kinematics calculations on gait trials from 5 new subjects. The purpose of adding DoF motion constraints was to provide physiological ranges of motion rather than absolute values to guide the system's resolution, as well as minimize errors introduced by soft tissue artifact created by skin mounted marker tracking.

As expected, introducing bone pin derived constraints resulted in smaller ranges of motion especially notable in the internal/external knee rotation (from 24.7^o to 6.1^o) as well as knee anterior/posterior (3.1cm to 0.6cm) and medial/lateral translation (2.1cm to 0.4cm; Figure 1.3, table 1.1). More specifically, unconstrained knee internal/external rotation and medial/lateral translation for the 4 and 5DoF model conditions showed large ranges of motion (4DoF: 21.2^o and 2.1cm, 5DoF: 24.7^o and 1.7cm respectively) during the gait cycle and were significantly different from the bone pin constrained ranges (5DoFb: 6.1^o and 0.4cm, 6DoFb: 6.5^o and 0.4cm respectively). Overall, the common bone pin constrained DoFs in both 5DoFb and 6DoFb model conditions showed very similar values over the gait cycle.

Soft tissue artifact present in motion capture has been shown in numerous studies to affect segment kinematics calculations (Andersen et al., 2010; Benoit et al., 2006; Gao & Zheng, 2010; Li et al., 2012). Large translational and rotational errors have been observed, more so at the thigh level than the lower leg, in the range of a few centimeters and more than 15 degrees respectively (Boeth, 2013; Leardini et al., 2005). When looking at knee joint flexion, errors of a few degrees can seem small in comparison to the magnitude of the motion. However, when comparing these errors to other DoFs at the knee where movements are proportionally much smaller, these errors become considerable (Benoit et al., 2006; Boeth, 2013; Leardini et al., 2005; Reinschmidt et al., 1997; Stagni, Fantozzi, Cappello, & Leardini, 2005). By definition, including these errors as inputs will lead to erroneous assumptions about joint motions and these errors will be propagated throughout the model.

Kinematic results for hip, knee and ankle flexion compared well with values observed in the literature in studies using motion capture with skin mounted markers (Kadaba et al., 1989; Kadaba, Ramakrishnan, & Wootten, 1990) as well as those using bone pin methodologies (Benoit et al., 2007; Lafortune, Cavanagh, Sommer, & Kalenak, 1992). This is consistent with observations from (Benoit et al., 2006; Boeth, 2013; Leardini et al., 2005; Reinschmidt et al., 1997; Stagni et al., 2005) showing that flexion/extension motions are typically well described when using reflective skin mounted markers to evaluate joint kinematics. When calculating inverse kinematics for the four model conditions, we found that there were no significant differences for hip flexion and for the large part of knee and ankle flexion (Figure 1.3). The differences that were observed are somewhat small when compared to the magnitude of motion: 6.8% or approximately 5^o of variation at the knee between bone pin constrained and unconstrained conditions over a range of about 73^o, and up to 20% or approximately 5^o, at the ankle between the unconstrained 4DoF model condition and the other three over a total range of about 25^o. These differences however could be the determining factor between clearing an obstacle on the floor and tripping resulting in a fall or loss of balance for example. For example, using Winter's data of a 180cm male (Winter 2004) and the gait kinematics and 1.29cm foot clearance during the oscillation phase as reported by Winter (1992), a 5^o change in ankle flexion angle would be enough (>1.29cm) to cause a trip. Thus the changes prescribed by our in vivo model are of clinical relevance.

Knee abduction results showed significant differences ($p<0.05$) between model conditions with and without bone pin constraints, although curve shapes were generally similar and not overly variable within themselves (Figure 1.3). In contrast, knee internal/external rotations were less consistent and showed striking differences between constrained and unconstrained model conditions (Figure 1.3). The modification of the knee joint's DoFs also had an impact on hip internal/external rotation. These results suggest that introducing knee joint kinematic constraints had some effect on the surrounding joints in addition to those of the knee joint, underlining the importance of creating a realistic musculoskeletal model in as many components as possible as all parts of the model interact with one another.

Anterior/posterior translation was significantly different (up to 3cm; figure 1.3) in the 5DoF model condition when compared to the other models at almost all time points1. It is in the 5DoF model condition that motion in anterior/posterior translation is not prescribed by a function nor is it constrained by bone pin envelopes but follows skin markers to determine its kinematics.

In the case of distal/proximal translation, curve shapes followed the same trends between the four model conditions, although the bone pin constrained 6DoF model showed a distal translation shift of approximately 5mm over the course of the gait cycle. A reason for this may be explained by the modified femur and tibia segment origin definitions to accommodate this additional un-prescribed DoF and the scaling protocol in OpenSim. This observation can also be expected based on Figure 1.2, where prescribed motion curves for distal/proximal translations are shifted slightly towards negative values from the bone pin interval definitions.

The medial/lateral translation DoF in the original 4DoF model used in this study is guided by skin mounted markers and is not prescribed, as opposed to the other two translations. The addition of bone pin constraints had a clear and significant effect on this DoF throughout the gait cycle, notably in the first 25%, near the 50% time point and at the end of the gait cycle, showing differences on the scale of 15mm.

Studies such as that of (Gao & Zheng, 2010) that rely on skin mounted markers, even in complex arrangements, to determine the smaller magnitude DoFs show translations from 1.5 to 3.5cm, which are large considering the size of the femoral condyles and tibial plateau, and when compared to in vivo results (Benoit et al., 2006; Lafortune et al., 1992; Reinschmidt et al., 1997). These differences underline the presence of soft tissue artifact in motion capture. Before accepting or using such results, they should be considered in terms of other tissues in the knee joint such as ligaments and their capacity to stretch and deform to such lengths without damage. For example, Butler et al. (Butler & Guan, 1992; Butler, Kay, & Stouffer, 1986) and Zavatski et al. (Zavatsky & Wright, 2001) reported that, depending on knee flexion angle, anterior tibial translations of as little as 6.65mm caused rupture of at least part of the ACL. Results from the 5DoF model in this study (Figure 1.3) would therefore imply an ACL rupture from excessive anterior translation during normal walking. The use of bone pin derived constraints maintained more reasonable translation values.

Although inverse kinematics differences between model conditions were easily observable, hip, knee and ankle moments and forces were not as pronounced (Figure 1.4). Torque results for hip, knee and ankle flexion from the model conditions without bone pins compare well with other studies (Kadaba et al., 1989; Lee & Hidler, 2008; Ren, Jones, & Howard, 2008) as may be expected since they are calculated in much the same way with similar gait data. The addition of bone pin constraints did not create many significant differences at the joint torque level (Figure 1.4) . Hip and knee rotation and abduction moment profiles from the 4 model conditions are also similar in shape to literature values although magnitudes varied (Lee & Hidler, 2008; Ren et al., 2008). The lack of significant differences may be due to small sample sizes, normalization methods and the inherent variability typical of joint moment calculations we observed.

Anterior/posterior forces, distal/proximal forces and medial/lateral forces curve shapes and magnitude of results are also similarly represented in (Kim et al., 2009; Ren et al., 2008). These results suggest that although kinematics are improved using bone pin constraints, knee joint torques are less affected by these changes after averaging of trials. Kinematic changes are observed more significantly in the secondary DoFs at the knee and torques are also respectively smaller in magnitude in these types of motions. The change in these secondary kinematics may not have been remarkable enough to create large changes in muscle moment arms and thus joint torques.

There are a few limitations in this study that must be noted. Bone pin data were collected from healthy young males and therefore the derived ranges of motion are representative of this population. The experimental data also only reflects values observed between 0-45^{o} of knee flexion. Beyond this range of knee flexion, bone pin boundaries were approximated, although final kinematic results remained similar to those of other studies. The bone pin sample size was also small (6 participants) and increasing this group size may reveal different ranges of bone motion. These may also be different in female populations or within those with various knee joint pathologies or different ages. The bone pin study could be repeated in different populations of varying demographics and health conditions. However, this may be difficult from a participant recruitment point of view and for participant health (Boeth, 2013; Ramsey, Wretenberg, Benoit, Lamontagne, & Nemeth, 2003). Despite these limitations, the in-vivo boundaries used here represent the best available data describing knee joint motions over a wide range of dynamic movements and are therefore a significant improvement over current practice. It is clear that relying on skin mounted markers may not be a reliable method in studying 5 of the 6 DoFs of the knee joint.

As with any musculoskeletal model simulation, results will only be as good as the model itself and the quality of the motion capture trial data. Muscle moment arms, muscle sizes and insertion points for example, are generally based on cadaveric studies (Delp et al., 1990; Pandy, 2001; Shelburne, Torry, & Pandy, 2006). Limitations arise from the populations on which these cadaveric studies are done as they are often older individuals who may have muscle atrophy or tissue degeneration (Buchanan, Lloyd, Manal, & Besier, 2005; Buchanan & Shreeve, 1996). These factors will therefore affect model prescribed motions in the DoFs of joints that are not free to move. In the case of this study however, prescribed motions were close to those derived from bone pin boundaries, especially in the anterior/posterior translation DoF.

From a technical standpoint, adding the bone pin constraints to the MatLab-OpenSim API did slow down the inverse kinematics simulation time as the model had to be updated with new boundaries at every time frame of the simulation. This delay was on the time scale of approximately 20 minutes/trial with the bone pin constraints compared to less than a minute/trial when unconstrained using OpenSim 3.2 and MatLab 2013a on a computer with a 3.4GHz processor and 16GB of RAM. In a study requiring many participants with many motion trials, this would considerably increase computation time. Nonetheless, it is a process that can be automated through MatLab programming without much user input. Following testing, visual checking of model scaling and motion was done to verify reasonable results had been calculated for all model conditions.

CONCLUSION

Soft tissue artifact is an important source of kinematic errors in human movement studies. It is important to consider that skin marker tracking is best suited for gross joint movement analysis such as flexion/extension of the knee as the other DoFs are not accurately represented. The methods in this paper describe a process to reduce soft tissue artifact in musculoskeletal modeling of health individuals by the application of boundaries derived from in vivo tibio femoral motions and presented in an easily implemented manner. Constraining joint motions to physiologically relevant ranges allows the resulting simulations to provide more representative joint motions although does not affect resulting joint moments and forces in an equally significant manner at least when looking at gait trials. If biofidelity is the goal of musculoskeletal modeling, this work represents a step in that direction.

REFERENCES

Andersen, M. S., Benoit, D. L., Damsgaard, M., Ramsey, D. K., & Rasmussen, J. (2010). Do Kinematic Models Reduce the Effects of Soft Tissue Artefacts in Skin Marker-Based Motion analysis? An In-Vivo Study of Knee Kinematics. *Journal of Biomechanics*, *43*, 268–273.

Andersen, M. S., Damsgaard, M., Rasmussen, J., Ramsey, D. K., & Benoit, D. L. (2012). A linear soft tissue artefact model for human movement analysis: Proof of concept using in vivo data. *Gait & Posture*, *35*(4), 606–611.

Anderson, F. C., & Pandy, M. G. (2001). Dynamic Optimization of Human Walking. *Journal of Biomechanical Engineering*, *123*.

Arnold, E. M., Ward, S. R., Lieber, R. L., & Delp, S. L. (2010). A Model of the Lower Limb for Analysis of Human Movement. *Annals of Biomedical Engineering*, *38*(2), 269–279.

Benoit, D. L., Damsgaard, M., & Andersen, M. S. (2015). Surface marker cluster translation, rotation, scaling and deformation: Their contribution to soft tissue artefact and impact on knee joint kinematics. *Journal of Biomechanics*, *48*(10).

Benoit, D. L., Ramsey, D. K., Lamontagne, M., Xu, L., Wretenberg, P., & Renstrom, P. (2006). Effect of skin movement artifact on knee kinematics during gait and cutting motions measured in vivo. *Gait & Posture*, *24*, 152–164.

Benoit, D. L., Ramsey, D. K., Lamontagne, M., Xu, L., Wretenberg, P., & Renstrom, P. (2007). In Vivo Knee Kinematics during Gait Reveals New Rotation Profiles and Smaller Translations. *Clinical Orthopaedics and Related Research*, *454*, 81–88.

Boeth, H. (2013). *Evaluation and characterization of knee joint instability in ACL deficient patients* (PhD Thesis). Technical University of Berlin, Germany.

Buchanan, T. S., Lloyd, D. G., Manal, K., & Besier, T. F. (2005). Estimation of Muscle Forces and Joint Moments Using a Forward-Inverse Dynamics Model. *Medicine and Science in Sports & Exercise*.

Buchanan, T. S., & Shreeve, D. A. (1996). An evaluation of optimization techniques for the prediction of muscle activation patterns during isometric tasks. *Journal of Biomechanical Engineering*, *118*.

Butler, D. L., & Guan, Y. (1992). Location-dependent variations in the material properties of the anterior cruciate ligament. *Journal of Biomechanics*, *25*.

Butler, D. L., Kay, M. D., & Stouffer, D. C. (1986). Comparison of material properties in fascicle-bone units from human patellar tendon and knee ligaments. *Journal of Biomechanics, 19*.

Coughlin, K. M., Incavo, S. J., Churchill, D. L., & Beynnon, B. D. (2003). Tibial Axis and Patellar Position Relative to the Femoral Epicondylar Axis During Squatting. *The Journal of Arthroplasty, 18*(8).

Delp, S. L., Loan, P., Hoy, M. G., Zajac, F. E., Topp, E. L., & Rosen, J. M. (1990). An Interactive Graphics-Based Model of the Lower Extremity to Study Orthopaedic Surgical Procedures. *IEEE Transactions on Biomedical Engineering*, *37*(8).

Duprey, S., Cheze, L., & Dumas, R. (2010). Influence of joint constraints on lower limb kinematics estimation from skin markers using global optimization. *Journal of Biomechanics, 43*, 2858–2862.

Fregly, B. J., Besier, T. F., Lloyd, D. G., Delp, S. L., Banks, S. A., Pandy, M. G., & D'Lima, D. D. (2011). Grand Challenge Competition to predict in vivo knee loads. *Journal of Orthopaedic Research*.

Gao, B., & Zheng, N. (2008). Investigation of soft tissue movement during level walking: translations and rotations of skin markers. *Journal of Biomechanics, 41*(15).

Gao, B., & Zheng, N. (2010). Alterations in three-dimensional joint kinematics of anterior cruciate ligament-deficient and -reconstructed knees during walking. *Clinical Biomechanics*, *25*, 222–229.

Gasparutto, X., Sancisi, N., Jacquelin, E., Parenti-Castelli, V., & Dumas, R. (2015). Validation of a multi-body optimization with knee kinematic models including ligament constraints. *Journal of Biomechanics*, *48*, 1141–1146.

Kadaba, M. P., Ramakrishnan, H. K., & Wootten, M. E. (1990). Measurement of lower extremity kinematics during level walking. *Journal of Orthopaedic Research*, *8*, 383–392.

Kadaba, M. P., Ramakrishnan, H. K., Wootten, M. E., Gainey, J., Gorton, G., & Cochran, G. V. B. (1989). Repeatability of kinematic, kinetic and electromyographic data in normal adult gait. *Journal of Orthopaedic Research*, *7*, 849–860.

Kim, H. J., Fernandez, J. W., Akbarshahi, M., Walter, J. P., Fregly, B. J., & Pandy, M. G. (2009). Evaluation of predicted knee-joint muscle forces during gait using and instrumented knee implant. *Journal of Orthopaedic Research*.

Kinney, A. L., Besier, T. F., D'Lima, D. D., & Fregly, B. J. (2013). Update on Grand Challenge competition to predict in vivo knee loads. *Journal of Biomechanical Engineering*, *135*.

Komistek, R. D., Kane, T. R., Mahfouz, M., Ochoa, J. A., & Dennis, D. A. (2005). Knee mechanics: a review of past and present techniques to determine in vivo loads. *Journal of Biomechanics*, *38*, 215–228.

Lafortune, M. A., Cavanagh, P. R., Sommer, H. J., & Kalenak, A. (1992). Three-dimensional kinematics of the human knee during walking. *Journal of Biomechanics*, *25*(4), 347–357.

Leardini, A., Chiari, L., Della Croce, U., & Cappozzo, A. (2005). Human movement analysis using stereophotogrammetry Part 3. Soft tissue artifact assessment and compensation. *Gait & Posture*, *21*, 212–225.

Lee, S. J., & Hidler, J. (2008). Biomechanics of overground vs treadmill walking in healthy individuals. *Journal of Applied Physiology*, *104*(3), 747–755.

Li, K., Zheng, L., Tashman, S., & Zhang, X. (2012). The inaccuracy of surface-measured model-derived tibiofemoral kinematics. *Journal of Biomechanics*, *45*(15), 2719–2723.

Modenese, L., Phillips, A. T. M., & Bull, A. M. J. (2011). An open source lower limb model: Hip joint validation. *Journal of Biomechanics*, *44*(12), 2185–2193.

Pandy, M. G. (2001). Computer modeling and simulation of human movement. *Annual Review of Biomedical Engineering*, *3*, 245–273.

Pataky, T. C. (2010). Generalized n-dimensional biomechanical field analysis using statistical parametric mapping. *Journal of Biomechanics*, *43*, 1976–1982.

Pataky, T. C. (2012). One-Dimensional statistical parametric mapping in Python. *Computer Methods in Biomechanics and Biomedical Engineering*, *15*(3), 295–301.

Pataky, T. C., Varenterghem, J., & Robinson, M. A. (2015). Zero- vs. one-dimensional, parametric vs. non-parametric, and confidence interval vs. hypothesis testing procedures in one-dimensional biomechanical trajectory analysis. *Journal of Biomechanics*, *48*, 1277–1285.

Ramsey, D. K., Wretenberg, P. F., Benoit, D. L., Lamontagne, M., & Nemeth, G. (2003). Methodological concerns using intra-cortical pins to measure tibiofemoral kinematics. *Knee Surgery Sports Traumatology Artrosc*, *11*, 344–349.

Reinbolt, J. A., Schutte, J. F., Fregly, B. J., Koh, B. I., Haftka, R. T., George, A. D., & Mitchell, K. H. (2005). Determination of patient-specific multi-joint kinematic models through two-level optimization. *Journal of Biomechanics*, *38*, 621–626.

Reinschmidt, C., Van Den Bogert, A. J., Nigg, B. M., Lundberg, A., & Murphy, N. (1997). Effect of skin movement on the analysis of skeletal knee joint motion during running. *Journal of Biomechanics*, *30*(7), 729–732.

Ren, L., Jones, R. K., & Howard, D. (2008). Whole body inverse dynamics over a complete gait cycle based only on measured kinematics. *Journal of Biomechanics*, *41*, 2750–2759.

Sasaki, K., & Neptune, R. R. (2010). Individual Muscle Contributions to the Axial Knee Joint Contact Force during Normal Walking. *Journal of Biomechanics*, *43*(14), 2780–2784.

Shelburne, K. B., Torry, M. R., & Pandy, M. G. (2006). Contributions of muscles, ligaments and the ground reaction force to tibiofemoral joint loading during normal gait. *Journal of Orthopaedic Research*.

Stagni, R., Fantozzi, S., Cappello, A., & Leardini, A. (2005). Quantification of soft tissue artefact in motion analysis by combining 3D fluoroscopy and stereophotogrammetry: a study on two subjects. *Clinical Biomechanics*, *20*, 320–329.

Worsley, P., Stokes, M., & Taylor, M. (2011). Predicted knee kinematics and kinetics during functional activities using motion capture and musculoskeletal modelling in healthy older people. *Gait & Posture*, *33*(2), 268–273.

Xu, H. (2013). *Development of a Musculoskeletal Model to Determine Knee Contact Force During Walking on Ballast Using Opensim Simulation*. University of Utah, Utah, United States.

Xu, H., Bloswick, D., & Merryweather, A. (2014). An improved OpenSim gait model with multiple degrees of freedom knee joint and knee ligaments. *Computer Methods in Biomechanics and Biomedical Engineering*.

Yamaguchi, G. T., & Zajac, F. E. (1989). A planar model of the knee joint to characterize the knee extensor mechanism. *Journal of Biomechanics*, *22*(1), 1–10.

Zavatsky, A. B., & Wright, H. J. K. (2001). Injury initiation and progression in the anterior cruciate ligament. *Clinical Biomechanics, 16*, 47–53.

Musculoskeletal Knee Joint Stability Inspired Optimization of Forward-Inverse Dynamics Simulations to Predict Muscle Activations

Brigitte M. Potvin,
University of Ottawa, School of Biomedical Engineering

Dr. Mohammad S. Shourijeh
University of Ottawa, School of Rehabilitation Sciences

Kenneth B. Smale
University of Ottawa, School of Human Kinetics

Dr. Davide Spinello
University of Ottawa, School of Mechanical Engineering

Dr. Daniel L. Benoit
University of Ottawa, School of Human Kinetics and Rehabilitation

ABSTRACT

Musculoskeletal modeling and simulation frameworks show promise in becoming important clinical tools. However, they must be validated before they can be widely used. Calculating muscle activations during motion around the knee joint is an under-determinate problem as the number of muscles involved is considerably larger than the joint's number of degrees of freedom. Therefore the solution of the problem must be found by optimization, adding an appropriate set of constraints to close the system. The true muscle activation strategies implemented by the central nervous system remain unknown. Many studies use optimization functions minimizing metabolic costs although results have shown inadequate accuracy with experimental data. This study used a simlation framework to predict muscle activations in 25 dominant leg muscles over a gait cycle with optimization objective functions inspired by musculoskeletal joint stability (maximization of total muscle activation, minimization of shear knee joint contact loading and maximization of knee joint compression loading) rather than a common efficiency functions (minimization of total muscle activation) using a forward-inverse dynamics simulation framework. EMG data for 8 of the model's muscles were used to compare simulation outputs to experimental data. Results showed that minimizing total muscle activations resulted in the strongest correlations and visual similarities to available experimental electromyographical data, notably for the tibialis anterior muscle (r=0.658 ±0.133). Medial gastrocnemius and soleus were well correlated for this function (r=0.718±0.137 and 0.725±0.095 respectively), for maximization of muscle activation (r=0.731±0.156 and 0.725±0.121 respectively) and minimization of shear loading (r=0.670±0.103 and 0.518±0.406 respectively). Maximizing knee joint compression forces did not show strong correlations. Other muscles did not show significant correlations with available EMG.

Optimization objective functions have an effect on final muscle activation and joint contact loading predictions. Although the joint stability inspired objective functions did not show marked improvements on simulation results, this supports the importance of considering optimization choices carefully in regards to the studied motion and the purposes of a given research question.

KEY WORDS

Musculoskeletal modeling, optimization, objective function, stability, electromyography, simulation framework

BACKGROUND

Musculoskeletal disorders and injuries affect large amounts of individuals, hundreds of thousands in the US only, and have high financial repercussions on the health care system (Frank & Jackson, 1997; Fregly et al., 2011; Mansouri & Reinbolt, 2012; McLean & Van Den Bogert, 2003; Reinbolt, Seth, & Delp, 2011; Roux et al., 2005). A better understanding of how muscles contribute to human movement and joint stability could help alleviate this problem.

Musculoskeletal modeling and computer simulations have become increasingly attractive in this regard (Delp et al., 1990; Fregly et al., 2011; Hicks, Uchida, Seth, Rajagopal, & Delp, 2015; Kinney, Besier, D'Lima, & Fregly, 2013; Komistek, Kane, Mahfouz, Ochoa, & Dennis, 2005; Reinbolt et al., 2005). As of yet however, models have not been validated sufficiently to be used reliably in health care environments (Hicks et al., 2015; Kinney et al., 2013), with one difficulty in validating muscle forces from these models related to making direct measurements on muscle fibers inside a live subject (Buchanan & Shreeve, 1996; Erdemir, McLean, Herzog, & Van Den Bogert, 2007; Hicks et al., 2015; Kim et al., 2009; Reinbolt et al., 2011). This knowledge however, is of crucial importance in understanding how movement is achieved in healthy and pathological conditions to develop treatment and rehabilitation protocols for various injuries or joint diseases (Delp et al., 1990; Fregly et al., 2011; Hicks et al., 2015; Reinbolt et al., 2005).

In knee joint modeling, there are many muscles to consider and considerably fewer joint degrees of freedom (and therefore governing equations) to solve for muscle activation profiles. Optimization methods are therefore employed with objective functions to guide the resolution of the systems in determining muscle activations, forces and joint contact loading (Buchanan & Shreeve, 1996; Crowninshield & Brand, 1981; Dul, Johnson, Shiavi, & Townsend, 1984; Kaufman, An, Litchy, & Chao, 1991; Pedotti, Krishman, & Stark, 1978). Choosing appropriate objective functions is difficult as results are sensitive to these choices, especially when faced with few constraints (Ackermann & van den Bogert, 2010; Buchanan, Lloyd, Manal, & Besier, 2004; Lin, Walter, Banks, Pandy, & Gregly, 2010; Sanford, Williams, Zucker-Levin, & Mihalko, 2013; Shourijeh & McPhee, 2013). Various functions have been used in recent models with the assumption that the human musculoskeletal system works to maximize efficiency such as minimizing total muscle activations (Kaufman et al., 1991; Kim et al., 2009; Shourijeh & McPhee, 2013; Walter et al., 2013), forces (Buchanan & Shreeve, 1996; Pedotti et al., 1978), fatigue (Buchanan & Shreeve, 1996; Cao, Inoue, Liu, & Shibata, 2013; Dul et al., 1984), or metabolic energy expenditure (Anderson & Pandy, 2001; Shourijeh & McPhee, 2013). The validity of these functions has been questioned as experimental data often poorly matches with predicted muscle activity or models require extensive subject specific model customization (Buchanan & Shreeve, 1996; Herzog & Leonard, 1991; Winby, Lloyd, Besier, & Kirk, 2009).

Numerous biomechanical and neuromuscular control studies have investigated the contributions of different structures of the knee joint (bones, ligaments, muscles) and muscle activation patterns in altering the stability and loading of a healthy or damaged joint to prevent or treat injuries and diseases and thus improving people's mobility in daily activities and sports (Baratta et al., 1988; Boeth, 2013; Doorenbosch & Harlaar, 2003; Giesl & Wagner, 2007; Lloyd & Buchanan, 1996; Maitland, Ajemian, & Suter, 1997; Schmitt & Rudolph, 2008; Senavongse et al., 2003; Solomonow et al., 1987; Sturnieks, Besier, & Lloyd, 2011). One of the challenges here, however, lies in the definition of the term *stability* and how it is applied in these studies (Hasan, 2005; Senavongse et al., 2003).

Studies show that co-contraction, the simultaneous activation of antagonistic muscles, plays an important role in supporting varus/valgus and flexion/extension moments, thus enhancing joint stability by increasing joint stiffness and protecting ligaments (Ambegaonkar et al., 2011; Doorenbosch & Harlaar, 2003; Lloyd & Buchanan, 1996, 2001; Maitland et al., 1997; Milner, 2002; Schipplein & Andriacchi, 1991; Schmitt & Rudolph, 2008; Senavongse et al., 2003; Shelburne, Torry, & Pandy, 2006; Solomonow et al., 1987; Sturnieks et al., 2011; Winby et al., 2009). Increases in synergistic muscle activity could help stiffen and stabilize a joint, but would consequently elevate compression loads between articular surfaces (Schipplein & Andriacchi, 1991) while also being a metabolically inefficient mechanism (Milner, 2002). This strategy could compensate joint stability when the passive mechanical properties of surrounding tissues are insufficient in accomplishing this task (Riemann & Lephart, 2002). These increases in co-activations and resulting increases in joint contact loading have been hypothesized to lead to damage of the articular surfaces (Lloyd & Buchanan, 1996; Schmitt & Rudolph, 2008; Winby et al., 2009; Wu, Burr, Boyd, & Radin, 1990), while cellular/tissue level studies have shown that physiological levels of dynamic loading of cartilage promote tissue health and integrity, although type and duration of loading could have negative effects (Lee, Grad, Wimmer, & Alini, 2006).

In musculoskeletal modeling, studies have used principles of mechanical control theories to describe muscle contributions in joint stabilization in using equilibrium (static with constant muscle activations and joint position) states (Derouin & Potvin, 2005; Giesl, Meisel, Scheurle, & Wagner, 2004; Pel, Spoor, Pool-Goudzwaard, Hoek Van Dijke, & Snijders, 2008; Wagner, Giesl, & Blickhan, 2007).

Considering the potential approaches to stability noted above, we will explore the effect of the objective function of the optimization protocol within a forward/inverse dynamics simulation framework by using as comparison standard the commonly used minimization of total muscle activation function. Different objective functions were defined, inspired by various definitions of musculoskeletal joint stability, and their effects on muscle activation pattern predictions was observed to show if changing the objective of an optimization protocol had an impact on final simulation outputs (muscle activation predictions) and thus should be chosen carefully.

METHODOLOGY

Data Collection:

Gait data from 5 healthy young adult males (mean age, bodyweight and height 24±1.9yr, 80.8±9.1kg and 177.3±8.1cm respectively) were collected and time normalized to two consecutive dominant heel strikes using a 10 camera motion capture system Nexus 1.8.3 (MX-40, Vicon Motion Systems ltd, UK). Fifty two passive marker trajectories, of which 38 described the lower limbs, were positioned using a Plug-in Gait model (Kadaba, Ramakrishnan, & Wootten, 1990) augmented with marker clusters on the pelvis, thigh, shank and foot, then sampled at 200 Hz. Ground reaction force data was sampled at 1000Hz using a Bertec force platform (FP4060-08, Bertec, USA). Trajectories and force plate data were filtered with a 4th order zero lag dual pass Butterworth filter with a cut-off frequency of 10Hz.

Muscle electromyography (EMG) data of the gluteus maximus (GLTMAX), gluteus medius (GLTMED), tensor fascia latae (TFL), rectus femoris (RFEM), vastus medials (VMED), vastus lateralis (VLAT), biceps femoris (BFEM), semitendinosus (STEN), tibialis anterior (TA), medial gastrocnemius (MGAS), lateral gastrocnemius (LGAS) and the soleus (SOL) were recorded from the dominant leg using a Delsys DS-B04 Bagnoli 16 EMG system (Delsys, USA). EMG signals were sampled at 1000 Hz, amplified by a gain of 1000, and band-pass filtered at 20-450 Hz before digital conversion using a 16-bit A/D conversion board (NI PCI 6229, National Instruments Corp., Austin, TX). The signal was then full wave rectified and low-pass filtered with a 4th order zero-lag Butterworth filter with cut-off frequency of 8Hz, chosen by residual analysis and visual observation. Trials were normalized to time and maximum voluntary isometric contraction (MVIC) trials.

Musculoskeletal Model

We adapted a musculoskeletal model based on the work of Xu et al. (Xu, Bloswick, & Merryweather, 2014) and Delp et al (Delp et al., 1990) available in the OpenSim model repository at *https://simtk.org/home/kneeligament* (last visited December 2015). It has 56 muscles (25/leg + 6 abdominals) and 29 degrees of freedom (DoF), specifically 4 at the knee joint (3 rotations and medio/lateral translation) (Xu, 2013; Xu et al., 2014) where the other two DoFs are prescribed functions. Ligaments were omitted from the model's definition and the muscle model used in the original script was updated from the “Thelen2003Muscle” muscle model (Thelen, 2003) to that of the Millard et al.’s model

"Millard2012EquilibriumMusclemodel" (Millard, Uchida, Seth, & Delp, 2013), as is the current OpenSim standard.

Muscles included in both EMG data collection and in the musculoskeletal model were the GLTMAX, GLTMED, TFL, RFEM, BFEM, TA, MGAS and SOL. In the musculoskeletal model, the GLTMAX and GLTMED were represented by three muscle segments each (GLTMAX1, GLTMAX2, GLTMAX3 and GLTMED1, GLTMED2, GLTMED3 respectively) and the BFEM muscle is divided into two muscle segments (BFEMLH - biceps femoris long head, and BFEMSH - biceps femoris short head).

Forward/Inverse Dynamics Simulation Framework

A forward-inverse dynamics (FID) simulation framework was developed within our research team and is illustrated in Figure 2.1. Details of this framework can be found in (Shourijeh & Benoit, 2015; Shourijeh, Smale, Potvin, & Benoit, 2016). The FID method calculates knee joint torques by first scaling a generic sized musculoskeletal model to subject specific marker placement, height and weight using the MatLab-OpenSim API (MatLab 2014a, The Mathworks, USA and OpenSim 3.2 , simtk.org, Simbios, National NIH Center for Biomedical Computing, USA), followed by inverse kinematics (IK) and inverse dynamics (ID) calculations as shown in the right hand side of Figure 2.1. The static optimization (SO) protocol built into OpenSim 3.2 that minimizes overall muscle activations squared was run for each trial to obtain initial muscle activation approximations for the forward dynamics (FD) element of the simulation framework.

FD with prescribed IK motion estimates muscle activations and forces that yield knee joint torques as close as possible to those calculated by the ID method (left hand side of Figure 2.1). Conversion from muscle activation level to muscle force and thus torque with the prescribed kinematics is determined using a Hill-type muscle model built into OpenSim (the Millard2012equilibrium muscle model) that considers activation level, force-length and force velocity muscle relationships as well as models muscle and tendon mechanical properties with parallel and series spring constants. More information on this muscle model can be found on the OpenSim website http://simtk-confluence.stanford.edu/. An optimization protocol is defined to determine the best combination of muscle activation levels with the objective of both minimizing this difference between the two sets of joint torques as well as a physiological objective function.

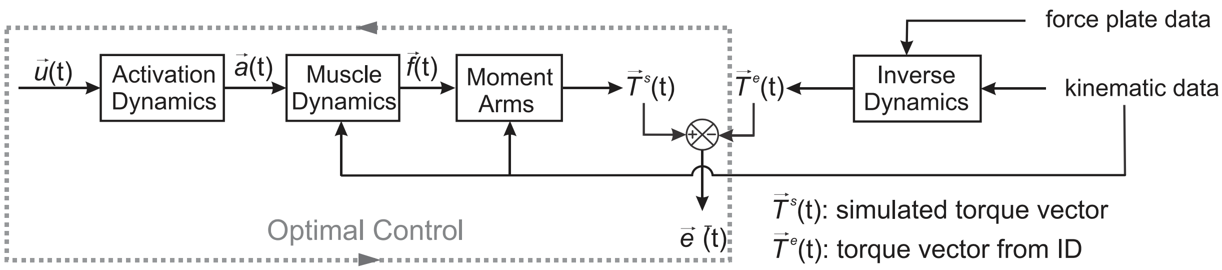

Figure 2.1 : Forward-inverse dynamics simulation framework minimizing joint torque prediction error $e(t)$. Other variables are defined as follows: $u(t)$: muscle excitation, $a(t)$: muscle activation, $f(t)$:tendon-muscle forces, T^S:simulated torque vector, T^e:torque vector from inverse dynamics (ID). Adapted from (Shourijeh & Benoit, 2015; Shourijeh & McPhee, 2014).

Optimization and Objective Function Definitions for Physiological Joint Stability

The mathematical component of the objective function (J_{Tmin}) of the optimization protocol minimizes the torque error (*TE*) normalized to torque magnitude for hip, knee and ankle flexion/extension and rejects combinations of values where predicted normalized muscle activations (*a*) are outside the range of 0 to100% of maximal activation.

$$J_{Tmin} = \min\big(\Sigma(TE)\big) / \left|ID_{Torques}\right|) \qquad \text{(eq1)}$$

A non-physiological mathematical objective is insufficient in providing biologically realistic results as it can yield an almost infinite number of muscle activation possibilities. Therefore biologically inspired functions focused on joint stability were added to the total objective function with an approximate 50/50 weighting to see what impact they had on final muscle activation outputs: minimizing and maximizing the sum of squared muscle activations ($\sum(a_i)^2$), (eq2 and eq3 respectively) maximizing knee joint compression contact loading on the tibia ($\sum F_{compr}$) (eq4) and minimizing knee joint shear contact loading on the tibia ($\sum F_{shear}$) (eq5).

$$J_{Amin} = min\Sigma(a_i)^2 \qquad \text{(eq2)}$$

$$J_{Amax} = \min \frac{1}{\Sigma(a_i)^2} \qquad \text{(eq3)}$$

$$J_{Jmax} = |\min (\frac{1}{\Sigma\left(F_{compr}\right)})| \qquad \text{(eq4)}$$

$$J_{Smin} = |\min\ \Sigma(F_{shear})| \qquad \text{(eq5)}$$

For example, using eq2, the total equation was defined as:

$$\begin{aligned} &Objective\ function\ value \qquad \text{(eq6)} \\ &= \sum_{for\ each\ 25\ muscles} \frac{J_{Amin}}{J_{Amin} + J_{Tmin}} * J_{Tmin} + \frac{J_{Tmin}}{J_{Amin} + J_{Tmin}} * J_{Amin} \\ &+\ (if\ a > 1) * 1e6 + (if\ a < 0) * 1e6 \end{aligned}$$

The optimizations were run with a MatLab 2014a script, using the functions *fmincon* (find minimum of constrained nonlinear multivariable function), *GA* (find minimum of function using a genetic algorithm) and *fminsearchbnd* (find minimum constrained multivariable function using derivative-free method) as described in (Shourijeh & McPhee, 2013; Shourijeh et al., 2016) with the specific parameters found in appendices. The simulation framework divided each motion trial into 50 time steps and optimized muscle activations for the dominant leg's 25 muscles for each step independently.

Data Analysis

For each subject individually, muscle activation patterns predicted from the different objective functions were compared to their respective experimental EMG data using Pearson's correlations (r) and root mean squared error (RMSE) tests for pattern trend and magnitude comparisons respectively. The strength of the correlations was classified as no relation (0.00>0.25), fair (0.25>0.50), moderate to good (0.50>0.75) and good to excellent (>0.75) (Portney & Watkins, 2000). Initial results showed that there was some observed delay between EMG peaks and muscle activation results due to the electrochemical delay between muscle excitation and production of force (Cavanagh & Komi, 1979; Hof, 1997; Hug, Hodges, & Tucker, 2015; Roberts & Gabaldon, 2008) as well as electrode placement (Hug et al., 2015; Van Dieen, Thissen, Van de Ven, & Toussaint, 1991; Wong & Ng, 2006). This delay was of the order of 30-150ms, consistent with literature values (Cavanagh & Komi, 1979; Hof, 1997) and varied between different muscles. Cross-correlation between muscle activations and EMG were therefore calculated and the curves correspondingly shifted in the time domain to remove the effect of the time offset of up to approximately 150ms using MatLab scripting and its *xcorr* function. Predicted muscle activity patterns were also compared to EMG data and simulation results from the literature.

Joint contact loading patterns were qualitatively compared between the predicted results of each physiological objective function, as well as with values found in the literature.

RESULTS

The cross-correlation adjusted activation results from the simulations of each physiological objective function's muscle activation levels were compared to their corresponding EMG channel. Figure 2.2 displays results for minimization of torque error combined with minimization of total muscle activation ($J_{Tmin+Amin}$) and also with maximization of total muscle activation ($J_{Tmin+Amax}$). Figure 2.3 displays results for minimization of torque error combined with maximization of knee joint compression ($J_{Tmin+Jmax}$) and combined with minimization of knee joint shear force ($J_{Tmin+Smin}$), as well as results from OpenSim's SO. Average time shifted correlations with standard deviations between relevant muscles with EMG profiles are detailed in Table 2.2.

Muscle activation patterns (Figure 2.2) indicate good correlation for the TA (r=0.658), MGAS (r=0.718) and SOL (r=0.725) muscles for the $J_{Tmin+Amin}$ objective function. The TA muscle is not well correlated (r=-0.099) in the case of the $J_{Tmin+Amax}$ function although MGAS (r=0.731) and SOL (r=0.725) remain good.

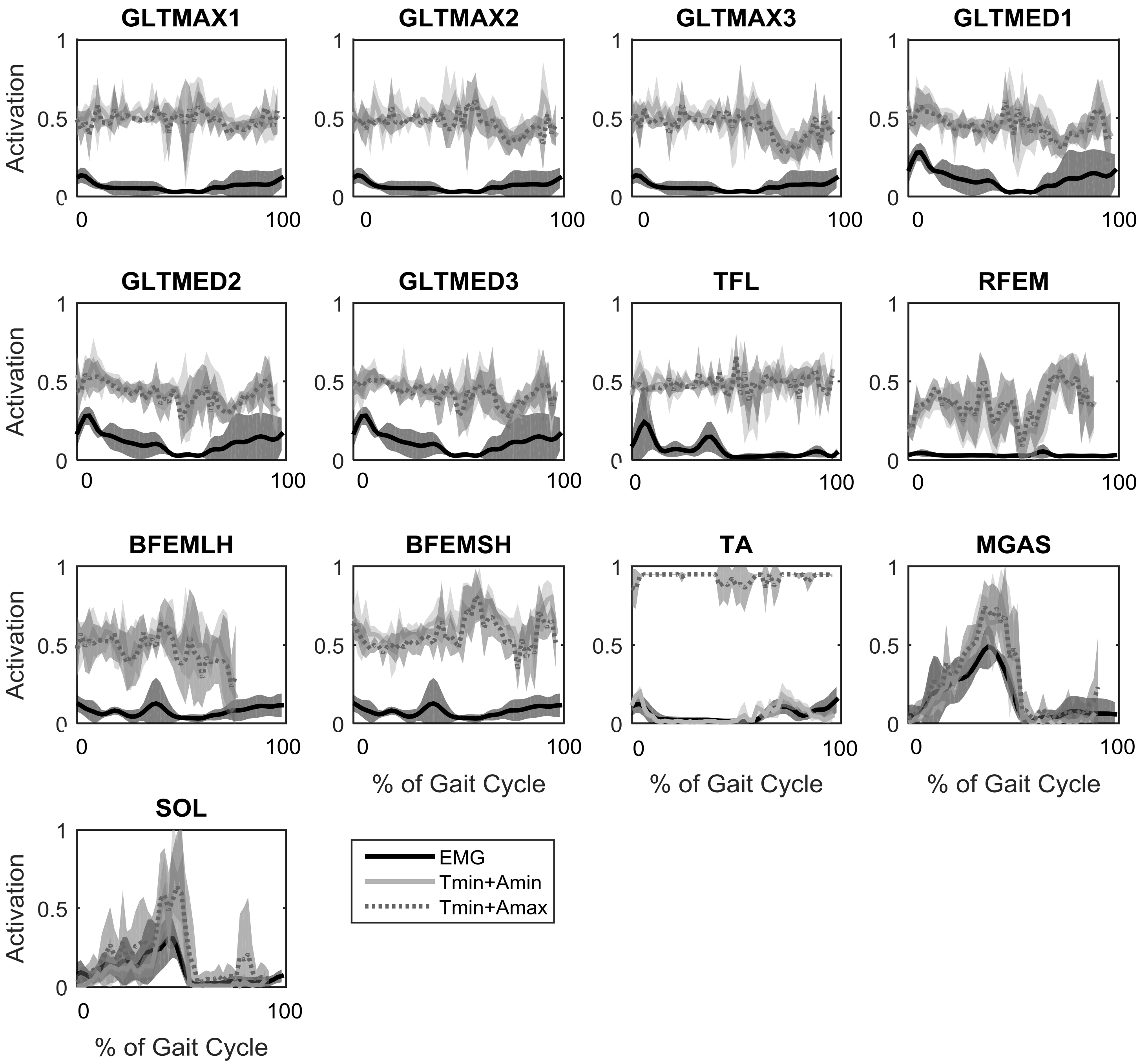

Figure 2.2: Across-subject average muscle activation predictions with standard deviation clouds for muscles with EMG channels and present in the musculoskeletal model following simulations with two of the tested objective functions: minimization of torque error combined with minimization of total muscle activation ($\boldsymbol{T_{min}} + \boldsymbol{A_{min}}$) and also with maximization of total muscle activation ($\boldsymbol{T_{min}} + \boldsymbol{A_{max}}$)).

Similarly to the $J_{Tmin+Amax}$ objective function results, the MGAS (r=0.670) and SOL (r=0.518) for the $J_{Tmin+Smin}$ function, and SO (r=0.796 and 0.772 respectively) all have good correlations (Figure 2.3). However, residual errors in joint torque that the FID framework is meant to minimize was quite high in the case of SO activation predictions and this may indicate technical issues within the OpenSim function. The $J_{Tmin+Jmax}$ did not show particular correlations with any muscle.

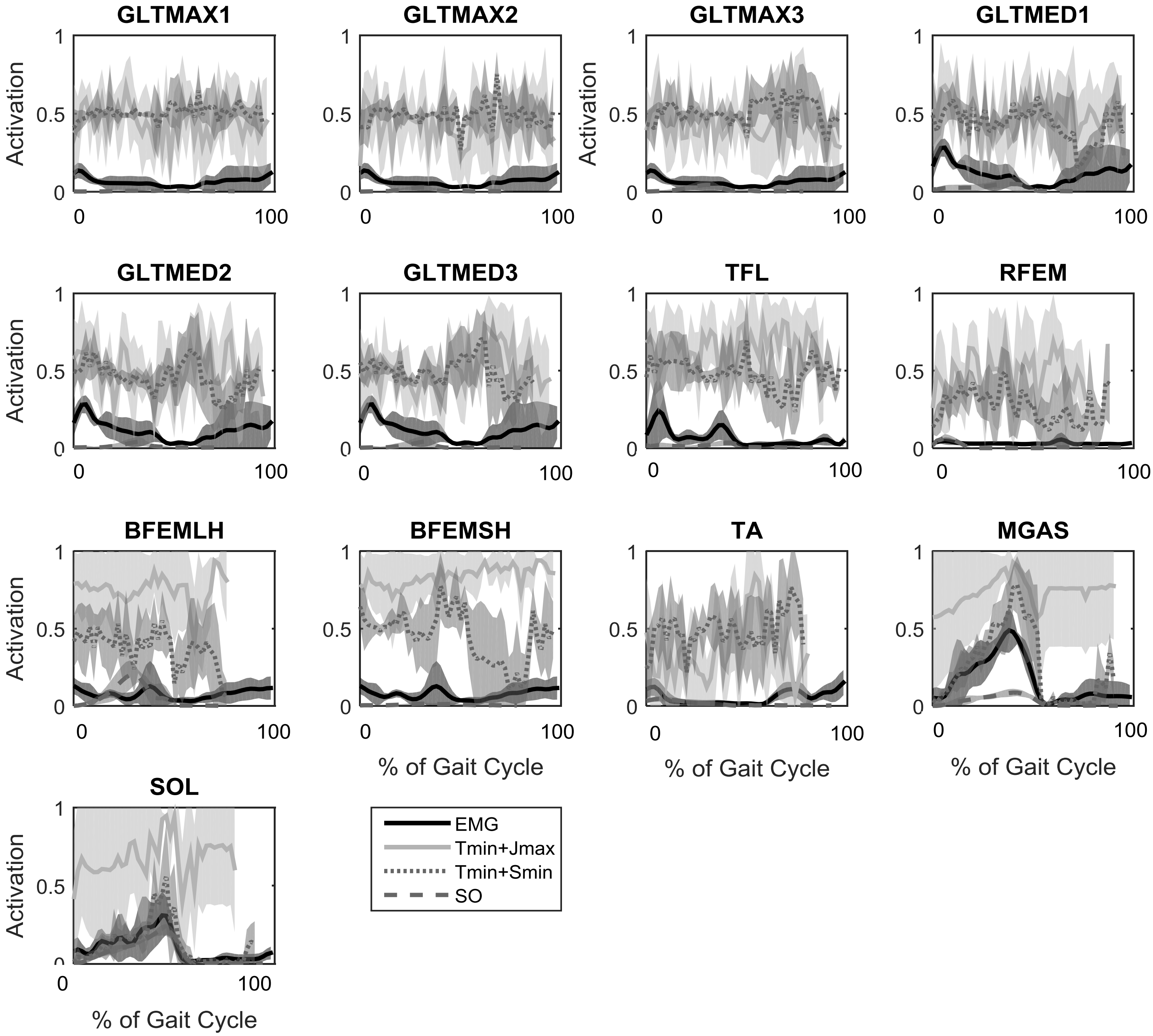

Figure 2.3 : Across-subject average muscle activation predictions with standard deviation clouds for muscles with EMG channels and present in the musculoskeletal model following simulations with three of the tested objective functions: minimization of torque error combined with maximization of knee joint compression ($T_{min} + J_{max}$) and combined with minimization of knee joint shear force ($T_{min} + S_{min}$) as well as results from OpenSim's static optimization process (SO).

Table 2.1 : Across-subject average (+/-std dev) correlations (r) following removal of time offset using cross-correlation between muscle activation predictions and corresponding EMG signal resulting from simulations using the different objective functions.

	$\boldsymbol{T_{min}} + \boldsymbol{A_{min}}$	$\boldsymbol{T_{min}} + \boldsymbol{A_{max}}$	$\boldsymbol{T_{min}} + \boldsymbol{J_{max}}$	$\boldsymbol{T_{min}} + \boldsymbol{S_{min}}$	**SO**
GLTMAX1	-0.010 (0.157)	-0.042 (0.233)	0.027 (0.115)	-0.179 (0.117)	-0.316 (0.148)
GLTMAX2	-0.082 (0.092)	-0.002 (0.122)	0.000 (0.117)	-0.024 (0.125)	-0.300 (0.125)
GLTMAX3	0.031 (0.246)	-0.005 (0.229)	0.094 (0.157)	-0.033 (0.221)	-0.233 (0.180)
GLTMED1	0.217 (0.315)	0.259 (0.197)	0.094 (0.224)	0.124 (0.343)	0.056 (0.310)
GLTMED2	0.266 (0.382)	0.298 (0.350)	0.121 (0.286)	0.150 (0.376)	-0.060 (0.148)
GLTMED3	0.042 (0.464)	0.269 (0.240)	0.026 (0.280)	0.047 (0.392)	-0.149 (0.234)
TFL	0.057 (0.272)	-0.055 (0.088)	-0.173 (0.128)	0.018 (0.158)	0.303 (0.453)
RFEM	0.128 (0.278)	0.097 (0.267)	0.052 (0.126)	-0.127 (0.211)	0.175 (0.167)
BFEMLH	-0.114 (0.332)	0.065 (0.271)	0.130 (0.149)	-0.003 (0.203)	-0.255 (0.330)
BFEMSH	-0.142 (0.343)	-0.184 (0.333)	0.094 (0.208)	-0.061 (0.132)	-0.443 (0.298)
TA	0.658 (0.133)	-0.099 (0.383)	-0.106 (0.133)	0.080 (0.221)	0.194 (0.203)
MGAS	0.718 (0.137)	0.731 (0.156)	0.054 (0.310)	0.670 (0.103)	0.796 (0.170)
SOL	0.725 (0.095)	0.725 (0.121)	0.325 (0.502)	0.518 (0.406)	0.772 (0.128)

Overall, GLTMAX, GLTMED, TFL, RFEM and BFEM muscle activation pattern predictions did not show particular correlations with EMG curve shapes for any of the tested objective function conditions.

RMSE values detailed in Table 2.2 support the observations that correlations with the $J_{Tmin+Amin}$ where the highest (RMSE values were the lowest). Overall results suggest that for gait motion, the $J_{Tmin+Amin}$ objective function may yield the best results although there remains room for improvement with other muscles.

Table 2.2: RMSE between predicted activations and experimental EMG resulting from the FID simulations using the different optimization objectives ($\boldsymbol{T_{min} + A_{min}}$, $\boldsymbol{A_{max}}$, $\boldsymbol{J_{max}}$, $\boldsymbol{S_{min}}$) as well as SO results from OpenSim 3.2 functionality.

	$\boldsymbol{T_{min} + A_{min}}$	$\boldsymbol{T_{min} + A_{max}}$	$\boldsymbol{T_{min} + J_{max}}$	$\boldsymbol{T_{min} + S_{min}}$	**SO**
GLTMAX1	3.084	2.923	2.670	3.031	0.420
GLTMAX2	2.939	2.763	2.552	2.913	0.314
GLTMAX3	2.773	2.662	2.544	3.072	0.307
GLTMED1	2.411	2.364	2.561	2.216	0.505
GLTMED2	2.233	2.103	2.665	2.342	0.555
GLTMED3	2.262	2.168	2.684	2.533	0.618
TFL	2.816	2.783	3.906	2.757	0.478
RFEM	2.042	2.260	2.782	1.713	0.127
BFEMLH	2.596	2.380	4.758	1.812	0.144
BFEMSH	3.949	3.457	5.365	2.671	0.383
TA	0.253	6.109	2.159	2.879	0.231
MGAS	0.464	0.579	3.884	0.523	0.986
SOL	0.533	1.008	3.908	0.520	0.397

Average joint contact loading applied to the tibia resulting from the various muscle activation patterns are shown in Figure 2.4. As expected, axial joint contact loading is at its greatest for the $J_{Tmin+Jmax}$ condition.

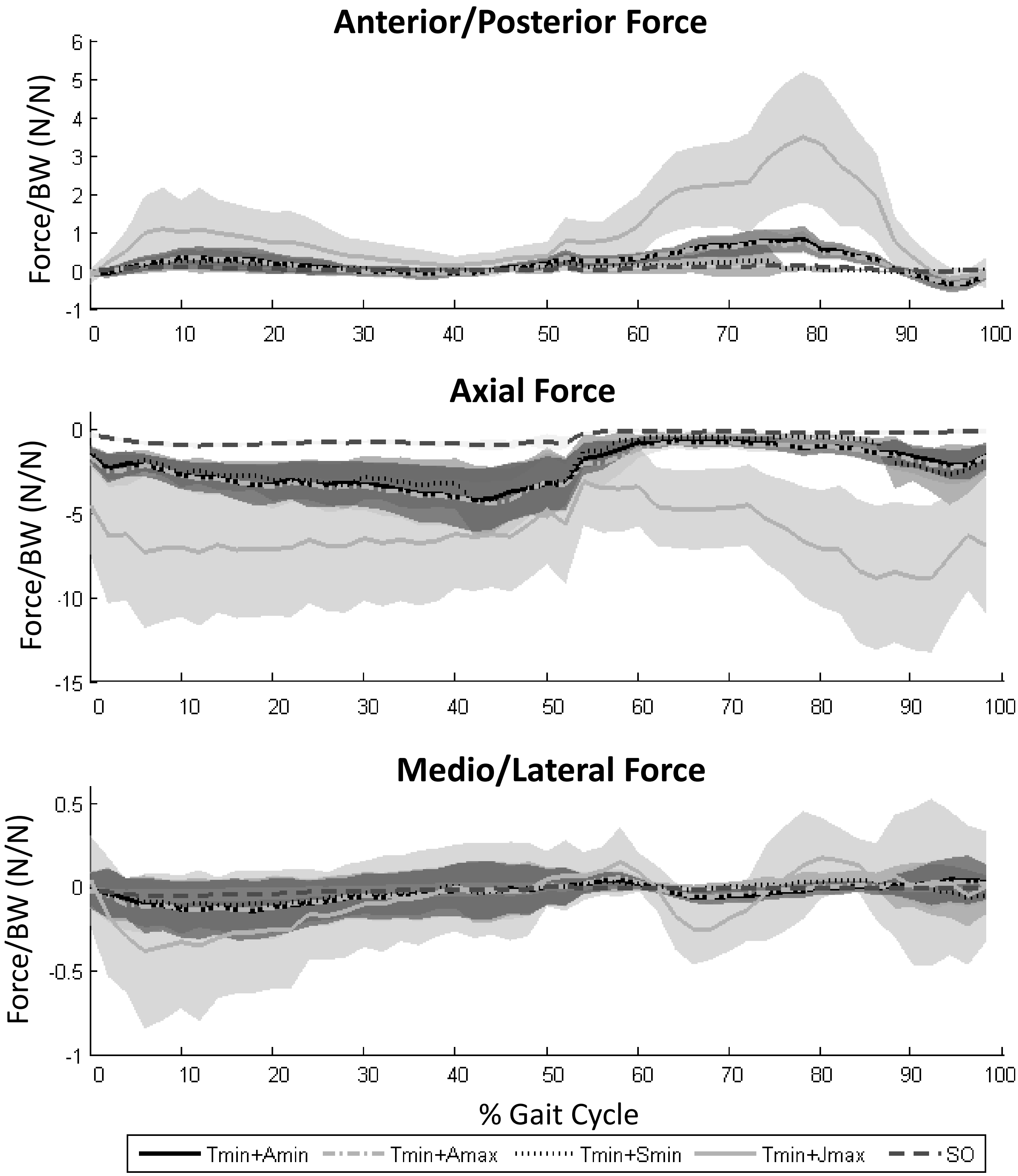

Figure 2.4: Average knee joint forces (N) normalized to bodyweight (N) in relation to the tibial coordinate system resulting from each objective function's simulation muscle activation results. Objective functions are $T_{min} + A_{min}$: Addition of minimization of total muscle activation. $T_{min} + A_{max}$: Addition of maximizing total muscle activation. $T_{min} + J_{max}$: Addition of maximizing axial knee compression. $T_{min} + S_{min}$: Addition of minimizing shear forces at the knee. SO: OpenSim static optimization results obtained from inverse dynamics only.

DISCUSSION

The purpose of this study was to evaluate the effect of a range of objective functions based on potential neuromuscular stabilisation strategies on simulated muscle activations within a musculoskeletal modeling framework. These predicted activations were compared to experimental EMG measurements collected during gait trials of healthy young adult males, simultaneously with kinematics and ground reaction forces. Our experimental gait kinematics (Besier, Sturnieks, Alderson, & Lloyd, 2003; Gao & Zheng, 2010; Kadaba et al., 1989, 1990; Lafortune, Cavanagh, Sommer, & Kalenak, 1992; Potvin, Shourijeh, Smale, & Benoit, 2015; Sartori, Farina, & Lloyd, 2014) and EMG data (Sartori et al., 2014; Van Den Bogert, Geijtenbeek, Even-Zohar, Steenbrink, & Hardin, 2013) are consistent with the literature, indicating that our in vivo data is an appropriate source to validate the muscle activations predicted by the various objective functions used in this study.

The tested objective functions for optimization were chosen based on J_{Amax} and also J_{Jmax} potentially increasing joint stiffness and promoting muscle co-contraction and thus stable support. J_{Smin} was thought to promote co-contraction of muscles while also protecting the important ligaments supporting the knee from excessive stress. J_{Amin} was used as a comparison, as this particular function is often used in musculoskeletal modeling under the assumption that the body moves efficiently (Kaufman et al., 1991; Kim et al., 2009; Shelburne et al., 2006; Shourijeh & McPhee, 2013; Walter et al., 2013).

Muscle Activation Predictions

Previous studies have noted that gait tends to follow patterns that minimize fatigue or promote efficiency (Ackermann & van den Bogert, 2010). Results illustrated in Figure 2.2 and

2.3 show that J_{Amin} produced predicted muscle activation patterns consistent with EMG curves in 3 of the 8 muscles groups that could be compared between the model and experimental EMG data: the TA (r=0.658), MGAS (r=0.718) and SOL (r=0.725) muscles.

Although correlations were low, visual inspection showed some trends for the RFEM and BFEM predicted activation patterns. Curve shapes for $J_{Tmin+Amin}$, $J_{Tmin+Amax}$ and $J_{Tmin+Smin}$ in Figure 2.2 and 2.3, suggest that muscle activation predictions followed EMG peaks with some delay, although EMG signal amplitudes were quite low. Timing of predicted muscle activations and force production for these muscle groups are also consistent with what may be expected during a gait cycle (Sartori et al., 2014; Van Den Bogert et al., 2013). Co-contraction of the RFEM and BFEM muscle groups was observed in the predicted activations of all optimization protocols as well as experimental EMG, suggesting both groups work together to maintain joint stability.

The timing of predicted activations for the RFEM and MGAS is also consistent with past studies suggesting that quadriceps muscles had an important role in early stance followed by gastrocnemius activity in later stance phase (Shelburne et al., 2006; Winby et al., 2009). Muscle force curves for the MGAS, RFEM and BFEM muscle group studies by Kim et al. (Kim et al., 2009) and by Lin et al. (Lin et al., 2010) also resemble activation curves shown in Figure 2.2 for their corresponding muscles.

Although results of the $J_{Tmin+Jmax}$ objective function did not yield muscle activation predictions consistent with EMG data, the high activations (>50% activation throughout the gait cycle; Figure 2.3) of the BFEM, MGAS and SOL muscles suggest that these muscles can play an important role in tightening the knee joint and increasing compression forces.

Overall, high magnitudes of predicted muscle activations were observed for many muscles as shown in Figure 2.2 and 2.3, notably for the GLTMAX, GLTMED, BFEM and TFL which hovered around 50% activation throughout the gait cycle. These values are normalized based on maximum strengths of muscles defined in the musculoskeletal model. Increasing the strength properties of these within the musculoskeletal model to subject or population specific ones may yield lower activation values and be more physiologically representative. As the musculoskeletal model used in this study was a simplified one that did not include all muscles, there may have been compensation by the existing muscles to act on behalf of the missing muscles and thus the model needed to have higher activations to resolve the system.

Many studies and simulation platforms like OpenSim and AnyBody (AnyBody Technology, Denmark) have built in the minimization of total muscle activation as their ideal objective (Cao et al., 2013; Kim et al., 2009) Although it may be fitting in some simulations, it is important to realize that this has not yet been fully validated. It is possible that testing other types of motions (squats, sprints, jumps, etc.) or injured populations may show that this function is no longer appropriate. The objective functions tested in this study show that some functions are better predictors than others but that these objective functions have important effects on simulation outputs, as also noted in previous research (Cleather & Bull, 2011; Lin et al., 2010). Given that gait is considered highly efficient and presents little risk of injury, it is reasonable to conclude that the functions presented here in these studies may be better suited to more dynamic tasks where joint stability would be prioritized by the CNS.

Knee Joint Contact Forces

Predicted joint contact loading results shown in Figure 2.4 confirm that, as expected, the $J_{Tmin+Jmax}$ objective function resulted in the highest predicted loading values compared to the other optimization conditions. This also led to higher predicted loading in the medio/lateral and antero/posterior directions, although not at all time points. Predicted axial forces were quite large, reaching almost 8x bodyweight when using this objective function. This is not surprising since the objective of this function was to maximize this force. It does, however, show the potential for muscles to contribute in important ways to knee loading. Predicted axial loading patterns resulting from the three other objective function optimization conditions showed comparatively reduced axial loading magnitudes and resembled the double peak knee loading curves found in other musculoskeletal modeling studies (D’Lima, Patil, Steklov, Slamin, & Colwell Jr., 2006; Fregly et al., 2011; Kim et al., 2009; Winby et al., 2009). Figure 2.4 shows compression loads of up to approximately 4.2N/BW for these objective function conditions. Many studies have reported values in the range near 2.5x bodyweight (D’Lima et al., 2006; Fregly et al., 2011; Heinlein et al., 2009; Kim et al., 2009; Kutzner et al., 2010; Lin et al., 2010; Schipplein & Andriacchi, 1991; Shelburne et al., 2006; Thambyah, Pereira, & Wyss, 2005) including studies reporting joint contact loading recorded from instrumented knee joint prostheses (Bergmann et al., 2014; Heinlein et al., 2009) but the range increases up to more than double this range in other works (Fregly et al., 2011; Mikosz, Andriacchi, & Andersson, 1988; Seireg & Arvikar, 1975; Winby et al., 2009). Predicted joint contact loading values obtained in the current study fit within these ranges but remain on the higher end of reported values, possibly due to model simplifications. It should be kept in mind that since some predicted muscle activation patterns were not well correlated with experimental EMG, resulting knee joint contact loading is likely inaccurate.

Limitations

In terms of the FID simulation framework, the addition of physiological objectives to the optimization protocol resulted in slightly reduced quality in torque error minimization as the focus of the optimization was split between the two elements in the function. ID joint torques are themselves imperfect due to noise in measurements and approximations of anthropometric data. Joint torque errors observed using $J_{Tmin+Jmax}$ and OpenSim's SO functions were large, suggesting that muscle activations predicted by these methods are incorrect, especially noting the few similarities with EMG. In the case of the SO protocol built into OpenSim 3.2, errors may be of a technical nature. The SO function predicts muscle activations based on minimizing total muscle activation squared that should reconstruct the joint torques calculated through inverse dynamics. When the SO predicted activation results were used with muscle moment arms, it was found that this net torque value was not recreated. In the case of $J_{Tmin+Jmax}$, minimizing joint torque error was weighed equally with maximization of axial joint forces. Perhaps with a different weigthing scheme, the final torque error would be better reconstructed although the physiological element of the optimization sequence would have to be reduced.

Only sagittal plane joint torque error was optimized. Other non-principal DoFs were not considered as their kinematics and dynamics are not reliable when using skin surface markers in motion capture systems due to soft tissue artifact (Benoit et al., 2006; Gao & Zheng, 2008; Gasparutto, Sancisi, Jacquelin, Parenti-Castelli, & Dumas, 2015; Li, Zheng, Tashman, & Zhang, 2012; Reinschmidt, Van Den Bogert, Nigg, Lundberg, & Murphy, 1997). The simulation framework was unable to reduce the joint torque errors to acceptable levels for all degrees of freedom simultaneously, possibly from lack of sufficient muscles or ligaments within the musculoskeletal model. Incorporating more muscles within the model could improve this flexibility and physiological realism but also comes at a higher computational price (Buchanan & Shreeve, 1996). The model used in this study included 25 muscles in each leg, which we considered to be a good balance between keeping the model realistic enough without requiring exceedingly long simulation times.

There are a few additional general sources of errors to consider in these simulations. Measurement errors can originate at the initial data collection, affecting model inputs and the reliability of simulation outputs. Many of the musculoskeletal model's variables are determined from cadaveric studies, often from older individuals, and therefore do not always scale well to younger healthy populations (Anderson & Pandy, 2001; Buchanan, Lloyd, Manal, & Besier, 2005; Buchanan & Shreeve, 1996; Delp et al., 1990; Shelburne et al., 2006). The flexibility of a model in terms of its DoFs can affect joint kinematics and thus muscle moment arms and predicted muscle forces (Buchanan & Shreeve, 1996). The model created by Xu et al. based on the work of (Delp et al., 1990) offered 4DoF at the knee joint (Xu et al., 2014) giving it more flexibility to follow experimental kinematics data around the joint than hinge knee joint models.

Finally, knee ligaments were omitted in this study which may have led to underestimation of joint contact loading (Sasaki & Neptune, 2010; Winby et al., 2009; Xu, 2013) and may have contributed to the increased muscle activation magnitudes to compensate for this lack of passive tissue, as noted by (Doorenbosch & Harlaar, 2003) in a model with reduced anterior cruciate ligament function.

CONCLUSION

The purpose of this study was to evaluate the effectiveness of optimizing muscle activation predictions using different objective functions than one that is commonly used in musculoskeletal modeling today. In the case of gait, a motion recognized as an efficient and well practiced task, the optimization objective minimizing muscle activation and thus efficiency showed the most similarities to experimental muscle excitation patterns. It is possible that for less familiar tasks or motions that occur in multiple DoFs rather than principally in the sagittal plane for walking, the optimization objectives suggested in this work would be more suitable. Researchers have not yet defined how it is exactly that the neuro-musculoskeletal system controls muscle activity and thus body motion. Our work explored a small sample of physiologically inspired possibilities and revealed that the choice of objective is an important one in the musculoskeletal simulation process.

REFERENCES

Ackermann, M., & van den Bogert, A. J. (2010). Optimality principles for model-based prediction of human gait. *Journal of Biomechanics*, *43*(6), 1055–1050.

Ambegaonkar, J. P., Shultz, S. J., Perrin, D. H., Schmitz, R. J., Ackerman, T. A., & Schulz, M. R. (2011). Lower Body Stiffness and Muscle Activity Differences Between Female Dancers and Basketball Players During Drop Jumps. *Sport Health*, *3*(1).

Anderson, F. C., & Pandy, M. G. (2001). Dynamic Optimization of Human Walking. *Journal of Biomechanical Engineering*, *123*.

Baratta, R., Solomonow, M., Zhou, B. H., Letson, D., Chuinard, R., & D'Ambrosia, R. (1988). Muscular coactivation - The role of the antagonist musculature in maintaining knee stability. *The American Journal of Sports Medicine*, *16*(2).

Benoit, D. L., Ramsey, D. K., Lamontagne, M., Xu, L., Wretenberg, P., & Renstrom, P. (2006). Effect of skin movement artifact on knee kinematics during gait and cutting motions measured in vivo. *Gait & Posture*, *24*, 152–164.

Bergmann, G., Bender, A., Graichen, F., Dymke, J., Rohlmann, A., Trepczynski, A., … Kutzner, I. (2014). Standardized loads acting in knee implants. *PLOS One*, *9*(1).

Besier, T. F., Sturnieks, D. L., Alderson, J. A., & Lloyd, D. G. (2003). Repeatability of gait data using a functional hip joint centre and a mean helical knee axis. *Journal of Biomechanics*, *36*, 1159–1168.

Boeth, H. (2013). *Evaluation and characterization of knee joint instability in ACL deficient patients* (PhD Thesis). Technical University of Berlin, Germany.

Buchanan, T. S., Lloyd, D. G., Manal, K., & Besier, T. F. (2004). Neuromusculoskeletal Modeling : Estimation of Muscle Forces and Joint Moments and Movements from Measurements of Neural Command. *Journal of Applied Biomechanics*, *20*(4), 367–395.

Buchanan, T. S., Lloyd, D. G., Manal, K., & Besier, T. F. (2005). Estimation of Muscle Forces and Joint Moments Using a Forward-Inverse Dynamics Model. *Medicine and Science in Sports & Exercise*.

Buchanan, T. S., & Shreeve, D. A. (1996). An evaluation of optimization techniques for the prediction of muscle activation patterns during isometric tasks. *Journal of Biomechanical Engineering*, *118*.

Cao, E., Inoue, Y., Liu, T., & Shibata, K. (2013). An inverse dynamic approach for quantitative muscle force estimation during human standing-up process. *Journal of Biomechanical Science and Engineering*, *8*(1).

Cavanagh, P. R., & Komi, P. V. (1979). Electromechanical delay in human skeletal muscle under concentric and eccentric contractions. *European Journal of Applied Physiology and Occupational Physiology*, *42*(3), 159–163.

Cleather, D. J., & Bull, A. M. J. (2011). An optimization-based simultaneous approach to the determination of muscular, ligamentous, and joint contact forces provides insight into musculoligamentous interaction. *Annals of Biomedical Engineering*, *39*(7), 1925–1934.

Crowninshield, R. D., & Brand, R. A. (1981). A physiologically based criterion of muscle force prediction in locomotion. *Journal of Biomechanics*, *14*(11), 793–801.

Delp, S. L., Loan, P., Hoy, M. G., Zajac, F. E., Topp, E. L., & Rosen, J. M. (1990). An Interactive Graphics-Based Model of the Lower Extremity to Study Orthopaedic Surgical Procedures. *IEEE Transactions on Biomedical Engineering*, *37*(8).

Derouin, A., & Potvin, J. (2005). Knee Stability: Mechanical Contributions of Individual Muscles. Presented at the ISB XXth congress - ASB 29th Annual Meeting.

D'Lima, D. D., Patil, S., Steklov, N., Slamin, J. E., & Colwell Jr., C. W. (2006). Tibial forces measured in vivo after total knee arthroplasty. *The Journal of Arthroplasty*, *21*(2).

Doorenbosch, C. A. M., & Harlaar, J. (2003). A clinically applicable EMG-force model to quantify active stabilization of the knee after a lesion of the anterior cruciate ligament. *Clinical Biomechanics*, *18*, 142–149.

Dul, J., Johnson, G. E., Shiavi, R., & Townsend, M. A. (1984). Muscle Synergism - II. A minimum-fatigue criterion for load sharing between synergistic muscles. *Journal of Biomechanics*, *17*.

Erdemir, A., McLean, S., Herzog, W., & Van Den Bogert, A. J. (2007). Model-based estimation of muscle forces exerted during movements. *Clinical Biomechanics*, *22*, 131–154.

Frank, C. B., & Jackson, D. W. (1997). Current Concepts Review - The Science of Reconstruction of the Anterior Cruciate Ligament. *Journal of Bone & Joint Surgery, American Version*, *79*(10), 1556–1576.

Fregly, B. J., Besier, T. F., Lloyd, D. G., Delp, S. L., Banks, S. A., Pandy, M. G., & D'Lima, D. D. (2011). Grand Challenge Competition to predict in vivo knee loads. *Journal of Orthopaedic Research*.

Gao, B., & Zheng, N. (2008). Investigation of soft tissue movement during level walking: translations and rotations of skin markers. *Journal of Biomechanics*, *41*(15).

Gao, B., & Zheng, N. (2010). Alterations in three-dimensional joint kinematics of anterior cruciate ligament-deficient and -reconstructed knees during walking. *Clinical Biomechanics*, *25*, 222–229.

Gasparutto, X., Sancisi, N., Jacquelin, E., Parenti-Castelli, V., & Dumas, R. (2015). Validation of a multi-body optimization with knee kinematic models including ligament constraints. *Journal of Biomechanics*, *48*, 1141–1146.

Giesl, P., Meisel, D., Scheurle, J., & Wagner, H. (2004). Stability analysis of the elbow with a load. *Journal of Theoretical Biology*, *228*, 115–125.

Giesl, P., & Wagner, H. (2007). Lyapunov function and the basin of attraction for a single-joint muscle-skeletal model. *Journal of Mathematical Biology*, *54*, 453–464.

Hasan, Z. (2005). The human motor-control system's response to mechanical perturbation:should it, can it and does it ensure stability? *Journal of Motor Behavior*, *37*, 484–493.

Heinlein, B., Kutzner, I., Graichen, F., Bender, A., Rohlmann, A., Halder, A., … Bergmann, G. (2009). ESB clinical biomechanics award 2008: Complete data of total knee replacement loading for level walking and stair climbing measured in vivo with a follow-up of 6-10 months. *Clinical Biomechanics*, *24*, 315–326.

Herzog, W., & Leonard, T. R. (1991). Validation of optimization models that estimate the forces exerte by synergistic muscles. *Journal of Biomechanics*, *24*(S1), 31–39.

Hicks, J. L., Uchida, T. K., Seth, A., Rajagopal, A., & Delp, S. L. (2015). Is my model good enough? Best practices for verification and validation of musculoskeletal models and simulations of movement. *Journal of Biomechanical Engineering*, *137*.

Hof, A. L. (1997). The relationship between electromyogram and muscle force. *Sportverletz Sportschaden*, *11*(3), 79–86.

Hug, F., Hodges, P. W., & Tucker, K. (2015). Muscle force cannot be directly inferred fom muscle activation: Illustrated by the proposed imbalance of force between vasus medialis and lateralis in people with patellofemoral pain. *Journal of Orthopaedic & Sports Physical Therapy*, *45*(5).

Kadaba, M. P., Ramakrishnan, H. K., & Wootten, M. E. (1990). Measurement of lower extremity kinematics during level walking. *Journal of Orthopaedic Research*, *8*, 383–392.

Kadaba, M. P., Ramakrishnan, H. K., Wootten, M. E., Gainey, J., Gorton, G., & Cochran, G. V. B. (1989). Repeatability of kinematic, kinetic and electromyographic data in normal adult gait. *Journal of Orthopaedic Research*, *7*, 849–860.

Kaufman, K. R., An, K. N., Litchy, W. J., & Chao, E. Y. S. (1991). Physiological prediction of muscle forces - I. Theoretical Formulation. *Neuroscience*, *40*.

Kim, H. J., Fernandez, J. W., Akbarshahi, M., Walter, J. P., Fregly, B. J., & Pandy, M. G. (2009). Evaluation of predicted knee-joint muscle forces during gait using and instrumented knee implant. *Journal of Orthopaedic Research*.

Kinney, A. L., Besier, T. F., D'Lima, D. D., & Fregly, B. J. (2013). Update on Grand Challenge competition to predict in vivo knee loads. *Journal of Biomechanical Engineering*, *135*.

Komistek, R. D., Kane, T. R., Mahfouz, M., Ochoa, J. A., & Dennis, D. A. (2005). Knee mechanics: a review of past and present techniques to determine in vivo loads. *Journal of Biomechanics*, *38*, 215–228.

Kutzner, I., Heinlein, B., Graichen, F., Bender, A., Rohlmann, A., Halder, A., … Bergmann, G. (2010). Loading of the knee joint during activities of daily living measured in vivo in five subjects. *Journal of Biomechanics*, *43*(11).

Lafortune, M. A., Cavanagh, P. R., Sommer, H. J., & Kalenak, A. (1992). Three-dimensional kinematics of the human knee during walking. *Journal of Biomechanics*, *25*(4), 347–357.

Lee, C., Grad, S., Wimmer, M., & Alini, M. (2006). The Influence of Mechanical Stimuli on Articular Cartilage Tissue Engineering. *Topics in Tissue Engineering*, *2*.

Li, K., Zheng, L., Tashman, S., & Zhang, X. (2012). The inaccuracy of surface-measured model-derived tibiofemoral kinematics. *Journal of Biomechanics*, *45*(15), 2719–2723.

Lin, Y., Walter, J. P., Banks, S. A., Pandy, M. G., & Gregly, B. J. (2010). Simultaneous prediction of muscle and contact forces in the knee during gait. *Journal of Biomechanics*, *43*, 945–952.

Lloyd, D. G., & Buchanan, T. S. (1996). A model of load sharing between muscles and soft tissues at the human knee during static tasks. *Journal of Biomechanical Engineering*, *118*.

Lloyd, D. G., & Buchanan, T. S. (2001). Strategies of muscular support of varus and valgus isometric loads at the human knee. *Journal of Biomechanics*, *34*, 1257–1267.

Maitland, M. E., Ajemian, S. V., & Suter, E. (1997). Quadriceps Femoris and Hamstring Muscle Function in a Person with an Unstable Knee. *Physical Therapy Journal*, *79*(1).

Mansouri, M., & Reinbolt, J. A. (2012). A platform for dynamic simulation and control of movement based on OpenSim and MatLab. *Journal of Biomechanics*, *45*, 1517–1521.

McLean, S. G., & Van Den Bogert, A. J. (2003). Development and validation of a 3D model to predict knee joint loading during dynamic movement. *Transactions of the ASME*, *125*, 864–874.

Mikosz, R. P., Andriacchi, T. P., & Andersson, G. B. J. (1988). Model analysis of factors influencing the prediction of muscle forces at the knee. *Journal of Orthopaedic Research*, *6*, 205–214.

Millard, M., Uchida, T., Seth, A., & Delp, S. L. (2013). Flexing computational muscle: modeling and simulation of musculotendon dynamics. *ASME Journal of Biomechanical Engineering*, *135*(2).

Milner, T. E. (2002). Contribution of geometrey and joint stiffness to mechanical stability of the human arm. *Experimental Brain Research*, *143*, 515–519.

Pedotti, A., Krishman, V. V., & Stark, L. (1978). Optimization of muscle force sequencing in human locomotion. *Mathematical Biosciences*, *38*, 57–76.

Pel, J. J. M., Spoor, C. W., Pool-Goudzwaard, A. L., Hoek Van Dijke, G. A., & Snijders, C. J. (2008). Biomechanical Analysis of Reducing Sacroiliac Joint Shear Load by Optimization of Pelvic Muscle and Ligament Forces. *Annals of Biomedical Engineering*, *36*(3), 415–424.

Portney, L., & Watkins, M. (2000). *Foundations of clinical research: Applications to practice* (Third Edition). Upper Saddle River, NJ: Pearson Prentice Hall.

Potvin, B. M., Shourijeh, M. S., Smale, K. B., & Benoit, D. L. (2015). Effect of adding in-vivo based kinematic knee joint constraints on inverse kinematics and dynamics results in musculoskeletal modeling using OpenSim. *(Unpublished)*.

Reinbolt, J. A., Schutte, J. F., Fregly, B. J., Koh, B. I., Haftka, R. T., George, A. D., & Mitchell, K. H. (2005). Determination of patient-specific multi-joint kinematic models through two-level optimization. *Journal of Biomechanics*, *38*, 621–626.

Reinbolt, J. A., Seth, A., & Delp, S. L. (2011). Simulation of human movement: applications using OpenSim. *Procedia IUTAM*, *2*, 186–198.

Reinschmidt, C., Van Den Bogert, A. J., Nigg, B. M., Lundberg, A., & Murphy, N. (1997). Effect of skin movement on the analysis of skeletal knee joint motion during running. *Journal of Biomechanics*, *30*(7), 729–732.

Riemann, B. L., & Lephart, S. M. (2002). The Sensorimotor System, Part II: The Role of Proprioception in Motor Control and Functional Joint Stability. *Journal of Athletic Training*, *37*(1), 80–84.

Roberts, T. J., & Gabaldon, A. M. (2008). Interpreting muscle function from EMG: Lessons learned from direct measurements of muscle force. *Integrative and Comparative Biology*, *48*(2), 312–320.

Roux, C. H., Guillemin, F., Boini, S., Longuetaud, F., Arnault, N., Hercberg, S., & Briancon, S. (2005). Impact of musculoskeletal disorders on quality of life: an inception cohort study. *Annals of the Rheumatic Diseases*, *64*, 606–611.

Sanford, B. A., Williams, J. L., Zucker-Levin, A. R., & Mihalko, W. M. (2013). Tibiofemoral joint forces during the stance phase of gait after ACL reconstruction. *Open Journal of Biophysics*, *3*, 277–284.

Sartori, M., Farina, D., & Lloyd, D. G. (2014). Hybrid neuromusculoskeletal modeling to best track joint moments using a balance between muscle excitations derived from electromyograms and optimization. *Journal of Biomechanics*, *47*, 3613–3621.

Sasaki, K., & Neptune, R. R. (2010). Individual Muscle Contributions to the Axial Knee Joint Contact Force during Normal Walking. *Journal of Biomechanics*, *43*(14), 2780–2784.

Schipplein, O. D., & Andriacchi, T. P. (1991). Interaction Between Active and Passive Knee Stabilizers During Level Walking. *Journal of Orthopaedic Research*, *9*, 113–119.

Schmitt, L. C., & Rudolph, K. S. (2008). Muscle Stabilization Strategies in People with Medial Knee Osteoarthritis: The Effect of Instability. *Journal of Orthopaedic Research*, *26*, 1180–1185.

Seireg, A., & Arvikar, R. J. (1975). The prediction of muscular load sharing and joint forces in the lower extremities during walking. *Journal of Biomechanics*, *8*, 89–102.

Senavongse, W., Farahmand, F., Jones, J., Andersen, H., Bull, A. M. J., & Amis, A. A. (2003). Quantitative measurement of patellofemoral joint stability: force-displacement behavior of the human patella in vitro. *Journal of Orthopaedic Research*, *21*, 780–786.

Shelburne, K. B., Torry, M. R., & Pandy, M. G. (2006). Contributions of muscles, ligaments and the ground reaction force to tibiofemoral joint loading during normal gait. *Journal of Orthopaedic Research*.

Shourijeh, M. S., & Benoit, D. L. (2015). Hybrid forward inverse dynamics framework for human musculoskeletal simulations. Presented at the International Society of Biomechanics, Glasgow.

Shourijeh, M. S., & McPhee, J. (2013). Optimal Control and Forward Dynamics of Human Periodic Motions Using Fourier Series for Muscle Excitation Patterns. *Journal of Computational and Nonlinear Dynamics*, *9*(2).

Shourijeh, M. S., & McPhee, J. (2014). Forward Dynamic Optimization of Human Gait Simulations: A Global Parameterization Approach. *Journal of Computational and Nonlinear Dynamics*, *9*(3).

Shourijeh, M. S., Smale, K. B., Potvin, B. M., & Benoit, D. L. (2016). A Forward Inverse Dynamics Framework for Human Musculoskeletal Simulations. *Journal of Biomechanics*. http://doi.org/http://dx.doi.org/10.1016/j.jbiomech.2016.04.007

Solomonow, M., Baratta, R., Zhou, B. H., Shoji, H., Bose, W., Beck, C., & D'Ambrosia, R. (1987). The synergistic action of the anterior cruciate ligament and thigh muscles in maintaining joint stability. *The American Journal of Sports Medicine*, *15*(3).

Sturnieks, D. L., Besier, T. F., & Lloyd, D. G. (2011). Muscle activations to stabilize the knee following arthroscopic partial meniscectomy. *Clinical Biomechanics*, *26*, 292–297.

Thambyah, A., Pereira, B. P., & Wyss, U. (2005). Estimation of bone-on-bone contact forces in the tibiofemoral joint during walking. *The Knee*, *12*(5).

Thelen, D. G. (2003). Adjustment of Muscle Mechanics Model Parameters to Simulate Dynamic Contractions in Older Adults. *Transactions of the ASME*, *125*.

Van Den Bogert, A. J., Geijtenbeek, T., Even-Zohar, O., Steenbrink, F., & Hardin, E. C. (2013). A real time system for biomechanical analysis of human movement and muscle function. *Medical & Biological Engineering & Computing*, *51*.

Van Dieen, J. H., Thissen, C. E. A. M., Van de Ven, A. J. G. M., & Toussaint, H. M. (1991). The electro-mechanical delay of the erector spinae muscle: influence of rate of force development, fatigue and electrode location. *European Journal of Applied Physiology and Occupational Physiology*, *63*, 216–222.

Wagner, H., Giesl, P., & Blickhan, R. (2007). Musculoskeletal Stabilization of the Elbow - Complex or Real. *Journal of Mechanics in Medicine and Biology*, *7*(3).

Walter, J. P., Kinney, A. L., Banks, S. A., D'Lima, D. D., Besier, T. F., Lloyd, D. G., & Fregly, B. J. (2013). Muscle Synergies May Improve Optimization Prediction of Knee Contact Forces During Walking. *Journal of Biomechanical Engineering*, *136*(2).

Winby, C. R., Lloyd, D. G., Besier, T. F., & Kirk, T. B. (2009). Muscle and External Load Contribution to Knee Joint contact Loads During Normal Gait. *Journal of Biomechanics*, *42*, 2294–2300.

Wong, Y.-M., & Ng, G. Y. F. (2006). Surface electrode placement affects the EMG recordings of the quadriceps muscles. *Physical Therapy in Sport*, *7*(3), 122–127.

Wu, D. D., Burr, D. B., Boyd, R. D., & Radin, E. L. (1990). Bone and Cartilage Changes Following Experimental Varus or Valgus Tibial Angulation. *Journal of Orthopaedic Research*, *8*, 572–585.

Xu, H. (2013). *Development of a Musculoskeletal Model to Determine Knee Contact Force During Walking on Ballast Using Opensim Simulation*. University of Utah, Utah, United States.

Xu, H., Bloswick, D., & Merryweather, A. (2014). An improved OpenSim gait model with multiple degrees of freedom knee joint and knee ligaments. *Computer Methods in Biomechanics and Biomedical Engineering*.

APPENDICES

Appendix 2.1: Optimization function parameters used for *fmincon* (find minimum of constrained nonlinear multivariable function), *GA* (find minimum of function using a genetic algorithm) and *fminsearchbnd* (find minimum constrained multivariable function using derivative-free method) . TolFun: Termination tolerance on the function value, TolX: Termination tolerance on x, the current point, FinDiffRelStep: step size for finite difference, MaxFunEvals: maximum function evaluations, MaxIter: maximum iterations, StallGenLimit: maximum iteration of population update without improvement of the objective function, TolCon: tolerance on constraint

	fmincon	**GA**	**fminsearchbnd**
TolFun	1e-4	1e-4	1e-4
TolX	1e-6	--	1e-6
Algorithm	Interior-point	--	Nelder-Mead
FinDiffRelStep	1e-5	--	--
MaxFunEvals	5e2	--	5e2
MaxIter	2e2	--	2e2
StallGenLimit	--	5	--
Generations	--	25	--
PopulationSize	--	20	--
TolCon	1e-3	1e-3	1e-3

Using an In-Vivo Based Knee Kinematic Model in a Forward-Inverse Musculoskeletal Modeling Framework Alters Predicted Knee Joint Forces and Muscle Activations

Brigitte M. Potvin,
University of Ottawa, School of Biomedical Engineering

Dr. Mohammad S. Shourijeh
University of Ottawa, School of Rehabilitation Sciences

Kenneth B. Smale
University of Ottawa, School of Human Kinetics

Dr. Davide Spinello
University of Ottawa, School of Mechanical Engineering

Dr. Daniel L. Benoit
University of Ottawa, School of Human Kinetics and Rehabilitation

ABSTRACT

Musculoskeletal modeling and simulation of human movement is often used to describe motions and muscle activations about the knee joint. The knee is a 6 degree of freedom (DoF) joint that is often simplified in musculoskeletal modeling. Since there are very few studies describing tibio-femoral kinematics in vivo during dynamic tasks, the effects of these simplifications is not well understood. The purpose of this study was to compare muscle activation predictions within an OpenSim framework when using a novel 5DoF knee joint kinematically defined from in vivo bone-pin derived tibio-femoral kinematics and one prescribed DoF and when using a free 4DoF knee joint model with two prescribed joint constraints. Two objective functions (minimization of total muscle activation squared and minimization of shear forces at the knee) within the optimization protocols of a forward-inverse dynamics simulation framework were also tested.

Using minimization of muscle activation as an objective function within the simulation framework, the in vivo model's muscle activations were more closely correlated to experimental EMG than the prescribed 4DoF model for the medial gastrocnemius (r=0.776 vs 0.725), soleus (r=0.771 vs 0.718) and showed good correlations with tibialis anterior predictions (r=0.600). Knee joint contact loading magnitudes were reduced and varied less among subjects in the in vivo model condition for compression and medio/lateral forces but increased for posterior/anterior loading, potentially due to increased degrees of freedom at the knee and tighter ranges of motion.

KEY WORDS

Musculoskeletal modeling, simulations, knee, stability, bone-pins, intra-cortical pins, soft tissue artifact, motion capture, kinematics, dynamics, muscle activation, electromyography, degree of freedom

BACKGROUND

Musculoskeletal modeling and computer simulations are becoming useful clinical and research tools to address musculoskeletal disorders and their costly effect on quality of life and on the health care system (Delp et al., 1990; Fregly et al., 2011; Kinney, Besier, D'Lima, & Fregly, 2013; Komistek, Kane, Mahfouz, Ochoa, & Dennis, 2005; Reinbolt et al., 2005). In order to closely represent the internal workings of the human body, models and simulations need to be as physiologically realistic as possible, in particular if they are to be used to gain clinical insight. There are a few challenges to address within musculoskeletal modeling, one of which lies in the quality of experimental kinematic data applied to models within simulation frameworks. Skin mounted reflective markers used with motion capture camera systems are affected by soft tissue artifact (STA) and do not reflect actual bone motions in any but the larger range DoFs (flexion/extension for the hip, knee and ankle) as has been demonstrated in multiple studies (Benoit et al., 2006; Duprey, Cheze, & Dumas, 2010; Gasparutto, Sancisi, Jacquelin, Parenti-Castelli, & Dumas, 2015; Li, Zheng, Tashman, & Zhang, 2012). Methods have been used to reduce STA effects at the motion capture level such as with the use of marker clusters (Alexander & Andriacchi, 2001; Andriacchi, Alexander, Toney, Dyrby, & Sum, 1998; Cappozzo, Capello, Croce, & Pensalfini, 1997), or at the computer model level by reducing joint DoFs to hinge, spherical, parallel and universal joints (Reinbolt et al., 2005), prescribing DoFs based on 2D motion (Cerveri, Pedotti, & Ferrigno, 2005), or introducing anatomical constraints

(Duprey et al., 2010; Gasparutto et al., 2015; Lu & O'Connor, 1999) such as modifying ligaments properties and simplifying joint contact surface shapes. However, some of these methods have been shown to worsen the error caused by STA or are only useful to specific types of motion (Andersen, Benoit, Damsgaard, Ramsey, & Rasmussen, 2010; Andersen, Damsgaard, Rasmussen, Ramsey, & Benoit, 2012).

The knee joint in particular is a complex load bearing joint that moves in 6 degrees of freedom (DoF). However, this joint is often simplified within musculoskeletal models by either reducing the DoF for example in (Anderson & Pandy, 2001; De Groote et al., 2009; Delp et al., 1990; Glitsch & Baumann, 1997; Modenese, Phillips, & Bull, 2011; Xu, Bloswick, & Merryweather, 2014; Yamaguchi & Zajac, 1989) and/or prescribing the motions of secondary rotations and translations based on sagittal (knee flexion/extension) rotations as was done in (Delp et al., 1990; Dumas, Moissenet, Gasparutto, & Cheze, 2012; Duprey et al., 2010; Xiao & Higginson, 2008; Xu et al., 2014).

A recently developed novel 5 DoF kinematic knee joint model (Potvin, Shourijeh, Smale, & Benoit, 2015) is based on experimental bone-pin derived tibio-femoral ranges of motion envelopes during dynamic tasks (Benoit et al., 2007; Benoit, Damsgaard, & Andersen, 2015). Significant differences were found in kinematics between the in vivo derived model and the 4 DoF model with prescribed kinematics, especially notable in knee abduction and translations. These kinematic differences change the musculoskeletal model's muscle moment arms, and therefore muscle activations predictions should be different between model conditions.

Once joint kinematics and dynamics are calculated, muscle activation predictions can be made through simulation frameworks and optimization protocols since the knee joint is an under-determinate system. Various types of simulation frameworks, inverse (ID) (Cao, Inoue, Liu, &

Shibata, 2013; De Groote et al., 2009; Glitsch & Baumann, 1997; Kim et al., 2009) or forward dynamics (FD) based/EMG driven (Besier, Fredericson, Gold, Beaupre, & Delp, 2009; Buchanan, Lloyd, Manal, & Besier, 2005; Winby, Gerus, Kirk, & Lloyd, 2013), have been described in the literature. Hybrid forward-inverse dynamics simulations are also used to cross-validate results between ID and FD methods (Buchanan et al., 2005; Lloyd & Buchanan, 1996; Sartori, Farina, & Lloyd, 2014). Optimizations using simple objective functions based on the premise of motion and metabolic efficiency have been used to predict muscle activations and forces (Anderson & Pandy, 2001; Cao et al., 2013; Cleather & Bull, 2011; Collins, 1995; Crowninshield & Brand, 1981; Glitsch & Baumann, 1997; Kim et al., 2009; Seireg & Arvikar, 1975; Shelburne, Torry, & Pandy, 2006; Winby, Lloyd, Besier, & Kirk, 2009). Nevertheless, the contributions of individual muscles to resulting knee joint contact loading is still an open research field as direct measurement is difficult (Buchanan et al., 2005; Crowninshield & Brand, 1981; Glitsch & Baumann, 1997; Shelburne et al., 2006; Winby et al., 2009). Ideally, in vivo activations can inform simulations, thus leading to improved predictions of in vivo activations (Sartori et al., 2014).We therefore developed a forward-inverse dynamics (FID) simulation framework that combined the advantages of both forward and inverse dynamics methods ((Shourijeh, Smale, Potvin, & Benoit, 2016), Figure 3.1).

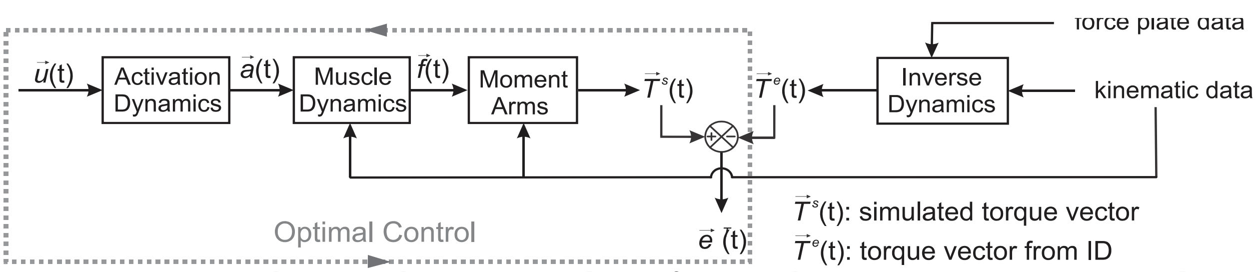

Figure 3.1: Forward-inverse dynamics simulation framework minimizing joint torque prediction error $e(t)$. Other variables are defined as follows: $u(t)$: muscle excitation, $a(t)$: muscle activation, $f(t)$:tendon-muscle forces, T^s:simulated torque vector, T^e:torque vector from inverse dynamics (ID). Adapted from (Shourijeh & Benoit, 2015; Shourijeh & McPhee, 2014).

Using this framework we found that changing the objective function from the commonly used minimizing total muscle activation (J_{Amin}) to functions based on joint stabilisation (minimization of shear forces (J_{Smin}) at the knee) had an impact on activation predictions during the gait cycle (Potvin, Shourijeh, Smale, Spinello, & Benoit, 2015). Physiological joint stability can also be defined using classic control theory as the system's ability to return to an original equilibrium state or remain within a feasible range of states described by constraints or boundaries for given parameters(Bergmark, 1989; Moengin, 2010, 2011; Murphy, 1974). This is similar to imposing boundaries with bone pin data for kinematic calculations and increasing a system's stability.

As such, the purpose of this study was to combine both the in vivo derived knee joint model (Potvin, Shourijeh, Smale, & Benoit, 2015) and the simulation framework's optimizations from (Potvin, Shourijeh, Smale, Spinello, et al., 2015) to determine if motion constrained by in-vivo bone-pin data had an impact on muscle activation predictions and joint contact loading during dynamic tasks, in addition to comparing the results to the built-in static optimization (SO) function of OpenSim 3.2.We hypothesize that the use of the in vivo knee kinematic model will improve muscle activation profiles and thus joint contact loading patterns. Furthermore, we hypothesize that combining this model with a joint stability-inspired objective function could improve the activation predictions when compared to a standard approach during gait.

METHODOLOGY

Musculoskeletal Model Definition and Modifications

Xu et al.'s musculoskeletal model (Xu et al., 2014), developed based on (Delp et al., 1990), was used in this study and is available from the OpenSim model database. This model includes 56 muscles (25/leg + 6 abdominals) and 29 DoFs. The knee joint has 4 free DoFs and the remaining two are functions of the knee flexion/extension angle. The Xu model was modified to omit ligaments and to update the muscle model from the "Thelen2003Muscle" muscle model (Thelen, 2003) to that of the Millard et al.(Millard, Uchida, Seth, & Delp, 2013), "Millard2012EquilibriumMusclemodel" as is OpenSim's current standard.

The knee joint model script was modified to have two conditions: 1- 4DoF: A 4DoF knee model with 2 prescribed DoFs (Distal/Proximal translation and anterior/posterior translations) without in-vivo data. 2- In-Vivo: A 5 DoF knee model with one prescribed DoFs (distal/proximal translation) and 4 DoFs (excluding flexion/extension) constrained by in-vivo bone-pin data. 4DoF and In-Vivo model kinematics were obtained following the procedure outlined in (Potvin, Shourijeh, Smale, & Benoit, 2015).

Motion Capture Data

Gait trials from 5 healthy young adult males (mean age, weight and height 24±1.9yr, 80.8±9.1kg and 177.3±8.1cm respectively) were collected, and time normalized between two consecutive dominant leg heel strikes with a 10 camera motion capture system (Nexus 1.8.3, Vicon Motion Systems ltd, UK). Fifty two marker trajectories, of which 38 described the lower limbs were placed according to the University of Ottawa Motion Analysis Cluster Model, a modified Plug-in-Gait model (Kadaba MP & Wootten, 1990), were sampled at 200 Hz and kinetics data (force plates) were collected at 1000Hz (FP4060-08, Bertec, USA). Marker trajectories and force plate data were filtered with a 4^{th} order zero lag Butterworth filter with a cut-off frequency of 10Hz.

Electromyography (EMG) collected at 1000Hz on the dominant leg was recorded for 12 muscles using a Delsys DS-B04 Bagnoli 16 EMG system (Delsys, USA): gluteus maximus (GLTMAX), gluteus medius (GLTMED), tensor fascia latae (TFL), rectus femoris (RFEM), vastus medials (VMED), vastus lateralis (VLAT), biceps femoris (BFEM), semitendinosus (STEN), tibialis anterior (TA), medial gastrocnemius (MGAS), lateral gastrocnemius (LGAS) and the soleus (SOL). EMG data from each motion trial was full wave rectified and low-pass filtered with a 4th order zero-lag Butterworth filter with cut-off frequency of 8Hz. Resulting EMG waveforms were normalized to maximum voluntary isometric contraction (MVIC) trials recorded on a Biodex System 4 (Biodex Medical Systems, NY-USA).

Forward-Inverse Dynamics Simulation Framework (FID)

We used a novel forward-inverse dynamics simulation framework (FID) (Figure 3.1; (Shourijeh et al., 2016)) to predict muscle activations and also joint contact forces using the kinematics from the In-Vivo model and the 4DoF model. This FID calculates knee joint torques using a scaled model through the MatLab-OpenSim API (MatLab 2014a, The Mathworks, USA and OpenSim 3.2 , simtk.org, Simbios, National NIH Center for Biomedical Computing, USA), followed by inverse kinematics (IK) and dynamics calculations (ID) as shown in the right hand side of Figure 3.1. The static optimization (SO) protocol built into OpenSim 3.2 that minimizes the sum of muscle activations squared was also run to predict muscle activations for all model muscles for both the in vivo 5DoF model and the 4 free DoF model to obtain initial muscle activation approximations for the FID framework's simulation of the 25 muscles from the dominant leg.

Forward dynamics with prescribed kinematic motion were run to estimate muscle activations yielding knee joint torques as close to those described by the ID results. Additional physiologically based objective functions were added since minimization of torque error could yield an infinite number of muscle activation combinations.

Optimization with Stability Inspired Objective Functions

The basic objective function (J_{Tmin}) of the framework minimizes the normalized torque error (*TE*) divided by absolute values of torque determined from inverse dynamics ($ID_{Torques}$). Simulation scripting rejected combinations of values where muscle activations (a) were outside the range of 0 to100% maximal activation. .

$$J_{Tmin} = \min\left(\Sigma\left(\frac{|TE|}{|ID_{Torques}|}\right)\right) \qquad \text{(eq1)}$$

The two most promising objective functions from a previous study (Potvin, Shourijeh, Smale, Spinello, et al., 2015) were added to eq1 and weighting of each element of the function was divided evenly: minimizing the sum of squared muscle activations ($\sum(a_i)^2$) and minimizing total shear loading ($\sum F_{shear}$).

$$J_{Amin} = min\Sigma(a_i)^2 \qquad \text{(eq2)}$$

$$J_{Smin} = min\Sigma(F_{shear}) \qquad \text{(eq3)}$$

For example, using eq2, the total equation was defined as

$$Objective\ function\ value \qquad \text{(eq4)}$$

$$= \sum_{for\ each\ 25\ muscles} \frac{J_{Amin}}{J_{Amin} + J_{Tmin}} * J_{Tmin} + \frac{J_{Tmin}}{J_{Amin} + J_{Tmin}} * J_{Amin}$$

$$+\ (if\ a > 1) * 1e6 + (if\ a < 0) * 1e6$$

The optimizations were run with a MatLab 2014a script, using the functions from the Global Optimization and Optimization toolboxes *fmincon* (find minimum of constrained nonlinear multivariable function), *GA* (find minimum of function using a genetic algorithm) and *fminsearchbnd* (find minimum constrained multivariable function using derivative-free method).

Data Analysis

Differences between inverse kinematics and dynamics results for both free and In-Vivo models conditions were reported in (Potvin, Shourijeh, Smale, & Benoit, 2015). Dominant leg muscle activation results from the FID framework simulations with the two objective functions (A_{min} and S_{min}) as well as SO for the two models were compared with corresponding experimental EMG for each subject for pattern trends using Pearson's correlation (r) test and for magnitude using root mean squared error (RMSE) through custom MatLab scripting. The FID framework predicted muscle activations for the 25 muscles on the dominant leg. Muscles present both in the musculoskeletal model and as EMG recordings included the GLTMAX, GLTMED, TFL, RFEM, BFEM, TA, MGAS and SOL. In the model, GLTMAX and GLTMED are represented by 3 muscle lines and the BFEM is represented by 2 muscle bundles, the biceps femoris long head and short head (BFEMLH and BFEMSH respectively).

In preliminary observations, there was some delay between EMG peaks and muscle activation results likely due to electrode placement on the muscles (Hug, Hodges, & Tucker, 2015; Van Dieen, Thissen, Van de Ven, & Toussaint, 1991; Wong & Ng, 2006) as well as the typical electrochemical delay seen between muscle excitation and production of force (Cavanagh & Komi, 1979; Hof, 1997; Hug et al., 2015; Roberts & Gabaldon, 2008). This delay was on the order of 30-150ms, consistent with literature values (Cavanagh & Komi, 1979; Hof, 1997). Cross-correlation between muscle activations and EMG were therefore calculated to remove the effect of the time offset using MatLab scripting and its *xcorr* function (this offset was set to a maximum of approximately 150ms). Predicted muscle activity patterns were also compared to EMG data from the literature and to simulation results obtained by other studies.

Knee joint contact loading patterns created by the muscle activation patterns were also qualitatively compared between the predicted results of each physiological objective function and both model conditions as well as with relevant literature.

RESULTS

Simulation framework results from the different objective function definitions (A_{min}, S_{min}, SO) and both model conditions (4DoF and In-Vivo) were averaged across subjects and are plotted in Figures 3.2, 3.3 and 3.4 with their respective average EMG data. According to cross-correlation analysis results, muscle activation predictions were shifted in these figures to represent the best fit between EMG and activation and minimize the effect of the delay between the two. Correlation values can be found in Table 3.1 and RMSE values between predicted results and experimental EMG are found in Table 3.2.

In the A_{min} case (Figure 3.2), TA, MGAS and SOL muscles were well and similarly predicted in the framework for both model conditions, with average correlation (+/- stdev) values for the 4DoF model of r=0.658(0.133), 0.718(0.137) and 0.725(0.095) respectively and for the In-Vivo model values of r=0.600(0.126), 0.771(0.113) and 0.776(0.084) respectively. As detailed in Table 3.2, RMSE values for these muscles were slightly lower for the 4DoF model than the In-Vivo model (0.253, 0.464, 0.533 respectively for the 4DoF model as compared to 0.417, 0.571 and 0.550 respectively for the In-Vivo model).

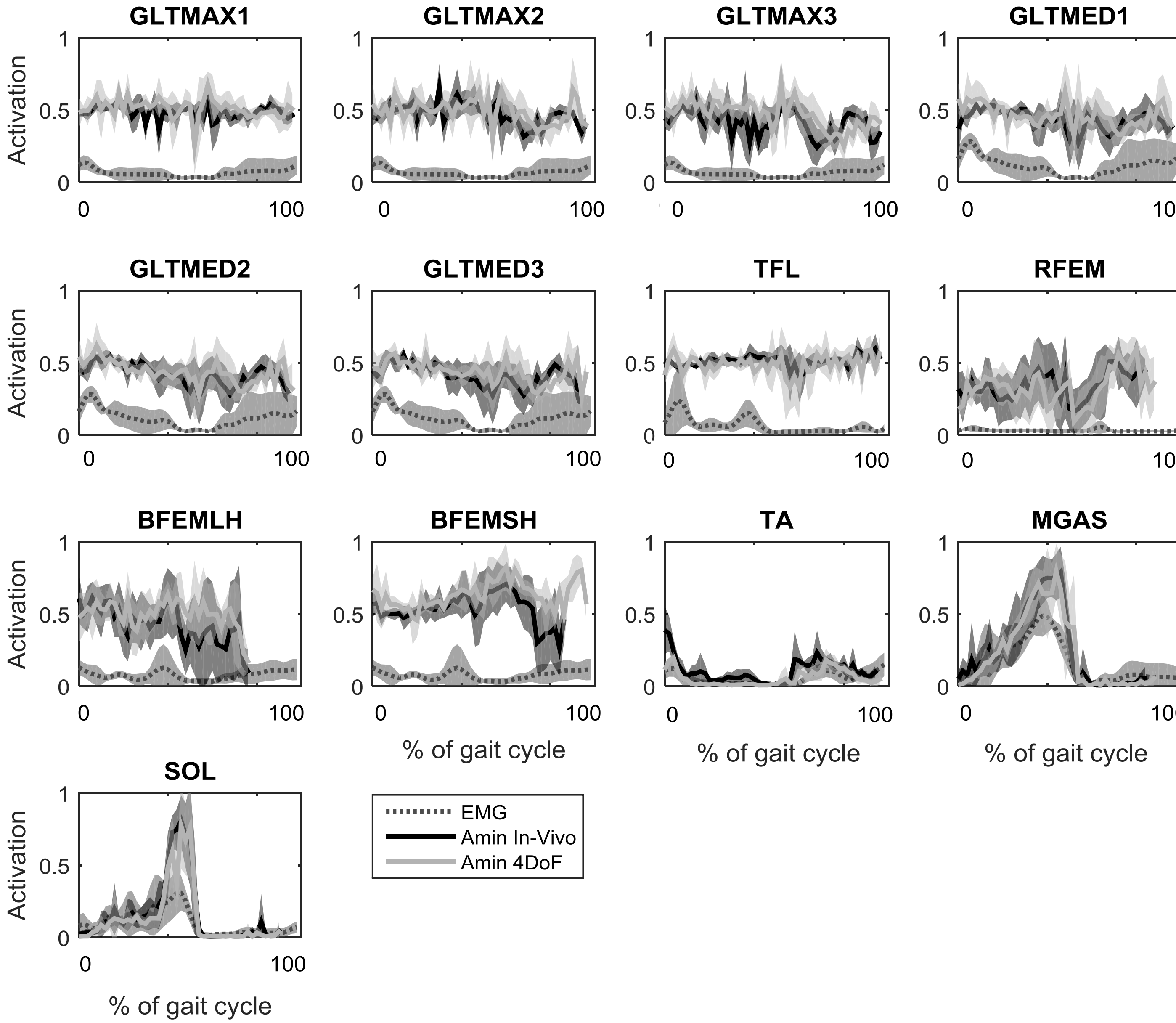

Figure 3.2: Comparison of muscle activation predictions adjusted to best experimental EMG correlation data for the simulation condition using a combination of minimization of torque error with minimization of total muscle activation for the musculoskeletal model with the 4DoF knee model (A_{min}, 4DoF) and for the In-Vivo model (A_{min}, In-Vivo)

In the case of the S_{min} objective function in Figure 3.3, muscle activation prediction results were similar between model conditions for the MGAS and SOL muscles (4DoF average r and (stdev): r=0.670(0.103) and 0.518(0.406) respectively and In-Vivo: 0.550(0.126) and 0.754(0.069) respectively) while other muscles did not show particular correlations. As in the

A_{min} objective function case, RMSE values were higher in the In-Vivo model compared to in the 4DoF model (In-Vivo: 1.164 and 1.257 respectively and 4DoF:0.523 and 0.520). This suggests that these muscle activation predictions were overestimated in the In-Vivo model more so than in the 4DoF model with prescribed motion when using the S_{min} objective function.

Muscle activation predictions simulated with the SO objective function as defined in OpenSim 3.2 showed much weaker activations across muscles. Similarities between predictions and experimental EMG were observed for the MGAS and SOL muscles (average correlation +/- stdev) for the 4DoF model r=0.796(0.170) and 0.772(0.128) respectively and for the In-Vivo model r=(-0.438(0.205) and 0.758(0.138) respectively). Predicted activation results from the In-Vivo model were similar or lower than those of the 4DoF model as illustrated in Figure 3.4. RMSE, detailed in Table 3.2, also showed higher values for the In-Vivo model for these muscles (MGAS: 1.083 and SOL: 0.413) than in the 4DoF model (MGAS: 0.986 and SOL: 0.397). Upon further analysis, it was revealed that knee joint torques calculated by inverse dynamics were not well replicated by the forward dynamics calculations using predicted muscle activations. This may be a technical issue in OpenSim 3.2.

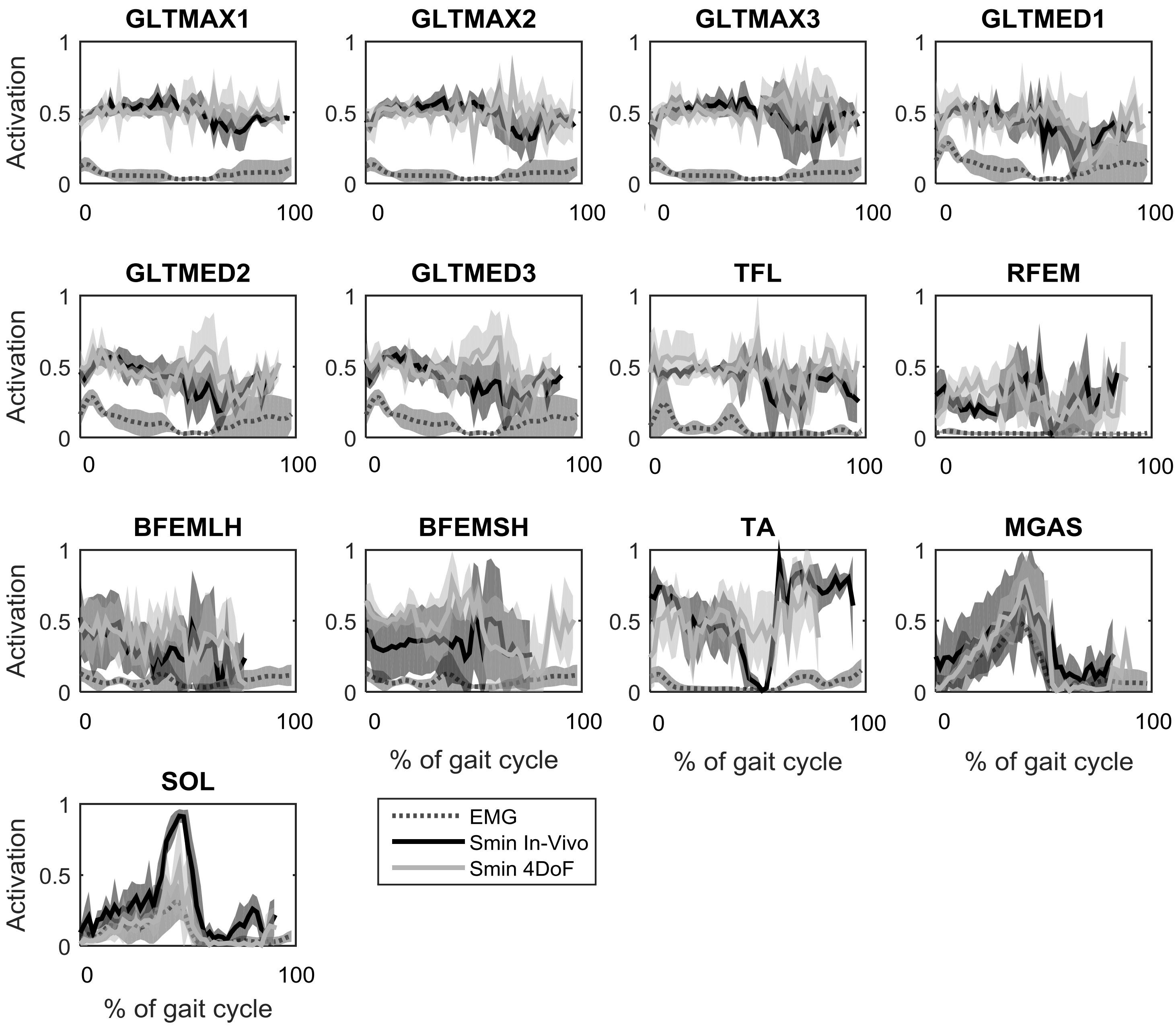

Figure 3.3: Comparison of muscle activation predictions adjusted to best correlate to experimental EMG for the simulation condition using a combination of minimization of torque error with minimization of shear force at the knee joint for the musculoskeletal model with the 4DoF knee model (S_{min} 4DoF) and for the In-Vivo model (S_{min} In-Vivo)

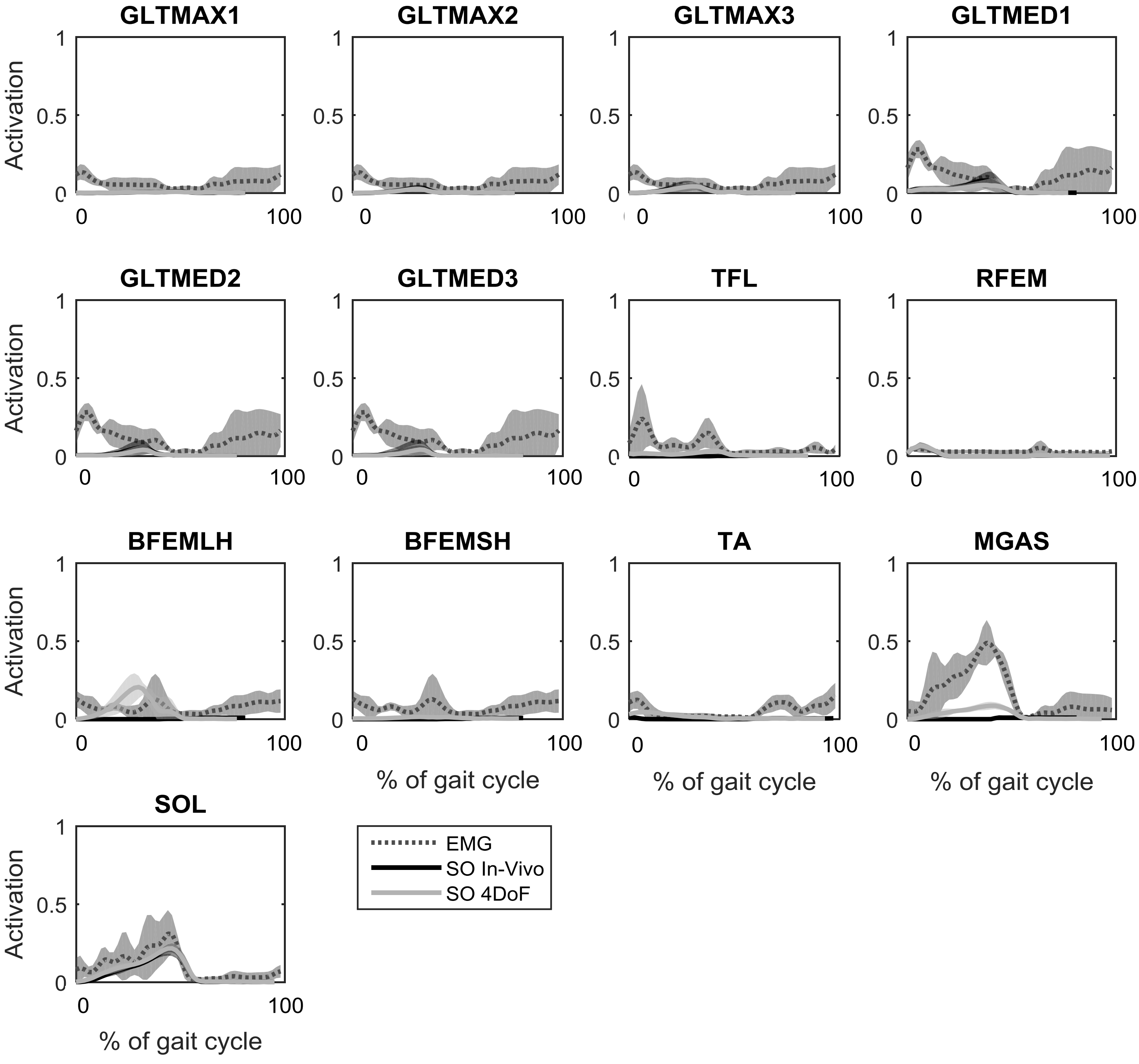

Figure 3.4: Comparison of muscle activation predictions adjusted to best correlate to experimental EMG as determined from the static optimization analysis script in OpenSim 3.2 for the musculoskeletal model with the 4DoF knee model (SO 4DoF) and for the In-Vivo model (SO In-Vivo)

Table 3.1: Across subject average (+/-std dev) Pearson's correlation results after adjustment with cross-correlation analysis between muscle activation predictions and corresponding EMG signal resulting from simulations using the different objective functions for the 4DoF model (clear cells) and In-Vivo model (shaded cells).

	$\boldsymbol{T_{min} + A_{min}}$ **(4DoF model)**	$\boldsymbol{T_{min} + A_{min}}$ **(In-Vivo model)**	$\boldsymbol{T_{min} + S_{min}}$ **(4DoF model)**	$\boldsymbol{T_{min} + S_{min}}$ **(In-Vivo model)**	**SO (4DoF model)**	**SO (In-Vivo model)**
GLTMAX1	-0.010 (0.157)	-0.009 (0.079)	-0.179 (0.117)	-0.125 (0.201)	-0.316 (0.148)	-0.345 (0.060)
GLTMAX2	-0.082 (0.092)	-0.098 (0.113)	-0.024 (0.125)	-0.141 (0.297)	-0.300 (0.125)	-0.222 (0.253)
GLTMAX3	0.031 (0.246)	0.009 (0.156)	-0.033 (0.221)	-0.098 (0.253)	-0.233 (0.180)	-0.205 (0.214)
GLTMED1	0.217 (0.315)	0.182 (0.296)	0.124 (0.343)	0.186 (0.427)	0.056 (0.310)	0.006 (0.150)
GLTMED2	0.266 (0.382)	0.249 (0.446)	0.150 (0.376)	0.264 (0.442)	-0.060 (0.148)	0.028 (0.160)
GLTMED3	0.042 (0.464)	0.241 (0.411)	0.047 (0.392)	0.273 (0.403)	-0.149 (0.234)	0.009 (0.375)
TFL	0.057 (0.272)	-0.170 (0.159)	0.018 (0.158)	0.108 (0.242)	0.303 (0.453)	-0.299 (0.392)
RFEM	0.128 (0.278)	0.130 (0.308)	-0.127 (0.211)	0.084 (0.381)	0.175 (0.167)	0.247 (0.173)
BFEMLH	-0.114 (0.332)	0.155 (0.241)	-0.003 (0.203)	0.088 (0.121)	-0.255 (0.330)	0.332 (0.281)
BFEMSH	-0.142 (0.343)	-0.018 (0.251)	-0.061 (0.132)	0.063 (0.168)	-0.443 (0.298)	0.330 (0.278)
TA	0.658 (0.133)	0.600 (0.126)	0.080 (0.221)	0.506 (0.221)	0.194 (0.203)	0.745 (0.140)
MGAS	0.718 (0.137)	0.771 (0.113)	0.670 (0.103)	0.550 (0.126)	0.796 (0.170)	-0.438 (0.205)
SOL	0.725 (0.095)	0.776 (0.084)	0.518 (0.406)	0.754 (0.069)	0.772 (0.128)	0.758 (0.138)

Table 3. 2: RMSE values between predicted activations and experimental EMG for the different model conditions (4DoF and In-Vivo model) and for the different objective function optimization protocols (A_{min}, S_{min} and SO)

	$T_{min} + A_{min}$ (4DoF model)	$T_{min} + A_{min}$ (In-Vivo model)	$T_{min} + S_{min}$ (4DoF model)	$T_{min} + S_{min}$ (In-Vivo model)	SO (4DoF model)	SO (In-Vivo model)
GLTMAX1	3.084	2.896	3.031	2.945	0.420	0.425
GLTMAX2	2.939	2.805	2.913	2.873	0.314	0.312
GLTMAX3	2.773	2.395	3.072	2.905	0.307	0.301
GLTMED1	2.411	2.197	2.216	2.024	0.505	0.516
GLTMED2	2.233	2.100	2.342	2.008	0.555	0.536
GLTMED3	2.262	2.058	2.533	2.066	0.618	0.662
TFL	2.816	2.977	2.757	2.339	0.478	0.541
RFEM	2.042	2.002	1.713	1.580	0.127	0.129
BFEMLH	2.596	2.142	1.812	1.431	0.144	0.417
BFEMSH	3.949	3.247	2.671	1.959	0.383	0.420
TA	0.253	0.417	2.879	3.484	0.231	0.306
MGAS	0.464	0.571	0.523	1.164	0.986	1.083
SOL	0.533	0.550	0.520	1.257	0.397	0.413

Average predicted knee joint contact loading results created by the muscle activation profiles between the physiological objective functions A_{min} and S_{min} as well as the static optimization results from OpenSim 3.2 for both model conditions (4DoF and In-Vivo) are shown in Figure 3.5. Mean curve shapes are similar in both models although medio-lateral forces show much less variability in the In-Vivo model (max stdev = 0.66N/Kg) than in the 4DoF model (max stdev = 2.02N/Kg), whereas anterior-posterior forces are more variable in the In-Vivo model (max stdev = 10.34N/Kg compared to 3.67N/Kg). Peak absolute forces were lower for axial and medio/lateral forces in the In-Vivo model (33.55N/Kg and 0.65N/Kg respectively) compared to the 4DoF model (41.53N/Kg and 1.36N/Kg respectively).

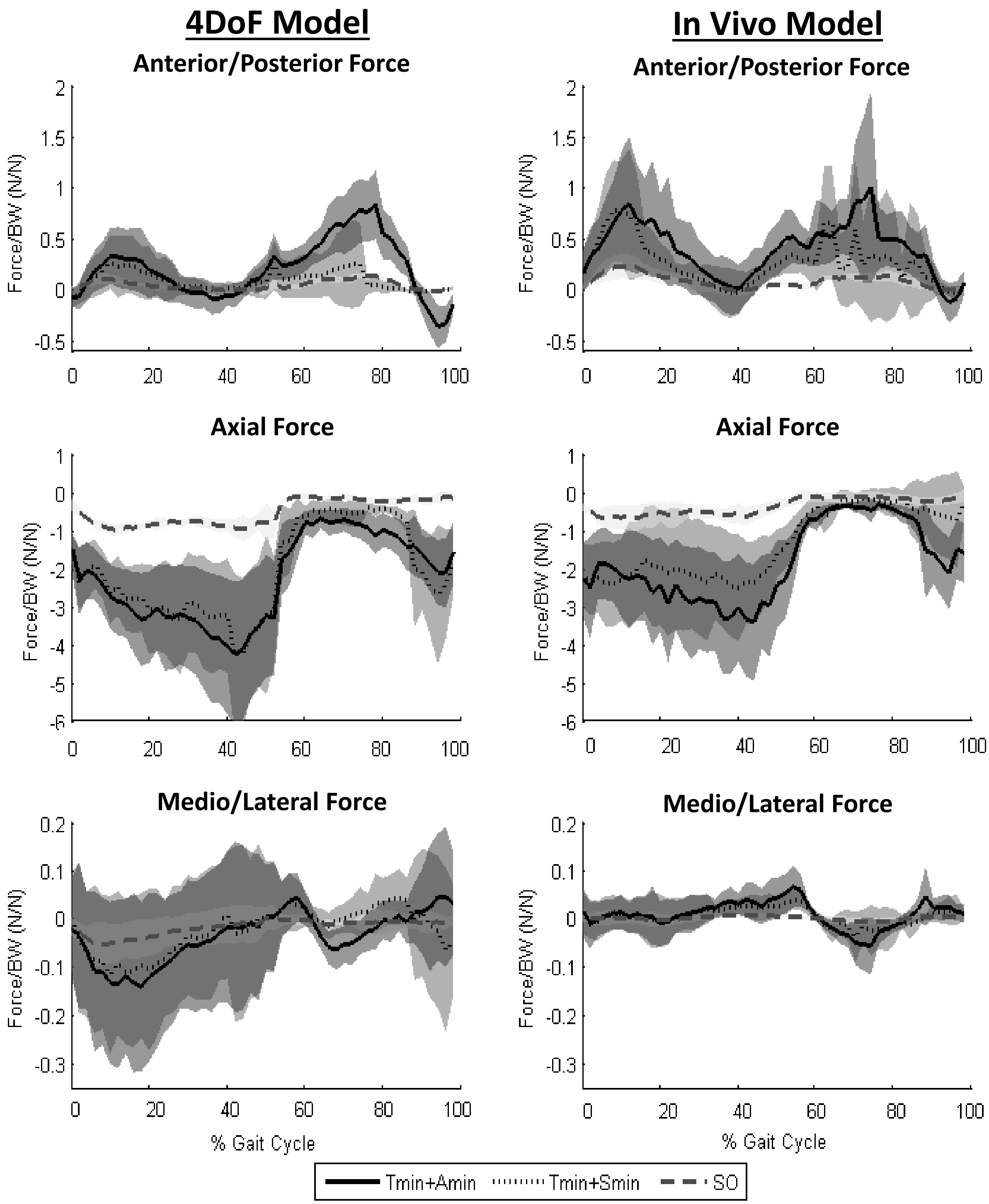

Figure 3.5: Average (±stdev) between subjects of bodyweight normalized knee joint contact loading in the tibial reference frame resulting from the predicted muscle activation profiles from each of the simulation conditions for the 4DoF knee model and for the In-Vivo knee model.

DISCUSSION

The main purpose of this study was to examine the effect of adding In-Vivo based joint kinematic constraints within a musculoskeletal model on muscle activation predictions from a forward-inverse dynamics simulation framework and subsequently on resulting knee joint contact loading. As an additional objective, the effect of changing the objective function within the optimization protocol of the FID framework using the In-Vivo or 4DoF models was observed.

Effect of Model Condition and Objective Function on Muscle Activation Predictions

When looking back at results obtained in (Potvin, Shourijeh, Smale, & Benoit, 2015), we see that although kinematics were changed significantly when adding bone-pin derived range of motion limits, hip, knee and ankle joint torques were not. Since the simulation framework optimizes its solution using knee joint net torque values, it could have been hypothesized that if this torque remains similar, predicted activation profiles would also be similar. On the other hand, the simulation framework also uses prescribed kinematic motion to determine moment arms of the muscles in the musculoskeletal model. As such, the change in joint kinematics introduced by the In-Vivo model should also have had an effect on simulation results. As demonstrated in (Potvin, Shourijeh, Smale, Spinello, et al., 2015) the change in objective function within the framework also had an influence on muscle activation predictions.

Comparing average correlation results using the physiologically inspired objective functions ($A_{min}$and S_{min}) from Table 3.1, we see that the MGAS and SOL muscles were well predicted (Pearson's correlation values 0.518<r<776), with higher values obtained with the In-Vivo model. TA muscle activation was also well predicted by the optimization protocol minimizing muscle activation (r=0.658 for the 4DoF model and r=0.600 for the In-Vivo model) but not as well by minimization of shear force loading at the knee (r=0.080 for the 4DoF model and r=0.506 for the In-Vivo model). As SO muscle activation predictions did not accurately recreate inverse dynamics calculated net joint torques in the simulation framework (see Appendices A4 of this thesis), the activation results appear questionable even though good correlations were identified for the MGAS (4DoF: r=0.796, In-Vivo: 0.72) and SOL (In-Vivo: r=0.758) muscles.

Overall, using minimization of muscle activation squared as the objective function within the optimization protocol of the FID simulation framework showed the strongest correlations for the most muscles although it was only for 3 muscles of the 8 that could be compared to EMG. These results are consistent with other studies that have shown gait patterns to be driven in such a way as to reduce energy expenditure and thus fatigue (Ackermann & van den Bogert, 2010).

Although correlation values were low for the other muscles, visual observations showed that RFEM and BFEM muscles did show some trend of increasing activation after peaks in EMG data although EMG values were low. Co-contraction of the BFEM and RFEM during the stance phase was also observed and suggests muscles working together to balance and stabilize the knee.

Correlation comparisons give us an idea of curve shape, but RMSE analysis also revealed if there were large differences between predicted muscle activity and experimental EMG magnitudes with both model conditions. Results for the TA, MGAS and SOL muscles suggest that the 4DoF model predicted values that were closer in magnitude to experimental EMG than the In-Vivo based model (0.253, 0.464, 0.533 respectively for the 4DoF model as compared to 0.417, 0.571 and 0.550 respectively for the In-Vivo model). For those muscles that did not show particular correlations with EMG data, RMSE values were generally lower by an average of 8% using the In-Vivo model rather than with the 4DoF model.

From both of these viewpoints, results show that changing the musculoskeletal model as well as changing the objective function will have an impact on final muscle activation predictions. Similar observations have been reported by (Cleather & Bull, 2011) although others report that changing the objective function within the simulation had minimal impacts on final predictions (Buchanan et al., 2005; Collins, 1995; Glitsch & Baumann, 1997). Such conclusions depend on how objective functions were defined within the simulation framework and to what degree each tested condition differed. The current study showed that the In-Vivo model using the A_{min} objective function had higher correlations for 2 of the three well correlated muscles (MGAS and SOL) than the 4DoF model. On the other hand, RMSE results showed higher values for the In-Vivo model. These results emphasize that choosing an objective function should be done carefully and its results reviewed with caution. As well, as was noted in (Crowninshield & Brand, 1981; Potvin, Shourijeh, Smale, Spinello, et al., 2015) observing good muscle activation correlations with experimental EMG does not necessarily guarantee the validity of the optimization's objective functions or the model. As can be seen in figures 3.2, 3.3 and 3.4, although some muscle activation patterns are well predicted, others have room for improvement. This could be achieved in various ways such as by modifying the musculoskeletal model parameters. For example, high levels of muscle activations were noted for the GLTMAX, GLTMED and TFL muscles. This could be adjusted by increasing the strength parameters of the various muscles within Xu et al.'s musculoskeletal model script. Improvements to the current model could also include the addition of synergistic muscle groups to actuate the various DoFs of the lower limb. This could reduce the forces applied to certain muscles by sharing the load with additional actuators and thus decrease each of their activations, which results of this experiment showed were higher than experimental EMG in many cases.

Effect of Model Condition on Joint Contact Loading

Multiple studies have reported estimated knee joint compressive loading values and maximal values range mostly around 2-3x bodyweight (D'Lima, Patil, Steklov, Slamin, & Colwell Jr., 2006; Fregly et al., 2011; Heinlein et al., 2009; Kim et al., 2009; Kutzner et al., 2010; Lin, Walter, Banks, Pandy, & Gregly, 2010; Schipplein & Andriacchi, 1991; Shelburne et al., 2006; Thambyah, Pereira, & Wyss, 2005) but also reached up to more double this value in certain cases (Fregly et al., 2011; Mikosz, Andriacchi, & Andersson, 1988; Seireg & Arvikar, 1975; Winby et al., 2009). The mean maximal compressive loading values shown in Figure 3.5 also fall within this range though perhaps on the high side high (approx. 4-4.5x bodyweight). Fewer studies like those using instrumented prostheses (Bergmann et al., 2014; Taylor, Heller, Bergmann, & Duda, 2004) report shear forces at the knee although values found in this study for medial/lateral and posterior/anterior forces are similar to those reported by (Bergmann et al., 2014; Heinlein et al., 2009; Mikosz et al., 1988).

Neglecting the knee joint ligaments in both model conditions likely resulted in some underestimation of joint contact loading as has been discussed in previous works (Sasaki & Neptune, 2010; Winby et al., 2009; Xu, 2013). Ligaments omitted in the musculoskeletal models used here are also important to provide additional moment arms to create forces counteracting joint contact loading when muscles are not sufficient (Cleather & Bull, 2011). It should also be kept in mind that since some predicted muscle activation patterns were not well correlated with experimental EMG, resulting knee joint contact loading is likely inaccurate.

In addition to changes in muscle activation predictions, the incorporation of bone-pin derived constraints in the In-Vivo model resulted in differences in joint contact loading compared to the 4DoF model as illustrated in Figure 3.5. Generally, force curves were somewhat similar between both model conditions, although a reduction of medio/lateral force (0.066 vs. 0.14 N/BW) and peak axial loading magnitude of the tibia (-3.42 vs -4.23 N/BW) was noted for the In-Vivo model. An increase in anterior/posterior loading is noted especially during the stance phase of gait with the In-Vivo model that may be caused by the increased activation levels from the BFEM muscles in the bone pin constrained simulation output compared to the unconstrained condition. As well, a sharp reduction variability, as evidenced by the decreased standard deviation was observed in the In-Vivo model, most notably for medio/lateral force (0.067N/BW vs 0.206 N/BW, or a 67% difference). This is to be expected as kinematic variability was limited when using the bone pin derived constraints (Potvin, Shourijeh, Smale, & Benoit, 2015).

CONCLUSION

The objective function guiding the control of muscles in the human body during various activities has yet to be defined and may be a combination of various strategies. The functions tested in this study and in a related previous one (Potvin, Shourijeh, Smale, Spinello, et al., 2015) are only a few simple examples meant to highlight the variety of possible options to be explored which are based on a physiological principle. Similarly, using an in vivo kinematics derived knee joint is a simple way in which to ensure realistic ranges of motion are obtained. Although the muscle activation changes were relatively small, gait is primarily a sagittal plane movement and its effects may be more pronounced for the simulation of more dynamic tasks, similar to those from which the In-Vivo model was derived (cutting and hoping motions). Nevertheless, if the goal of a musculoskeletal model is to achieve a physiological representation of muscle activations and forces, optimization strategies and joint models which are physiologically representative are crucial step in obtaining accurate information. Based on our results, the In-Vivo model showed more realistic kinematics for the knee joint, reduced simulated force variability, and remained consistent in muscle activation predictions when compared to the 4DoF model. Taken together, we believe that incorporating our in-vivo model into existing frameworks can improve the biofidelity of musculoskeletal models.

REFERENCES

Ackermann, M., & van den Bogert, A. J. (2010). Optimality principles for model-based prediction of human gait. *Journal of Biomechanics*, *43*(6), 1055–1050.

Alexander, E. J., & Andriacchi, T. P. (2001). Correcting for deformation in skin-based marker systems. *Journal of Biomechanics*, *34*(3), 355–361.

Andersen, M. S., Benoit, D. L., Damsgaard, M., Ramsey, D. K., & Rasmussen, J. (2010). Do Kinematic Models Reduce the Effects of Soft Tissue Artefacts in Skin Marker-Based Motion analysis? An In-Vivo Study of Knee Kinematics. *Journal of Biomechanics*, *43*, 268–273.

Andersen, M. S., Damsgaard, M., Rasmussen, J., Ramsey, D. K., & Benoit, D. L. (2012). A linear soft tissue artefact model for human movement analysis: Proof of concept using in vivo data. *Gait & Posture*, *35*(4), 606–611.

Anderson, F. C., & Pandy, M. G. (2001). Dynamic Optimization of Human Walking. *Journal of Biomechanical Engineering*, *123*.

Andriacchi, T. P., Alexander, E. J., Toney, M. K., Dyrby, C., & Sum, J. (1998). A point cluster method for in vivo motion analysis: applied to a study of knee kinematics. *Journal of Biomechanics*, *120*.

Benoit, D. L., Damsgaard, M., & Andersen, M. S. (2015). Surface marker cluster translation, rotation, scaling and deformation: Their contribution to soft tissue artefact and impact on knee joint kinematics. *Journal of Biomechanics*, *48*(10).

Benoit, D. L., Ramsey, D. K., Lamontagne, M., Xu, L., Wretenberg, P., & Renstrom, P. (2006). Effect of skin movement artifact on knee kinematics during gait and cutting motions measured in vivo. *Gait & Posture*, *24*, 152–164.

Benoit, D. L., Ramsey, D. K., Lamontagne, M., Xu, L., Wretenberg, P., & Renstrom, P. (2007). In Vivo Knee Kinematics during Gait Reveals New Rotation Profiles and Smaller Translations. *Clinical Orthopaedics and Related Research*, *454*, 81–88.

Bergmann, G., Bender, A., Graichen, F., Dymke, J., Rohlmann, A., Trepczynski, A., … Kutzner, I. (2014). Standardized loads acting in knee implants. *PLOS One*, *9*(1).

Bergmark, A. (1989). Stability of the lumbar spine - A study in mechanical engineering. *Acta Orthopaedica Scandinavica Supplementum*, *60*(230).

Besier, T., Fredericson, M., Gold, G. E., Beaupre, G. S., & Delp, S. L. (2009). Knee muscle forces during walking and running in patellofemoral pain patients and pain-free controls. *Journal of Biomechanics*, *42*(7).

Buchanan, T. S., Lloyd, D. G., Manal, K., & Besier, T. F. (2005). Estimation of Muscle Forces and Joint Moments Using a Forward-Inverse Dynamics Model. *Medicine and Science in Sports & Exercise*.

Cao, E., Inoue, Y., Liu, T., & Shibata, K. (2013). An inverse dynamic approach for quantitative muscle force estimation during human standing-up process. *Journal of Biomechanical Science and Engineering*, *8*(1).

Cappozzo, A., Capello, A., Croce, U. D., & Pensalfini, F. (1997). Surface-marker cluster design criteria for 3D bone movement reconstruction. *IEEE Transactions on Biomedical Engineering*, *44*(11).

Cavanagh, P. R., & Komi, P. V. (1979). Electromechanical delay in human skeletal muscle under concentric and eccentric contractions. *European Journal of Applied Physiology and Occupational Physiology*, *42*(3), 159–163.

Cerveri, P., Pedotti, A., & Ferrigno, G. (2005). Kinematical models to reduce the effect of skin artifact on marker-based human motion estimation. *Journal of Biomechanics*, *38*(11).

Cleather, D. J., & Bull, A. M. J. (2011). An optimization-based simultaneous approach to the determination of muscular, ligamentous, and joint contact forces provides insight into musculoligamentous interaction. *Annals of Biomedical Engineering*, *39*(7), 1925–1934.

Collins, J. J. (1995). The redundant nature of locomotor optimization laws. *Journal of Biomechanics*, *28*(3), 251–267.

Crowninshield, R. D., & Brand, R. A. (1981). A physiologically based criterion of muscle force prediction in locomotion. *Journal of Biomechanics*, *14*(11), 793–801.

De Groote, F., Pipeleers, G., Jonkers, I., Demeulenaere, B., Patten, C., Swevers, J., & De Schutter, J. (2009). A physiology based inverse dynamic analysis of human gait: potential and perspectives. *Computer Methods in Biomechanics and Biomedical Engineering*, *12*(5).

Delp, S. L., Loan, P., Hoy, M. G., Zajac, F. E., Topp, E. L., & Rosen, J. M. (1990). An Interactive Graphics-Based Model of the Lower Extremity to Study Orthopaedic Surgical Procedures. *IEEE Transactions on Biomedical Engineering*, *37*(8).

D'Lima, D. D., Patil, S., Steklov, N., Slamin, J. E., & Colwell Jr., C. W. (2006). Tibial forces measured in vivo after total knee arthroplasty. *The Journal of Arthroplasty*, *21*(2).

Dumas, R., Moissenet, F., Gasparutto, X., & Cheze, L. (2012). Influence of joint models on lower-limb musculo-tendon forces and three-dimensional joint reaction forces during gait. *Journal of Engineering in Medicine*, *226*(2), 146–160.

Duprey, S., Cheze, L., & Dumas, R. (2010). Influence of joint constraints on lower limb kinematics estimation from skin markers using global optimization. *Journal of Biomechanics*, *43*, 2858–2862.

Fregly, B. J., Besier, T. F., Lloyd, D. G., Delp, S. L., Banks, S. A., Pandy, M. G., & D'Lima, D. D. (2011). Grand Challenge Competition to predict in vivo knee loads. *Journal of Orthopaedic Research*.

Gasparutto, X., Sancisi, N., Jacquelin, E., Parenti-Castelli, V., & Dumas, R. (2015). Validation of a multi-body optimization with knee kinematic models including ligament constraints. *Journal of Biomechanics*, *48*, 1141–1146.

Glitsch, U., & Baumann, W. (1997). The three-dimensional determination of internal loads in the lower extremity. *Journal of Biomechanics*, *30*(11/12), 1123–1131.

Heinlein, B., Kutzner, I., Graichen, F., Bender, A., Rohlmann, A., Halder, A., … Bergmann, G. (2009). ESB clinical biomechanics award 2008: Complete data of total knee replacement loading for level walking and stair climbing measured in vivo with a follow-up of 6-10 months. *Clinical Biomechanics*, *24*, 315–326.

Hof, A. L. (1997). The relationship between electromyogram and muscle force. *Sportverletz Sportschaden*, *11*(3), 79–86.

Hug, F., Hodges, P. W., & Tucker, K. (2015). Muscle force cannot be directly inferred fom muscle activation: Illustrated by the proposed imbalance of force between vasus medialis and lateralis in people with patellofemoral pain. *Journal of Orthopaedic & Sports Physical Therapy*, *45*(5).

Kadaba MP, R. H., & Wootten, M. E. (1990). Measurement of lower extremity kinematics during level walking. *Orthopaedic Research*, *8*(3), 383–392.

Kim, H. J., Fernandez, J. W., Akbarshahi, M., Walter, J. P., Fregly, B. J., & Pandy, M. G. (2009). Evaluation of predicted knee-joint muscle forces during gait using and instrumented knee implant. *Journal of Orthopaedic Research*.

Kinney, A. L., Besier, T. F., D'Lima, D. D., & Fregly, B. J. (2013). Update on Grand Challenge competition to predict in vivo knee loads. *Journal of Biomechanical Engineering*, *135*.

Komistek, R. D., Kane, T. R., Mahfouz, M., Ochoa, J. A., & Dennis, D. A. (2005). Knee mechanics: a review of past and present techniques to determine in vivo loads. *Journal of Biomechanics*, *38*, 215–228.

Kutzner, I., Heinlein, B., Graichen, F., Bender, A., Rohlmann, A., Halder, A., … Bergmann, G. (2010). Loading of the knee joint during activities of daily living measured in vivo in five subjects. *Journal of Biomechanics*, *43*(11).

Li, K., Zheng, L., Tashman, S., & Zhang, X. (2012). The inaccuracy of surface-measured model-derived tibiofemoral kinematics. *Journal of Biomechanics*, *45*(15), 2719–2723.

Lin, Y., Walter, J. P., Banks, S. A., Pandy, M. G., & Gregly, B. J. (2010). Simultaneous prediction of muscle and contact forces in the knee during gait. *Journal of Biomechanics*, *43*, 945–952.

Lloyd, D. G., & Buchanan, T. S. (1996). A model of load sharing between muscles and soft tissues at the human knee during static tasks. *Journal of Biomechanical Engineering*, *118*.

Lu, T. W., & O'Connor, J. J. (1999). Bone position estimation from skin marker coordinates using global optimisation with joint constraints. *Journal of Biomechanics*, *32*(2), 129–134.

Mikosz, R. P., Andriacchi, T. P., & Andersson, G. B. J. (1988). Model analysis of factors influencing the prediction of muscle forces at the knee. *Journal of Orthopaedic Research*, *6*, 205–214.

Millard, M., Uchida, T., Seth, A., & Delp, S. L. (2013). Flexing computational muscle: modeling and simulation of musculotendon dynamics. *ASME Journal of Biomechanical Engineering*, *135*(2).

Modenese, L., Phillips, A. T. M., & Bull, A. M. J. (2011). An open source lower limb model: Hip joint validation. *Journal of Biomechanics*, *44*(12), 2185–2193.

Moengin, P. (2010). Polynomial Penalty Method for Solving Linear Programming Problems. *IAENG International Journal of Applied Mathematics*, *40*(3).

Moengin, P. (2011). Exponential Penalty Methods for Solving Linear Programming Problems (Vol. 2). Presented at the World Congress on Engineering and Computer Science, San Fransisco, USA.

Murphy, F. H. (1974). A Class of Exponential Penatly Functions. *SIAM J.*, *12*(4).

Potvin, B. M., Shourijeh, M. S., Smale, K. B., & Benoit, D. L. (2015). Effect of adding in-vivo based kinematic knee joint constraints on inverse kinematics and dynamics results in musculoskeletal modeling using OpenSim. *(Unpublished)*.

Potvin, B. M., Shourijeh, M. S., Smale, K. B., Spinello, D., & Benoit, D. L. (2015). Musculoskeletal Knee Joint Stability Inspired Optimization of Forward-Inverse Dynamics Simulations to Predict Muscle Activations. *(Unpublished)*.

Reinbolt, J. A., Schutte, J. F., Fregly, B. J., Koh, B. I., Haftka, R. T., George, A. D., & Mitchell, K. H. (2005). Determination of patient-specific multi-joint kinematic models through two-level optimization. *Journal of Biomechanics*, *38*, 621–626.

Roberts, T. J., & Gabaldon, A. M. (2008). Interpreting muscle function from EMG: Lessons learned from direct measurements of muscle force. *Integrative and Comparative Biology*, *48*(2), 312–320.

Sartori, M., Farina, D., & Lloyd, D. G. (2014). Hybrid neuromusculoskeletal modeling to best track joint moments using a balance between muscle excitations derived from electromyograms and optimization. *Journal of Biomechanics*, *47*, 3613–3621.

Sasaki, K., & Neptune, R. R. (2010). Individual Muscle Contributions to the Axial Knee Joint Contact Force during Normal Walking. *Journal of Biomechanics*, *43*(14), 2780–2784.

Schipplein, O. D., & Andriacchi, T. P. (1991). Interaction Between Active and Passive Knee Stabilizers During Level Walking. *Journal of Orthopaedic Research*, *9*, 113–119.

Seireg, A., & Arvikar, R. J. (1975). The prediction of muscular load sharing and joint forces in the lower extremities during walking. *Journal of Biomechanics*, *8*, 89–102.

Shelburne, K. B., Torry, M. R., & Pandy, M. G. (2006). Contributions of muscles, ligaments and the ground reaction force to tibiofemoral joint loading during normal gait. *Journal of Orthopaedic Research*.

Shourijeh, M. S., & Benoit, D. L. (2015). Hybrid forward inverse dynamics framework for human musculoskeletal simulations. Presented at the International Society of Biomechanics, Glasgow.

Shourijeh, M. S., & McPhee, J. (2014). Forward Dynamic Optimization of Human Gait Simulations: A Global Parameterization Approach. *Journal of Computational and Nonlinear Dynamics*, *9*(3).

Shourijeh, M. S., Smale, K. B., Potvin, B. M., & Benoit, D. L. (2016). A Forward Inverse Dynamics Framework for Human Musculoskeletal Simulations. *Journal of Biomechanics*. http://doi.org/http://dx.doi.org/10.1016/j.jbiomech.2016.04.007

Taylor, W. R., Heller, M. O., Bergmann, G., & Duda, G. N. (2004). Tibio-femoral loading during human gait and stair climbing. *Journal of Orthopaedic Research*, *22*(3), 625–32.

Thambyah, A., Pereira, B. P., & Wyss, U. (2005). Estimation of bone-on-bone contact forces in the tibiofemoral joint during walking. *The Knee*, *12*(5).

Thelen, D. G. (2003). Adjustment of Muscle Mechanics Model Parameters to Simulate Dynamic Contractions in Older Adults. *Transactions of the ASME*, *125*.

Van Dieen, J. H., Thissen, C. E. A. M., Van de Ven, A. J. G. M., & Toussaint, H. M. (1991). The electro-mechanical delay of the erector spinae muscle: influence of rate of force development, fatigue and electrode location. *European Journal of Applied Physiology and Occupational Physiology*, *63*, 216–222.

Winby, C. R., Gerus, P., Kirk, T. B., & Lloyd, D. G. (2013). Correlation between EMG-based co-activation measures and medial and lateral compartment loads of the knee during gait. *Clinical Biomechanics*, *28*, 1014–1019.

Winby, C. R., Lloyd, D. G., Besier, T. F., & Kirk, T. B. (2009). Muscle and External Load Contribution to Knee Joint contact Loads During Normal Gait. *Journal of Biomechanics*, *42*, 2294–2300.

Wong, Y.-M., & Ng, G. Y. F. (2006). Surface electrode placement affects the EMG recordings of the quadriceps muscles. *Physical Therapy in Sport*, *7*(3), 122–127.

Xiao, M., & Higginson, J. S. (2008). Muscle function may depend on model selection in forward simulation of normal walking. *Journal of Biomechanics*, *41*(15), 3236–3242.

Xu, H. (2013). *Development of a Musculoskeletal Model to Determine Knee Contact Force During Walking on Ballast Using Opensim Simulation*. University of Utah, Utah, United States.

Xu, H., Bloswick, D., & Merryweather, A. (2014). An improved OpenSim gait model with multiple degrees of freedom knee joint and knee ligaments. *Computer Methods in Biomechanics and Biomedical Engineering*.

Yamaguchi, G. T., & Zajac, F. E. (1989). A planar model of the knee joint to characterize the knee extensor mechanism. *Journal of Biomechanics*, *22*(1), 1–10.

Chapter 4 – Summary of Research Findings and Closing Remarks

4.1 Summary of Key Results

The first step in the work of this thesis, described in the first manuscript, involved creating boundary envelopes within which to constrain kinematics in the non-principal degrees of freedom of the knee joint in order to reduce the effect of soft tissue artifact. Results showed that adding these constraints to a musculoskeletal model with a knee joint with 4, 5 and 6 DoFs resulted in significant differences in kinematics, especially for the knee joint`s internal/external rotation and translation degrees of freedom as shown in Figure 1.3 of the first manuscript.

The addition of kinematic bone-pin constraints created more physiologically realistic motion profiles than what skin-mounted marker derived joint kinematics described. Since the original work of this part of the thesis was completed, additional work has applied these constraints to other motion trials (cutting and hopping) and also found significant differences and more realistic segment motions (unpublished). Kinematics in the principal DoFs as in the case of hip, knee and ankle flexion/extension, remain adequately accurate when using only skin mounted markers. Results also showed similar trends as those shown in other studies using intra-cortical pins to determine kinematics (Benoit et al., 2007; Lafortune, Cavanagh, Sommer, & Kalenak, 1992). The data used in this part of the work was based on experimental data from young and healthy adult males. It should therefore be noted that kinematic constraints may be different in other populations such as those with pathological musculoskeletal disorders.

Following the determination of kinematics derived from bone pin data, and as described in the second and third journal manuscripts in Chapter 3, a forward/inverse dynamics simulation framework was adapted to the musculoskeletal model and set up to predict muscle activation profiles during a gait cycle utilizing different optimization objective functions addressing the muscle redundancy problem presented by the knee joint and the lower limb's multiple muscles. The main objective of the second manuscript in Chapter 3 was to observe differences in muscle activation predictions between optimizations using several objective functions. Some of these results were also presented at the International Society of Biomechanics conference in Glasgow in 2015. The poster for this conference can be found in Appendices A5. In the third manuscript, the main goal was to see if incorporating the kinematics derived from bone pin data to the simulations made differences as well.

In many studies, objective functions within optimization protocols are defined to reduce energetic or metabolic costs, assuming the human body moves in an efficient manner (Anderson & Pandy, 2001; Cao et al., 2013; Kim et al., 2009; Lloyd & Buchanan, 1996; Winby et al., 2009). In this thesis, this assumption was challenged by implementing new objectives for the optimization script. These objectives were inspired by multiple and various definitions of musculoskeletal joint stability and were defined to maximize total muscle activation, minimize knee joint shear loading and to maximize knee joint compression (axial) loading. These simulation results were also compared to simulations aiming to minimize total muscle activations, a commonly used objective function promoting efficiency. Simulations were run for gait trials using a musculoskeletal model with 4 DoFs at the knee and by a more flexible knee joint model with 5DoFs at the knee of which 4 were constrained by bone pin data (all but knee flexion/extension and distraction/compression).

Results, shown in Figures 2.2 and 2.3 of the second manuscript, of the unconstrained 4DoF knee model show that, at least for gait motion, minimizing activation was the objective function leading to the most similarities between muscle activation predictions and experimental EMG. Correlations, root mean square error and visual observations suggest that the tibialis anterior, medial gastrocnemius and soleus muscles were best predicted with this objective function while other muscles were less accurately simulated. Some trends were visually observed between EMG and activation predictions for the rectus femoris and biceps femoris muscles as well, although correlation values were low. Timing of muscle activations and force production for these muscle groups are also consistent with what may be expected during a gait cycle. Co-contraction of the RFEM and BFEM muscle groups can also be seen from these figures, which suggests both groups work together to maintain joint stability.

Predictions from the maximization of knee joint contact loading should be interpreted carefully as it was observed that the joint torque error resulting from these activations within the forward-inverse dynamics simulation framework was high. (Joint torque errors resulting from this objective function as well as the other functions tested in this thesis can be found in Appendices A4. Such high levels of joint torque errors were also observed when static optimization outputs directly from OpenSim were input into the framework. The increased error in joint torques would suggest that muscle activation predictions are invalid as torques are not reconstructed correctly and may indicate a technical problem in the OpenSim 3.2 scripts.

Simulations were run once more with the musculoskeletal model having kinematics constrained with the in-vivo derived bone pin range of motion envelopes and using optimization objective functions of minimization of total muscle activation as well as minimization of shear forces at the knee joint. As in the model condition used in the previous experiment, minimization of muscle activation prove to be more effective in predicting muscle activation patterns and signal intensity than minimization of shear force.

Activation prediction results are shown in Figure 3.2 from the third manuscript and are adjusted for best correlation between EMG and activation results because of the effects of electrochemical delay and of electrode positioning (Hug, Hodges, & Tucker, 2015; Van Dieen, Thissen, Van de Ven, & Toussaint, 1991; Wong & Ng, 2006).There were some prediction differences between the 4DoF model and the In-Vivo model. The in vivo model's muscle activations were more closely correlated to experimental EMG than the prescribed 4DoF model for the medial gastrocnemius (r=0.776 vs 0.725), soleus (r=0.771 vs 0.718) and showed good correlations with tibialis anterior predictions (r=0.600). Root mean square error showed similar values although the 4DoF model had slightly lower results for these three muscles (0.533, 0.253 and 0.464 respectively) compared to the In-Vivo model (0.550, 0.417 and 0.571 respectively).

Other muscles (rectus femoris, biceps femoris, gluteus maximus, gluteus medius, tensor fascia latae) for both the 4DoF and In Vivo models were not as well predicted (Pearson's correlation $0<r<0.298$) for a variety of possible reasons. The musculoskeletal model is a simplification of the human body and did not include all muscles actually present in the human lower limb. The addition of more muscle segments may have helped to reduce the loading from the muscles present within the model. As well, it should be considered that normalization methods for EMG using experimental maximum voluntary isometric contraction (MVIC) is not the same as the method used for activation predictions which is based on theoretical muscle strengths and properties. Changing muscle mechanical properties within the model may help fine tune results or adapt them to different populations.

Knee joint contact loading magnitudes were reduced and varied less among subjects in the in vivo model condition for compression and medio/lateral forces but increased for posterior/anterior loading, potentially due to increased degrees of freedom at the knee and tighter ranges of motion. Loading patterns and magnitudes fell within values obtained elsewhere in the literature from model results and instrumented prosthesis devices for flexion/extension DoFs

(D'Lima, Patil, Steklov, Slamin, & Colwell Jr., 2006; Fregly et al., 2011, 2011; Heinlein et al., 2009; Kim et al., 2009; Kutzner et al., 2010; Lin, Walter, Banks, Pandy, & Gregly, 2010; Mikosz, Andriacchi, & Andersson, 1988; Mikosz et al., 1988; Schipplein & Andriacchi, 1991; Seireg & Arvikar, 1975; Shelburne et al., 2006; Thambyah, Pereira, & Wyss, 2005; Winby et al., 2013) as well as in shear loading (Bergmann et al., 2014; Heinlein et al., 2009; Mikosz et al., 1988). Joint contact loading is illustrated in Figure 3.5.

4.2 Conclusion

Defining accurate joint kinematics is an essential part of successful musculoskeletal modeling. However, determining such kinematics is challenging for various reasons, notably that we cannot easily see what is actually occurring within a joint without invasive or costly measurement techniques and that the alternative, using motion capture systems to track movement using skin mounted markers is heavily influenced by soft tissue artifact. This thesis first focused on developing an easy to use and implement tool constraining joint kinematics in the non-principal degrees of freedom to realistic ranges of motion that based itself on valuable joint motion data obtained from in-vivo experiments using intra-cortical pins equipped with tracking markers. This tool provided more biofidelic motion for the knee joint and is a step forward in the quest to obtaining accurate joint kinematics for musculoskeletal modeling.

Following this step, this thesis showed that changing the objective function of an optimization protocol within a musculoskeletal simulation framework had an important effect on final model outputs. Changing joint kinematics to more physiologically realistic ones obtained in the first part of this work also had an effect on simulation predictions. This underlines the importance of furthering research in this regard as we have yet to define, both physiologically and mathematically, how the neuromuscular system is governed during various activities.

Knowing which muscles activation patterns contribute to joint stability could improve treatment and training protocols to get a patient back on track, using objective testing and experimental data (Hicks et al., 2015).

This thesis focused on self-selected pace level ground gait trials, a movement that has been shown to favor efficiency (Kim et al., 2009). The new objective functions added to the simulation framework in this project were therefore not as adept at predicting muscle activation profiles as the original function minimizing total muscle activation. However, it would be interesting to see how all these objective functions perform with different motion types such as the one and two legged squat motions, cutting motions or jumping as well.

From this thesis we can conclude that (1) using in-vivo inspired knee constraints will modify and generally improve musculoskeletal model simulations; (2) simulation outputs should be analyzed cautiously and in light of the optimisation used to solve the indeterminate problem posed by the many muscles of the human body; (3) Changing the objective function is only one way in which to improve existing models. Continued modifications and optimizations of musculoskeletal model parameters and definitions can and should be made to improve results and achieve physiologically representative simulation results.

Glossary

Abduction: Moving away from the body's frontal plane central axis

Adduction: Moving towards the body's frontal plane central axis

Anterior: Meaning "in front of". For the knee joint, anterior translation refers to movement towards the front of the knee

Co-contraction: Simultaneous contraction of two opposing muscles

Cost Function: See "Objective Function"

Degree of Freedom: Directions of movement. For the knee joint, there are 6 degrees of freedom in which the bones can move with relation to one another, 3 rotations and 3 translations

Distal: Away from the body's trunk. Ex. The femur's epicondyles are distal to the femoral head in relation to the trunk of the body.

Dynamics: The study of mechanics and the motion of bodies under the influence of forces and moments

Electromyography: Electric signal measurement from muscle tissue, commonly measured through skin surface electrodes placed on the area closest to the muscle belly

Forward dynamics: The calculation of joint forces and torques by converting muscle excitation signals to activations to muscle forces and then joint torques

Inverse dynamics: The calculation of joint forces and torques using body segment kinematics and measured external forces

In-Silico: Computer based testing

In-Vitro: Lab based testing

In-Vivo: Real world, live testing

Joint contact loading: Forces and moments created within a joint from ground reaction forces as well as tightened muscles accross the joint

Joint reaction loading: Net joint forces/moments calculated from inverse dynamics based on ground reaction forces

Kinematics: The study of mechanical motion without considering masses or forces

Musculoskeletal Model: A representation of a body including an anatomical and geometrical representation of muscles, ligaments and bones and mechanical representations of muscle tissues

Objective Function: The function that an optimization protocol seeks to maximize or minimize in order to find a suitable solution to a given indeterminate problem

Pennation Angle: Angle formed between its line of action and direction of muscle fibers

Posterior: Meaning “behind”. For the knee joint, posterior translation refers to movement towards the back of the knee

Proximal: Close to the body’s trunk as opposed to distal. The femoral head is proximal to the femoral epicondyles

Simulation Framework: Protocol used to run a simulation with all of its components

Soft tissue artifact: The motion of skin affecting measurements of bone motion within the body segment, typically observed during motion capture data collection

Static Optimization: Optimization of solutions by individual steps such as time frames over the course of a trial

Statistical Parametric Mapping: Statistical method that considers 1-D continuous data trajectories to find significance between measures taken over time (ex: marker or force plate trajectories)

Varus/Valgus: Terms used to describe angled position of segments. At the knee, varus refers to outward angled knees and valgus describes knees pointed inwards in the frontal plane

References

Ambegaonkar, J. P., Shultz, S. J., Perrin, D. H., Schmitz, R. J., Ackerman, T. A., & Schulz, M. R. (2011). Lower Body Stiffness and Muscle Activity Differences Between Female Dancers and Basketball Players During Drop Jumps. *Sport Health*, *3*(1).

Andersen, M. S., Benoit, D. L., Damsgaard, M., Ramsey, D. K., & Rasmussen, J. (2010). Do Kinematic Models Reduce the Effects of Soft Tissue Artefacts in Skin Marker-Based Motion analysis? An In-Vivo Study of Knee Kinematics. *Journal of Biomechanics*, *43*, 268–273.

Anderson, F. C., & Pandy, M. G. (2001). Dynamic Optimization of Human Walking. *Journal of Biomechanical Engineering*, *123*.

Arnold, E. M., Ward, S. R., Lieber, R. L., & Delp, S. L. (2010). A Model of the Lower Limb for Analysis of Human Movement. *Annals of Biomedical Engineering*, *38*(2), 269–279.

Baratta, R., Solomonow, M., Zhou, B. H., Letson, D., Chuinard, R., & D'Ambrosia, R. (1988). Muscular coactivation - The role of the antagonist musculature in maintaining knee stability. *The American Journal of Sports Medicine*, *16*(2).

Behm, D. G., Anderson, K., & Curnew, R. S. (2002). Muscle force and activation under stable and unstable conditions. *Journal of Strength and Conditioning Research*, *16*(3), 416–422.

Benoit, D. L., Ramsey, D. K., Lamontagne, M., Xu, L., Wretenberg, P., & Renstrom, P. (2006). Effect of skin movement artifact on knee kinematics during gait and cutting motions measured in vivo. *Gait & Posture*, *24*, 152–164.

Benoit, D. L., Ramsey, D. K., Lamontagne, M., Xu, L., Wretenberg, P., & Renstrom, P. (2007). In Vivo Knee Kinematics during Gait Reveals New Rotation Profiles and Smaller Translations. *Clinical Orthopaedics and Related Research*, *454*, 81–88.

Bergmann, G., Bender, A., Graichen, F., Dymke, J., Rohlmann, A., Trepczynski, A., … Kutzner, I. (2014). Standardized loads acting in knee implants. *PLOS One*, *9*(1).

Bergmark, A. (1989). Stability of the lumbar spine - A study in mechanical engineering. *Acta Orthopaedica Scandinavica Supplementum*, *60*(230).

Besier, T., Fredericson, M., Gold, G. E., Beaupre, G. S., & Delp, S. L. (2009). Knee muscle forces during walking and running in patellofemoral pain patients and pain-free controls. *Journal of Biomechanics*, *42*(7).

Bisi, M. C., Riva, F., & Stagni, R. (2014). Measures of gait stability: performance on adults and toddlers at the beginning of independent walking. *Journal of Neuroengineering and Rehabilitation*, *11*(131).

Brand, R. A., Crowninshield, R. D., Wittstock, C. E., Pedersen, D. R., Clark, C. R., & Van Krieken, F. M. (1982). A model of lower extremity muscular anatomy. *Journal of Biomechanical Engineering*, *104*(4).

Buchanan, T. S., & Lloyd, D. G. (1995). Muscle activity is different for humands performing static tasks which require force control and position control. *Neuroscience Letters*, *194*, 61–64.

Buchanan, T. S., Lloyd, D. G., Manal, K., & Besier, T. F. (2004). Neuromusculoskeletal Modeling : Estimation of Muscle Forces and Joint Moments and Movements from Measurements of Neural Command. *Journal of Applied Biomechanics*, *20*(4), 367–395.

Buchanan, T. S., Lloyd, D. G., Manal, K., & Besier, T. F. (2005). Estimation of Muscle Forces and Joint Moments Using a Forward-Inverse Dynamics Model. *Medicine and Science in Sports & Exercise*.

Buchanan, T. S., & Shreeve, D. A. (1996). An evaluation of optimization techniques for the prediction of muscle activation patterns during isometric tasks. *Journal of Biomechanical Engineering*, *118*.

Cadova, M. (2013). Use of OpenSim and Anybody modelling software for dynamic simulation of the human masticatory system. *18th International Symposium on Computational Biomechanics in Ulm CBU.*

Cao, E., Inoue, Y., Liu, T., & Shibata, K. (2013). An inverse dynamic approach for quantitative muscle force estimation during human standing-up process. *Journal of Biomechanical Science and Engineering*, *8*(1).

Cappozzo, A., Catani, F., Leardini, A., Benedetti, M. G., & Della Croce, U. (1996). Position and orientation in space of bones during movement: experimental artifacts. *Clinical Biomechanics*, *11*.

Cleather, D. J., & Bull, A. M. J. (2011). An optimization-based simultaneous approach to the determination of muscular, ligamentous, and joint contact forces provides insight into musculoligamentous interaction. *Annals of Biomedical Engineering*, *39*(7), 1925–1934.

Collins, J. J. (1995). The redundant nature of locomotor optimization laws. *Journal of Biomechanics*, *28*(3), 251–267.

Corazza, S., Mundermann, L., Chaudhari, A. M., Demattio, T., Cobelli, C., & Andriacchi, T. P. (2006). A markerless motion capture system to study musculoskeletal biomechanics: Visual hull and simulated annealing approach. *Annals of Biomedical Engineering*, *34*(6), 1019–1029.

Coughlin, K. M., Incavo, S. J., Churchill, D. L., & Beynnon, B. D. (2003). Tibial Axis and Patellar Position Relative to the Femoral Epicondylar Axis During Squatting. *The Journal of Arthroplasty*, *18*(8).

Crowninshield, R. D., & Brand, R. A. (1981). A physiologically based criterion of muscle force prediction in locomotion. *Journal of Biomechanics*, *14*(11), 793–801.

Delp, S. L., Anderson, F. C., Arnold, A. S., Loan, P., Habib, A., John, C. T., … Thelen, D. G. (2007). OpenSim: Open-source software to create and analyze dynamic simulations of movement. *IEEE Transactions on Biomedical Engineering*, *54*(11).

Delp, S. L., Loan, P., Hoy, M. G., Zajac, F. E., Topp, E. L., & Rosen, J. M. (1990). An Interactive Graphics-Based Model of the Lower Extremity to Study Orthopaedic Surgical Procedures. *IEEE Transactions on Biomedical Engineering*, *37*(8).

De Luca, C. (1997). The Use of Surface Electromyography in Biomechanics. *Journal of Applied Biomechanics*, *13*(2), 125–163.

De Ridder, R., Willems, T., Vanrenterghem, J., Robinson, M. A., & Roosen, P. (2014). Lower limb landing biomechanics in subjects with chronic ankle instability. *Medicine and Science in Sports & Exercise*.

Derouin, A., & Potvin, J. (2005). Knee Stability: Mechanical Contributions of Individual Muscles. Presented at the ISB XXth congress - ASB 29th Annual Meeting.

D'Lima, D. D., Patil, S., Steklov, N., Slamin, J. E., & Colwell Jr., C. W. (2006). Tibial forces measured in vivo after total knee arthroplasty. *The Journal of Arthroplasty*, *21*(2).

Doorenbosch, C. A. M., & Harlaar, J. (2003). A clinically applicable EMG-force model to quantify active stabilization of the knee after a lesion of the anterior cruciate ligament. *Clinical Biomechanics*, *18*, 142–149.

Duprey, S., Cheze, L., & Dumas, R. (2010). Influence of joint constraints on lower limb kinematics estimation from skin markers using global optimization. *Journal of Biomechanics*, *43*, 2858–2862.

Epstein, M., & Herzog, W. (2003). Aspects of skeletal muscle modelling. *Philosophical Transactions of the Royal Society - Biological Sciences*, *358*, 1445–1452.

Erdemir, A., McLean, S., Herzog, W., & Van Den Bogert, A. J. (2007). Model-based estimation of muscle forces exerted during movements. *Clinical Biomechanics*, *22*, 131–154.

Flaxman, T. E., Speirs, A. D., & Benoit, D. L. (2012). Joint stabilisers or moment actuators: The role of knee joint muscles while weight-bearing. *Journal of Biomechanics*, *45*(15), 2570–2576.

Fregly, B. J., Besier, T. F., Lloyd, D. G., Delp, S. L., Banks, S. A., Pandy, M. G., & D'Lima, D. D. (2011). Grand Challenge Competition to predict in vivo knee loads. *Journal of Orthopaedic Research*.

Frigo, C., & Crenna, P. (2009). Multichannel SEMG in Clinical Gait Analysis: A Review and State-of-the-Art. *Clinical Biomechanics*, *24*, 236–245.

Friston, K. J., Holmes, A. P., Worsley, J. P., Frith, C. D., & Frackowiak, R. S. J. (1995). Statistical Parametric Maps in Functional Imaging: A General Linear Approach. *Human Brain Mapping*, *2*, 189–210.

Gasparutto, X., Sancisi, N., Jacquelin, E., Parenti-Castelli, V., & Dumas, R. (2015). Validation of a multi-body optimization with knee kinematic models including ligament constraints. *Journal of Biomechanics*, *48*, 1141–1146.

Giesl, P., Meisel, D., Scheurle, J., & Wagner, H. (2004). Stability analysis of the elbow with a load. *Journal of Theoretical Biology*, *228*, 115–125.

Giesl, P., & Wagner, H. (2007). Lyapunov function and the basin of attraction for a single-joint muscle-skeletal model. *Journal of Mathematical Biology*, *54*, 453–464.

Glitsch, U., & Baumann, W. (1997). The three-dimensional determination of internal loads in the lower extremity. *Journal of Biomechanics*, *30*(11/12), 1123–1131.

Hamner, S. R., Seth, A., & Delp, S. L. (2010). Muscle contributions to propulsion and support during running. *Journal of Biomechanics*, *43*(14).

Hasan, Z. (2005). The human motor-control system's response to mechanical perturbation:should it, can it and does it ensure stability? *Journal of Motor Behavior*, *37*, 484–493.

Heinlein, B., Kutzner, I., Graichen, F., Bender, A., Rohlmann, A., Halder, A., … Bergmann, G. (2009). ESB clinical biomechanics award 2008: Complete data of total knee replacement loading for level walking and stair climbing measured in vivo with a follow-up of 6-10 months. *Clinical Biomechanics*, *24*, 315–326.

Herzog, W. (1987). Considerations for predicting individual muscle forces in athletic movements. *International Journal of Sport Biomechanics*, *3*, 128–141.

Herzog, W. (1992). Sensitivity of muscle force estimations to changes in muscle input parameters using nonlinear optimization approaches. *Journal of Biomechanical Engineering*, *114*(2).

Hicks, J. L., Uchida, T. K., Seth, A., Rajagopal, A., & Delp, S. L. (2015). Is my model good enough? Best practices for verification and validation of musculoskeletal models and simulations of movement. *Journal of Biomechanical Engineering*, *137*.

Higginson, J. S., Ramsay, J. W., & Buchanan, T. S. (2012). Hybrid models of the neuromusculoskeletal system improve subject-specificity. *Proceedings of the Institution of Mechanical Engineers. Part H, Journal of Engineering in Medicine*, *226*(2), 113–119.

Hill, A. V. (1938). The heat of shortening and the dynamic constants of muscle. *Biophysics, Department of Physioogy, University College, London*.

Hof, A. L., & Van den Berg, J. W. (1981). EMG to force processing 1: An electrical analogue of the hill muscle model. *Journal of Biomechanics*, *14*(11), 747–753.

How RRA Works - OpenSim Documentation - Confluence. (2013). Retrieved October 10, 2014, from http://simtk-confluence.stanford.edu:8080/display/OpenSim/How+RRA+Works

Hug, F., Hodges, P. W., & Tucker, K. (2015). Muscle force cannot be directly inferred fom muscle activation: Illustrated by the proposed imbalance of force between vasus medialis and lateralis in people with patellofemoral pain. *Journal of Orthopaedic & Sports Physical Therapy*, *45*(5).

Hunter, L. C., Hendrix, E. C., & Dean, J. C. (2010). The cost of walking downhill: is the preferred gait energetically optimal? *Journal of Biomechanics*, *43*(10), 1910–1915.

Jacobs, J. J., Andersson, G. B. J., Bell, J. E., Weinstein, S. L., Dormans, J. P., Gnatz, S. M., … Yelin, E. H. (2008). The burden of musculoskeletal diseases. *Bone and Joint Decade*.

Kim, H. J., Fernandez, J. W., Akbarshahi, M., Walter, J. P., Fregly, B. J., & Pandy, M. G. (2009). Evaluation of predicted knee-joint muscle forces during gait using and instrumented knee implant. *Journal of Orthopaedic Research*.

Kinney, A. L., Besier, T. F., D’Lima, D. D., & Fregly, B. J. (2013). Update on Grand Challenge competition to predict in vivo knee loads. *Journal of Biomechanical Engineering*, *135*.

Knowlton, C. B., Wimmer, M. A., & Lundberg, H. J. (2012). Grand Challenge Competition: A Parametric Numerical model to Predict In-Vivo Medial and Lateral Knee Forces in Walking Gaits. In *Proceedings of the ASME 2012 Summer Bioengineering Conference*. Puerto Rico.

Kocmond, J. H., Delp, S. L., & Stern, S. H. (1995). Stability and Range of Motion of Insall-Burstein Condylar Prostheses - A Computer Simulation Study. *The Journal of Arthroplasty*, *10*(3).

Komistek, R. D., Kane, T. R., Mahfouz, M., Ochoa, J. A., & Dennis, D. A. (2005). Knee mechanics: a review of past and present techniques to determine in vivo loads. *Journal of Biomechanics*, *38*, 215–228.

Kuo, A. D. (1995). An Optimal Control Model for Analyzing Human Postural Balance. *IEEE Transactions on Biomedical Engineering*, *42*(1).

Kutzner, I., Heinlein, B., Graichen, F., Bender, A., Rohlmann, A., Halder, A., … Bergmann, G. (2010). Loading of the knee joint during activities of daily living measured in vivo in five subjects. *Journal of Biomechanics*, *43*(11).

Kwon, S., Kim, Y., & Kim, J. (2014). Movement Stability Analysis of Surface Electromyography-Based elbow Power Assistance. *IEEE Transactions on Biomedical Engineering*, *61*(4).

Lafortune, M. A., Cavanagh, P. R., Sommer, H. J., & Kalenak, A. (1992). Three-dimensional kinematics of the human knee during walking. *Journal of Biomechanics*, *25*(4), 347–357.

Leardini, A., Chiari, L., Della Croce, U., & Cappozzo, A. (2005). Human movement analysis using stereophotogrammetry Part 3. Soft tissue artifact assessment and compensation. *Gait & Posture*, *21*, 212–225.

Lin, Y., Walter, J. P., Banks, S. A., Pandy, M. G., & Gregly, B. J. (2010). Simultaneous prediction of muscle and contact forces in the knee during gait. *Journal of Biomechanics*, *43*, 945–952.

Lloyd, D. G., & Buchanan, T. S. (1996). A model of load sharing between muscles and soft tissues at the human knee during static tasks. *Journal of Biomechanical Engineering*, *118*.

Lloyd, D. G., & Buchanan, T. S. (2001). Strategies of muscular support of varus and valgus isometric loads at the human knee. *Journal of Biomechanics*, *34*, 1257–1267.

Maitland, M. E., Ajemian, S. V., & Suter, E. (1997). Quadriceps Femoris and Hamstring Muscle Function in a Person with an Unstable Knee. *Physical Therapy Journal*, *79*(1).

Manal, K., & Buchanan, T. S. (2003). A One-Parameter Neural Activation to Muscle Activation Model: Estimating Isometric Joint Moments from Electromyograms. *Journal of Biomechanics*, *36*, 1197–1202.

Manal, K., & Buchanan, T. S. (2013). An Electromyogram-Driven Musculoskeletal Model of the Knee to Predict In-Vivo Joint Contact Forces During Normal and Novel Gait Patterns. *Journal of Biomechanical Engineering*, *135*.

Mansouri, M., & Reinbolt, J. A. (2012). A platform for dynamic simulation and control of movement based on OpenSim and MatLab. *Journal of Biomechanics*, *45*, 1517–1521.

Marieb, E. (1998). *Anatomie et physiologie humaines* (2nd ed.). ERPI.

McLean, S. G., & Van Den Bogert, A. J. (2003). Development and validation of a 3D model to predict knee joint loading during dynamic movement. *Transactions of the ASME*, *125*, 864–874.

Menegaldo, L. L., & Oliveira, L. F. (2011). An EMG-driven model to evaluate quadriceps strengthening after and isokinetic training. *Procedia IUTAM*, *2*, 131–141.

Mikosz, R. P., Andriacchi, T. P., & Andersson, G. B. J. (1988). Model analysis of factors influencing the prediction of muscle forces at the knee. *Journal of Orthopaedic Research*, *6*, 205–214.

Millard, M., & Delp, S. (2012). A computationally efficient muscle model. In *Proceedings of the ASME 2012 Summer Bioengineering Conference*. Puerto Rico.

Millard, M., Uchida, T., Seth, A., & Delp, S. L. (2013). Flexing computational muscle: modeling and simulation of musculotendon dynamics. *ASME Journal of Biomechanical Engineering*, *135*(2).

Milner, T. E. (2002). Contribution of geometrey and joint stiffness to mechanical stability of the human arm. *Experimental Brain Research*, *143*, 515–519.

Modenese, L., Phillips, A. T. M., & Bull, A. M. J. (2011). An open source lower limb model: Hip joint validation. *Journal of Biomechanics*, *44*(12), 2185–2193.

Moengin, P. (2010). Polynomial Penalty Method for Solving Linear Programming Problems. *IAENG International Journal of Applied Mathematics*, *40*(3).

Moengin, P. (2011). Exponential Penalty Methods for Solving Linear Programming Problems (Vol. 2). Presented at the World Congress on Engineering and Computer Science, San Fransisco, USA.

Morrison, J. B. (1970). The mechanics of the knee joint in relation to normal walking. *Journal of Biomechanics*, *3*, 51–61.

Murphy, F. H. (1974). A Class of Exponential Penatly Functions. *SIAM J.*, *12*(4).

Pandy, M. G. (2001). Computer modeling and simulation of human movement. *Annual Review of Biomedical Engineering*, *3*, 245–273.

Pandy, M. G., Zajac, F. E., Sim, E., & Levine, W. S. (1990). An optimal control model for maximum-height human jumping. *Journal of Biomechanics*, *23*, 1185–1198.

Pataky, T. C. (2010). Generalized n-dimensional biomechanical field analysis using statistical parametric mapping. *Journal of Biomechanics*, *43*, 1976–1982.

Pataky, T. C. (2012). One-Dimensional statistical parametric mapping in Python. *Computer Methods in Biomechanics and Biomedical Engineering*, *15*(3), 295–301.

Pataky, T. C., Robinson, M. A., & Vanrenterghem, J. (2013). Vector field statistical analysis of kinematic and force trajectories. *Journal of Biomechanics*.

Pel, J. J. M., Spoor, C. W., Pool-Goudzwaard, A. L., Hoek Van Dijke, G. A., & Snijders, C. J. (2008). Biomechanical Analysis of Reducing Sacroiliac Joint Shear Load by Optimization of Pelvic Muscle and Ligament Forces. *Annals of Biomedical Engineering*, *36*(3), 415–424.

Petrella, A., Rasmussen, J., Al-Munajjed, A., Damsgaard, M., Lund, M., & Kiis, A. (2013). How good is good enough? Lessons in musculoskeletal model validation with the Anybody modeling system. *Journal of Medical Devices*, *7*.

Reinbolt, J. A., Schutte, J. F., Fregly, B. J., Koh, B. I., Haftka, R. T., George, A. D., & Mitchell, K. H. (2005). Determination of patient-specific multi-joint kinematic models through two-level optimization. *Journal of Biomechanics*, *38*, 621–626.

Reinbolt, J. A., Seth, A., & Delp, S. L. (2011). Simulation of human movement: applications using OpenSim. *Procedia IUTAM*, *2*, 186–198.

Riemann, B. L., & Lephart, S. M. (2002). The Sensorimotor System, Part II: The Role of Proprioception in Motor Control and Functional Joint Stability. *Journal of Athletic Training*, *37*(1), 80–84.

Roux, C. H., Guillemin, F., Boini, S., Longuetaud, F., Arnault, N., Hercberg, S., & Briancon, S. (2005). Impact of musculoskeletal disorders on quality of life: an inception cohort study. *Annals of the Rheumatic Diseases*, *64*, 606–611.

Rugh, W. J. (1996). *Linear System Theory* (2nd Edition). Prentice Hall.

Sanford, B. A., Williams, J. L., Zucker-Levin, A. R., & Mihalko, W. M. (2013). Tibiofemoral joint forces during the stance phase of gait after ACL reconstruction. *Open Journal of Biophysics*, *3*, 277–284.

Sartori, M., Farina, D., & Lloyd, D. G. (2014). Hybrid neuromusculoskeletal modeling to best track joint moments using a balance between muscle excitations derived from electromyograms and optimization. *Journal of Biomechanics*, *47*, 3613–3621.

Sasaki, K., & Neptune, R. R. (2010). Individual Muscle Contributions to the Axial Knee Joint Contact Force during Normal Walking. *Journal of Biomechanics*, *43*(14), 2780–2784.

Schipplein, O. D., & Andriacchi, T. P. (1991). Interaction Between Active and Passive Knee Stabilizers During Level Walking. *Journal of Orthopaedic Research*, *9*, 113–119.

Schmitt, L. C., & Rudolph, K. S. (2008). Muscle Stabilization Strategies in People with Medial Knee Osteoarthritis: The Effect of Instability. *Journal of Orthopaedic Research*, *26*, 1180–1185.

Seireg, A., & Arvikar, R. J. (1975). The prediction of muscular load sharing and joint forces in the lower extremities during walking. *Journal of Biomechanics*, *8*, 89–102.

Senavongse, W., Farahmand, F., Jones, J., Andersen, H., Bull, A. M. J., & Amis, A. A. (2003). Quantitative measurement of patellofemoral joint stability: force-displacement behavior of the human patella in vitro. *Journal of Orthopaedic Research*, *21*, 780–786.

Serrien, B., Blondeel, J., Clijsen, R., Goossens, M., & Baeyens, J. P. (2014). Analysis of 3D motion patterns with self-organising maps (SOM) and statistical parametric mapping (SPM): a methodological proposal. *Computer Methods in Biomechanics and Biomedical Engineering*, *17*(S1), 162–163.

Shelburne, K. B., Torry, M. R., & Pandy, M. G. (2006). Contributions of muscles, ligaments and the ground reaction force to tibiofemoral joint loading during normal gait. *Journal of Orthopaedic Research*.

Shourijeh, M. S., & Benoit, D. L. (2015). Hybrid forward inverse dynamics framework for human musculoskeletal simulations. Presented at the International Society of Biomechanics, Glasgow.

Shourijeh, M. S., & McPhee, J. (2014). Forward Dynamic Optimization of Human Gait Simulations: A Global Parameterization Approach. *Journal of Computational and Nonlinear Dynamics*, *9*(3).

Shourijeh, M. S., Smale, K. B., Potvin, B. M., & Benoit, D. L. (2016). A Forward Inverse Dynamics Framework for Human Musculoskeletal Simulations. *Journal of Biomechanics*. http://doi.org/http://dx.doi.org/10.1016/j.jbiomech.2016.04.007

Smith, A. J. J., Flaxman, T. E., Speirs, A. D., & Benoit, D. L. (2012). Reliability of knee joint muscle activity during weight bearing force control. *Journal of Electromyography and Kinesiology*, *22*(6), 914–922.

Solomonow, M., Baratta, R., Zhou, B. H., Shoji, H., Bose, W., Beck, C., & D'Ambrosia, R. (1987). The synergistic action of the anterior cruciate ligament and thigh muscles in maintaining joint stability. *The American Journal of Sports Medicine*, *15*(3).

Solomonow, M., & Krogsgaard, M. (2001). Sensorimotor control of knee stability. A review. *Scandinavian Journal of Medicine & Science in Sports*, *11*, 64–80.

Stashuk, D. (2001). EMG signal decomposition: how can it be accomplished and used? *Journal of Electromyography and Kinesiology*, *11*, 151–173.

Staudenmann, D. (2007). Effects of EMG processing on biomechanical models of muscle joint systems: Sensitivity of trunk muscle moments, spinal forces and stability. *Journal of Biomechanics*, *20*, 900–909.

Sturnieks, D. L., Besier, T. F., & Lloyd, D. G. (2011). Muscle activations to stabilize the knee following arthroscopic partial meniscectomy. *Clinical Biomechanics*, *26*, 292–297.

Szczerbik, E., & Kalinowska, M. (2011). The influence of knee marker placement error on evaluation of gait kinematic parameters. *Acta of Bioengineering and Biomechanics*, *13*(3), 43–46.

Thambyah, A., Pereira, B. P., & Wyss, U. (2005). Estimation of bone-on-bone contact forces in the tibiofemoral joint during walking. *The Knee*, *12*(5).

Thelen, D. G. (2003). Adjustment of Muscle Mechanics Model Parameters to Simulate Dynamic Contractions in Older Adults. *Transactions of the ASME, 125*.

Van Den Bogert, A. J., Gerritsen, K. G. M., & Cole, G. K. (1998). Human muscle modelling from a user's perspective. *Journal of Electromyography and Kinesiology*, *8*, 119–124.

Van Dieen, J. H., Thissen, C. E. A. M., Van de Ven, A. J. G. M., & Toussaint, H. M. (1991). The electro-mechanical delay of the erector spinae muscle: influence of rate of force development, fatigue and electrode location. *European Journal of Applied Physiology and Occupational Physiology*, *63*, 216–222.

Vanheule, V., Andersen, M. S., Wirix-Speetjens, R., Jonkers, I., Victor, J., & Vander Sloten, J. (2013). Modeling of patient-specific knee kinematics and ligament behavior using force dependent kinematics. *XXIV Congress of the International Society of Biomechanics*.

Vanrenterghem, J., Venables, E., Pataky, T. C., & Robinson, M. A. (2012). The effect of running speed on knee mechanical loading in females during side cutting. *Journal of Biomechanics*, *45*, 2444–2449.

Wagner, H., Giesl, P., & Blickhan, R. (2007). Musculoskeletal Stabilization of the Elbow - Complex or Real. *Journal of Mechanics in Medicine and Biology*, *7*(3).

Walter, J. P., Kinney, A. L., Banks, S. A., D'Lima, D. D., Besier, T. F., Lloyd, D. G., & Fregly, B. J. (2013). Muscle Synergies May Improve Optimization Prediction of Knee Contact Forces During Walking. *Journal of Biomechanical Engineering*, *136*(2).

Wibawa, A. D., Verdonschot, N., Halbertsma, J. P. K., Burgerhof, J. G. M., Diercks, R. L., & Verkerke, G. J. (2013). Lower limb musculoskeletal model validation during one legged forward hopping and side jumping in healthy subjects using EMG. Presented at the International Conference HCI International, Las Vegas, NV, USA.

Williams, G. N., Chmielewski, T., Rudolph, K. S., Buchanan, T. S., & Snyder-Mackler, L. (2001). Dynamic Knee Stability: Current Theory and Implications for clinicians and Scientists. *Journal of Orthopaedic & Sports Physical Therapy*, *31*(10), 546–566.

Winby, C. R., Gerus, P., Kirk, T. B., & Lloyd, D. G. (2013). Correlation between EMG-based co-activation measures and medial and lateral compartment loads of the knee during gait. *Clinical Biomechanics*, *28*, 1014–1019.

Winby, C. R., Lloyd, D. G., Besier, T. F., & Kirk, T. B. (2009). Muscle and External Load Contribution to Knee Joint contact Loads During Normal Gait. *Journal of Biomechanics*, *42*, 2294–2300.

Winter, D. (2004). *Biomechanics and Motor Control of Human Movement* (3rd Edition).

Winters, J. M. (1995). An improved muscle-reflex actuator for use in large-scale neuromusculoskeletal models. *Annals of Biomedical Engineering*, *23*, 359–374.

Wong, Y.-M., & Ng, G. Y. F. (2006). Surface electrode placement affects the EMG recordings of the quadriceps muscles. *Physical Therapy in Sport*, *7*(3), 122–127.

Xu, H. (2013). *Development of a Musculoskeletal Model to Determine Knee Contact Force During Walking on Ballast Using Opensim Simulation*. University of Utah, Utah, United States.

Xu, H., Bloswick, D., & Merryweather, A. (2014). An improved OpenSim gait model with multiple degrees of freedom knee joint and knee ligaments. *Computer Methods in Biomechanics and Biomedical Engineering*.

Yamaguchi, G. T., & Zajac, F. E. (1989). A planar model of the knee joint to characterize the knee extensor mechanism. *Journal of Biomechanics*, *22*(1), 1–10.

Appendices

Appendices A1: Patella definition scripts

Original model file: Note the parent body is the tibia and only flexion/extension(rotation1), anterior/posterior translation (translation1) and distal/proximal translation (translation2) are defined. Other DoFs are left at zero and omitted here for conciseness.

```
<CustomJoint name="tib_pat_r">
<!--Name of the parent body to which this joint connects its owner body.-->
<parent_body>tibia_r</parent_body>
<!--Location of the joint in the parent body specified in the parent reference frame. Default is (0,0,0).-->
<location_in_parent>0 0 0</location_in_parent>
<!--Orientation of the joint in the parent body specified in the parent reference frame. Euler XYZ body-fixed
rotation angles are used to express the orientation. Default is (0,0,0).-->
<orientation_in_parent>0 0 0</orientation_in_parent>
<!--Location of the joint in the child body specified in the child reference frame. For SIMM models, this vector is
always the zero vector (i.e., the body reference frame coincides with the joint). -->
<location>0 0 0</location>
<!--Orientation of the joint in the owing body specified in the owning body reference frame.  Euler XYZ body-
fixed rotation angles are used to express the orientation. -->
<orientation>0 0 0</orientation>
<!--Set holding the generalized coordinates (q's) that parmeterize this joint.-->
.....
<SpatialTransform>
    <!--3 Axes for rotations are listed first.-->
    <TransformAxis name="rotation1">
        <!--Names of the coordinates that serve as the independent variables        of the transform function.-->
        <coordinates>knee_extend_pat_r</coordinates>
        <!--Rotation or translation axis for the transform.-->
        <axis>0 0 1</axis>
        <!--Transform function of the generalized coordinates used to       represent the amount of
        transformation along a specified axis.-->
        <function>
            <SimmSpline>
                <x> -2.0944 -1.99997 -1.45752 -0.526391 0.0279253 0.174533</x>
                <y> 0.308051 0.308051 0.306305 0.270177 -0.037001 -0.279951</y>
            </SimmSpline>
        </function>
    </TransformAxis>
    <TransformAxis name="translation1">
        <!--Names of the coordinates that serve as the independent variables        of the transform function.-->
        <coordinates>knee_extend_pat_r</coordinates>
```

```
        <!--Rotation or translation axis for the transform.-->
        <axis>1 0 0</axis>
        <!--Transform function of the generalized coordinates used to       represent the amount of
        transformation along a specified axis.-->
        <function>
          <MultiplierFunction>
            <function>
              <SimmSpline>
                <x> -2.0944 -1.39626 -1.0472 -0.698132 -0.349066 -0.174533 0 0.00017453 0.00034907
                0.0872665 2.0944</x>
                <y> 0.0173 0.0324 0.0381 0.043 0.0469 0.0484 0.0496 0.0496 0.0496 0.0496 0.0496</y>
              </SimmSpline>
            </function>
            <scale>1</scale>
          </MultiplierFunction>
        </function>
      </TransformAxis>
      <TransformAxis name="translation2">
        <!--Names of the coordinates that serve as the independent variables       of the transform function.-->
        <coordinates>knee_extend_pat_r</coordinates>
        <!--Rotation or translation axis for the transform.-->
        <axis>0 1 0</axis>
        <!--Transform function of the generalized coordinates used to       represent the amount of
        transformation along a specified axis.-->
        <function>
          <MultiplierFunction>
            <function>
              <SimmSpline>
                <x> -2.0944 -1.5708 -1.39626 -1.0472 -0.698132 -0.349066 -0.174533 0 0.00017453
                0.00034907 0.0872665 2.0944</x>
                <y> -0.0219 -0.0202 -0.02 -0.0204 -0.0211 -0.0219 -0.0223 -0.0227 -0.0227 -0.0227 -0.0227 -
                0.0227</y>
              </SimmSpline>
            </function>
            <scale>1</scale>
          </MultiplierFunction>
        </function>
      </TransformAxis>
```

Modified model file: Note the parent body is the femur and only flexion/extension(rotation1), anterior/posterior translation (translation1) and distal/proximal translation (translation2) are defined. Other DoFs are left at zero and omitted here for conciseness.

```
  <CustomJoint name="fem_pat_r">
  <!--Name of the parent body to which this joint connects its owner body.-->
  <parent_body>femur_r</parent_body>
```

```xml
<!--Location of the joint in the parent body specified in the parent reference frame. Default is (0,0,0).-->
<location_in_parent>0.04 -0.395 0</location_in_parent>
<!--Orientation of the joint in the parent body specified in the parent reference frame. Euler XYZ body-fixed rotation angles are used to express the orientation. Default is (0,0,0).-->
<orientation_in_parent>0 0 0</orientation_in_parent>
<!--Location of the joint in the child body specified in the child reference frame. For SIMM models, this vector is always the zero vector (i.e., the body reference frame coincides with the joint). -->
<location>0 0 0</location>
<!--Orientation of the joint in the owing body specified in the owning body reference frame.  Euler XYZ body-fixed rotation angles are used to express the orientation. -->
<orientation>0 0 0</orientation>
<!--Set holding the generalized coordinates (q's) that parmeterize this joint.-->
<SpatialTransform>
    <!--3 Axes for rotations are listed first.-->
    <TransformAxis name="rotation1">
        <!--Names of the coordinates that serve as the independent variables        of the transform function.-->
        <coordinates>knee_extend_pat_r</coordinates>
        <!--Rotation or translation axis for the transform.-->
        <axis>0 0 1</axis>
        <!--Transform function of the generalized coordinates used to        represent the amount of transformation along a specified axis.-->
        <function>
            <PiecewiseLinearFunction>
                <x> -2.0944 -1.71743 -1.24969 -1.0472 -0.703922 -0.306391 -0.130644 0.00607367 0.127345 0.194133</x>
                <y> -1.85005 -1.26974 -0.846041 -0.733028 -0.476555 -0.207427 -0.0884463 -0.0590306 -0.0538727 -0.0566183</y>
            </PiecewiseLinearFunction>
        </function>
    </TransformAxis>
    <!--3 Axes for translations are listed next.-->
    <TransformAxis name="translation1">
        <!--Names of the coordinates that serve as the independent variables        of the transform function.-->
        <coordinates>knee_extend_pat_r</coordinates>
        <!--Rotation or translation axis for the transform.-->
        <axis>1 0 0</axis>
        <!--Transform function of the generalized coordinates used to        represent the amount of transformation along a specified axis.-->
        <function>
            <MultiplierFunction>
                <function>
                    <PiecewiseLinearFunction>
                        <x> -2.16868 -1.72496 -1.38149 -1.24969 -1.02358 -0.673697 -0.32898 -0.130644 0.0527228 0.334306 0.669892 1.26213 2.11637</x>
                        <y> -0.0722757 -0.0625827 -0.0468162 -0.0397108 -0.0318689 -0.016538 -0.00511909 0.000553575 0.00465652 0.00713944 0.0081561 0.00912147 0.00966838</y>
```

```
                </PiecewiseLinearFunction>
            </function>
            <scale>1</scale>
        </MultiplierFunction>
    </function>
</TransformAxis>
<TransformAxis name="translation2">
    <!--Names of the coordinates that serve as the independent variables        of the transform function.-->
    <coordinates>knee_extend_pat_r</coordinates>
    <!--Rotation or translation axis for the transform.-->
    <axis>0 1 0</axis>
    <!--Transform function of the generalized coordinates used to        represent the amount of transformation along a specified axis.-->
    <function>
        <MultiplierFunction>
            <function>
                <PiecewiseLinearFunction>
                    <x> -2.1612 -1.76797 -1.38153 -1.07282 -0.760551 -0.365625 -0.190483 -0.0139851 0.137468 0.528251 1.08032 1.41988 1.68543 1.98925 2.25075</x>
                    <y> -0.0277513 -0.0455888 -0.0518783 -0.0524016 -0.0479748 -0.0361534 -0.0249335 -0.0222212 -0.011389 -0.0107772 -0.0113565 -0.0111467 -0.0112391 -0.0111153 -0.011117</y>
                </PiecewiseLinearFunction>
            </function>
            <scale>1</scale>
        </MultiplierFunction>
    </function>
</TransformAxis>
</SpatialTransform>
</CustomJoint>
```

Appendices A2: OpenSim model scripts for the 4DoF and clamped 6DoF knee joint

Script for the 4DoF knee joint with 2 prescribed DoFs.

Tz refers to medio/lateral translation. The three rotation DoFs and medio/lateral translation are free to move depending on marker trajectories. Anterior/posterior and distal/proximal translations (translation 1 and 2 respectively) are defined as functions based on the flexion/extension angle. Ranges of motion are not clamped, meaning that they are not constrained to strenuous limitations.

```
<CustomJoint name="knee_r">
<!--Name of the parent body to which this joint connects its owner body.-->
<parent_body>femur_r</parent_body>
<!--Location of the joint in the parent body specified in the parent reference frame. Default is (0,0,0).-->
<location_in_parent>0 0 0</location_in_parent>
<!--Orientation of the joint in the parent body specified in the parent reference frame. Euler XYZ body-fixed
rotation angles are used to express the orientation. Default is (0,0,0).-->
<orientation_in_parent>0 0 0</orientation_in_parent>
<!--Location of the joint in the child body specified in the child reference frame. For SIMM models, this vector is
always the zero vector (i.e., the body reference frame coincides with the joint). -->
<location>0 0 0</location>
<!--Orientation of the joint in the owing body specified in the owning body reference frame.  Euler XYZ body-
fixed rotation angles are used to express the orientation. -->
<orientation>0 0 0</orientation>
<!--Set holding the generalized coordinates (q's) that parmeterize this joint.-->
<CoordinateSet>
  <objects>
    <Coordinate name="knee_extend_r">
      <!--Coordinate can describe rotational, translational, or coupled motion. Defaults to rotational.-->
      <motion_type>rotational</motion_type>
      <!--The value of this coordinate before any value has been set. Rotational coordinate value is in radians
      and Translational in meters.-->
      <default_value>0</default_value>
      <!--The speed value of this coordinate before any value has been set. Rotational coordinate value is in
      rad/s and Translational in m/s.-->
      <default_speed_value>0</default_speed_value>
      <!--The minimum and maximum values that the coordinate can range between. Rotational coordinate
      range in radians and Translational in meters.-->
      <range>-2.0943951 0.17453293</range>
      <!--Flag indicating whether or not the values of the coordinates should be limited to the range, above.--
      >
      <clamped>false</clamped>
      <!--Flag indicating whether or not the values of the coordinates should be constrained to the current
      (e.g. default) value, above.-->
      <locked>false</locked>
      <!--If specified, the coordinate can be prescribed by a function of time. It can be any OpenSim Function
      with valid second order derivatives.-->
```

```
        <prescribed_function />
        <!--Flag indicating whether or not the values of the coordinates should be prescribed according to the
        function above. It is ignored if the no prescribed function is specified.-->
        <prescribed>false</prescribed>
    </Coordinate>
    <Coordinate name="knee_rotation_r">
        <!--Coordinate can describe rotational, translational, or coupled motion. Defaults to rotational.-->
        <motion_type>rotational</motion_type>
        <!--The value of this coordinate before any value has been set. Rotational coordinate value is in radians
        and Translational in meters.-->
        <default_value>0</default_value>
        <!--The speed value of this coordinate before any value has been set. Rotational coordinate value is in
        rad/s and Translational in m/s.-->
        <default_speed_value>0</default_speed_value>
        <!--The minimum and maximum values that the coordinate can range between. Rotational coordinate
        range in radians and Translational in meters.-->
        <range>-0.78539815 0.52359877</range>
        <!--Flag indicating whether or not the values of the coordinates should be limited to the range, above.--
        >
        <clamped>false</clamped>
        <!--Flag indicating whether or not the values of the coordinates should be constrained to the current
        (e.g. default) value, above.-->
        <locked>false</locked>
        <!--If specified, the coordinate can be prescribed by a function of time. It can be any OpenSim Function
        with valid second order derivatives.-->
        <prescribed_function />
        <!--Flag indicating whether or not the values of the coordinates should be prescribed according to the
        function above. It is ignored if the no prescribed function is specified.-->
        <prescribed>false</prescribed>
    </Coordinate>
    <Coordinate name="knee_adduction_r">
        <!--Coordinate can describe rotational, translational, or coupled motion. Defaults to rotational.-->
        <motion_type>rotational</motion_type>
        <!--The value of this coordinate before any value has been set. Rotational coordinate value is in radians
        and Translational in meters.-->
        <default_value>0</default_value>
        <!--The speed value of this coordinate before any value has been set. Rotational coordinate value is in
        rad/s and Translational in m/s.-->
        <default_speed_value>0</default_speed_value>
        <!--The minimum and maximum values that the coordinate can range between. Rotational coordinate
        range in radians and Translational in meters.-->
        <range>-0.2617993 0.2617993</range>
        <!--Flag indicating whether or not the values of the coordinates should be limited to the range, above.--
        >
        <clamped>false</clamped>
        <!--Flag indicating whether or not the values of the coordinates should be constrained to the current
        (e.g. default) value, above.-->
```

```xml
            <locked>false</locked>
            <!--If specified, the coordinate can be prescribed by a function of time. It can be any OpenSim Function
            with valid second order derivatives.-->
            <prescribed_function />
            <!--Flag indicating whether or not the values of the coordinates should be prescribed according to the
            function above. It is ignored if the no prescribed function is specified.-->
            <prescribed>false</prescribed>
        </Coordinate>
        <Coordinate name="knee_tz_r">
            <!--Coordinate can describe rotational, translational, or coupled motion. Defaults to rotational.-->
            <motion_type>translational</motion_type>
            <!--The value of this coordinate before any value has been set. Rotational coordinate value is in radians
            and Translational in meters.-->
            <default_value>0</default_value>
            <!--The speed value of this coordinate before any value has been set. Rotational coordinate value is in
            rad/s and Translational in m/s.-->
            <default_speed_value>0</default_speed_value>
            <!--The minimum and maximum values that the coordinate can range between. Rotational coordinate
            range in radians and Translational in meters.-->
            <range>-0.02 0.02</range>
            <!--Flag indicating whether or not the values of the coordinates should be limited to the range, above.--
            >
            <clamped>false</clamped>
            <!--Flag indicating whether or not the values of the coordinates should be constrained to the current
            (e.g. default) value, above.-->
            <locked>false</locked>
            <!--If specified, the coordinate can be prescribed by a function of time. It can be any OpenSim Function
            with valid second order derivatives.-->
            <prescribed_function />
            <!--Flag indicating whether or not the values of the coordinates should be prescribed according to the
            function above. It is ignored if the no prescribed function is specified.-->
            <prescribed>false</prescribed>
        </Coordinate>
    </objects>
    <groups />
</CoordinateSet>
<!--Whether the joint transform defines parent->child or child->parent.-->
<reverse>false</reverse>
<!--Defines how the child body moves with respect to the parent as a function of the generalized coordinates.-->
<SpatialTransform>
    <!--3 Axes for rotations are listed first.-->
    <TransformAxis name="rotation1">
        <!--Names of the coordinates that serve as the independent variables        of the transform function.-->
        <coordinates>knee_extend_r</coordinates>
        <!--Rotation or translation axis for the transform.-->
        <axis>0 0 1</axis>
```

```
        <!--Transform function of the generalized coordinates used to       represent the amount of transformation
        along a specified axis.-->
        <function>
            <LinearFunction>
                <coefficients> 1 0</coefficients>
            </LinearFunction>
        </function>
    </TransformAxis>
    <TransformAxis name="rotation2">
        <!--Names of the coordinates that serve as the independent variables       of the transform function.-->
        <coordinates>knee_rotation_r</coordinates>
        <!--Rotation or translation axis for the transform.-->
        <axis>0 1 0</axis>
        <!--Transform function of the generalized coordinates used to       represent the amount of transformation
        along a specified axis.-->
        <function>
            <LinearFunction>
                <coefficients> 1 0</coefficients>
            </LinearFunction>
        </function>
    </TransformAxis>
    <TransformAxis name="rotation3">
        <!--Names of the coordinates that serve as the independent variables       of the transform function.-->
        <coordinates>knee_adduction_r</coordinates>
        <!--Rotation or translation axis for the transform.-->
        <axis>1 0 0</axis>
        <!--Transform function of the generalized coordinates used to       represent the amount of transformation
        along a specified axis.-->
        <function>
            <LinearFunction>
                <coefficients> 1 0</coefficients>
            </LinearFunction>
        </function>
    </TransformAxis>
    <!--3 Axes for translations are listed next.-->
    <TransformAxis name="translation1">
        <!--Names of the coordinates that serve as the independent variables       of the transform function.-->
        <coordinates>knee_extend_r</coordinates>
        <!--Rotation or translation axis for the transform.-->
        <axis>1 0 0</axis>
        <!--Transform function of the generalized coordinates used to       represent the amount of transformation
        along a specified axis.-->
        <function>
            <SimmSpline>
```

```xml
            <x> -2.0944 -1.74533 -1.39626 -1.0472 -0.698132 -0.349066 -0.174533 0.197344 0.337395 0.490178
            1.52146 2.0944</x>
            <y> -0.0032 0.00179 0.00411 0.0041 0.00212 -0.001 -0.0031 -0.005227 -0.005435 -0.005574 -
            0.005435 -0.00525</y>
          </SimmSpline>
        </function>
      </TransformAxis>
      <TransformAxis name="translation2">
        <!--Names of the coordinates that serve as the independent variables        of the transform function.-->
        <coordinates>knee_extend_r</coordinates>
        <!--Rotation or translation axis for the transform.-->
        <axis>0 1 0</axis>
        <!--Transform function of the generalized coordinates used to        represent the amount of transformation
        along a specified axis.-->
        <function>
          <SimmSpline>
            <x> -2.0944 -1.22173 -0.523599 -0.349066 -0.174533 0.159149 2.0944</x>
            <y> -0.4226 -0.4082 -0.399 -0.3976 -0.3966 -0.395264 -0.396</y>
          </SimmSpline>
        </function>
      </TransformAxis>
      <TransformAxis name="translation3">
        <!--Names of the coordinates that serve as the independent variables        of the transform function.-->
        <coordinates>knee_tz_r</coordinates>
        <!--Rotation or translation axis for the transform.-->
        <axis>0 0 1</axis>
        <!--Transform function of the generalized coordinates used to        represent the amount of transformation
        along a specified axis.-->
        <function>
          <LinearFunction>
            <coefficients> 1 0</coefficients>
          </LinearFunction>
        </function>
      </TransformAxis>
      </SpatialTransform>
      </CustomJoint>
    </Joint
```

Script for the 5DoF knee joint with clamped ranges of motion

Tz refers to medio/lateral translation and Tx refer to anterior/posterior translation. Distal/proximal translation remains prescribed in terms of the flexion/extension angle. The flexion/extension DoF is free to follow marker trajectories while the other 2 rotations, Tx and Tz DoFs are clamped to specific ranges of motion limits. These ranges of motion are updated within the model script during inverse kinematics calculations to reflect bone pin derived constraints.

```
<CustomJoint name="knee_r">
  <!--Name of the parent body to which this joint connects its owner body.-->
  <parent_body>femur_r</parent_body>
  <!--Location of the joint in the parent body specified in the parent reference frame. Default is (0,0,0).-->
  <location_in_parent>0 0 0</location_in_parent>
  <!--Orientation of the joint in the parent body specified in the parent reference frame. Euler XYZ body-fixed
  rotation angles are used to express the orientation. Default is (0,0,0).-->
  <orientation_in_parent>0 0 0</orientation_in_parent>
  <!--Location of the joint in the child body specified in the child reference frame. For SIMM models, this vector
  is always the zero vector (i.e., the body reference frame coincides with the joint). -->
  <location>0 0 0</location>
  <!--Orientation of the joint in the owing body specified in the owning body reference frame.  Euler XYZ body-
  fixed rotation angles are used to express the orientation. -->
  <orientation>0 0 0</orientation>
  <!--Set holding the generalized coordinates (q's) that parmeterize this joint.-->
  <CoordinateSet>
    <objects>
      <Coordinate name="knee_extend_r">
        <!--Coordinate can describe rotational, translational, or coupled motion. Defaults to rotational.-->
        <motion_type>rotational</motion_type>
        <!--The value of this coordinate before any value has been set. Rotational coordinate value is in
        radians and Translational in meters.-->
        <default_value>0</default_value>
        <!--The speed value of this coordinate before any value has been set. Rotational coordinate value is
        in rad/s and Translational in m/s.-->
        <default_speed_value>0</default_speed_value>
        <!--The minimum and maximum values that the coordinate can range between. Rotational
        coordinate range in radians and Translational in meters.-->
        <range>-2.0944 0.17453</range>
        <!--Flag indicating whether or not the values of the coordinates should be limited to the range,
        above.-->
        <clamped>false</clamped>
        <!--Flag indicating whether or not the values of the coordinates should be constrained to the current
        (e.g. default) value, above.-->
        <locked>false</locked>
        <!--If specified, the coordinate can be prescribed by a function of time. It can be any OpenSim
        Function with valid second order derivatives.-->
        <prescribed_function />
        <!--Flag indicating whether or not the values of the coordinates should be prescribed according to
        the function above. It is ignored if the no prescribed function is specified.-->
```

```xml
        <prescribed>false</prescribed>
    </Coordinate>
    <Coordinate name="knee_rotation_r">
        <!--Coordinate can describe rotational, translational, or coupled motion. Defaults to rotational.-->
        <motion_type>rotational</motion_type>
        <!--The value of this coordinate before any value has been set. Rotational coordinate value is in radians and Translational in meters.-->
        <default_value>0</default_value>
        <!--The speed value of this coordinate before any value has been set. Rotational coordinate value is in rad/s and Translational in m/s.-->
        <default_speed_value>0</default_speed_value>
        <!--The minimum and maximum values that the coordinate can range between. Rotational coordinate range in radians and Translational in meters.-->
        <range>-0.7854 0.5236</range>
        <!--Flag indicating whether or not the values of the coordinates should be limited to the range, above.-->
        <clamped>true</clamped>
        <!--Flag indicating whether or not the values of the coordinates should be constrained to the current (e.g. default) value, above.-->
        <locked>false</locked>
        <!--If specified, the coordinate can be prescribed by a function of time. It can be any OpenSim Function with valid second order derivatives.-->
        <prescribed_function />
        <!--Flag indicating whether or not the values of the coordinates should be prescribed according to the function above. It is ignored if the no prescribed function is specified.-->
        <prescribed>false</prescribed>
    </Coordinate>
    <Coordinate name="knee_adduction_r">
        <!--Coordinate can describe rotational, translational, or coupled motion. Defaults to rotational.-->
        <motion_type>rotational</motion_type>
        <!--The value of this coordinate before any value has been set. Rotational coordinate value is in radians and Translational in meters.-->
        <default_value>0</default_value>
        <!--The speed value of this coordinate before any value has been set. Rotational coordinate value is in rad/s and Translational in m/s.-->
        <default_speed_value>0</default_speed_value>
        <!--The minimum and maximum values that the coordinate can range between. Rotational coordinate range in radians and Translational in meters.-->
        <range>-0.2618 0.2618</range>
        <!--Flag indicating whether or not the values of the coordinates should be limited to the range, above.-->
        <clamped>true</clamped>
        <!--Flag indicating whether or not the values of the coordinates should be constrained to the current (e.g. default) value, above.-->
        <locked>false</locked>
        <!--If specified, the coordinate can be prescribed by a function of time. It can be any OpenSim Function with valid second order derivatives.-->
```

```xml
        <prescribed_function />
        <!--Flag indicating whether or not the values of the coordinates should be prescribed according to
        the function above. It is ignored if the no prescribed function is specified.-->
        <prescribed>false</prescribed>
    </Coordinate>
    <Coordinate name="knee_tx_r">
        <!--Coordinate can describe rotational, translational, or coupled motion. Defaults to rotational.-->
        <motion_type>translational</motion_type>
        <!--The value of this coordinate before any value has been set. Rotational coordinate value is in
        radians and Translational in meters.-->
        <default_value>0</default_value>
        <!--The speed value of this coordinate before any value has been set. Rotational coordinate value is
        in rad/s and Translational in m/s.-->
        <default_speed_value>0</default_speed_value>
        <!--The minimum and maximum values that the coordinate can range between. Rotational
        coordinate range in radians and Translational in meters.-->
        <range>-0.1 0.1</range>
        <!--Flag indicating whether or not the values of the coordinates should be limited to the range,
        above.-->
        <clamped>true</clamped>
        <!--Flag indicating whether or not the values of the coordinates should be constrained to the current
        (e.g. default) value, above.-->
        <locked>false</locked>
        <!--If specified, the coordinate can be prescribed by a function of time. It can be any OpenSim
        Function with valid second order derivatives.-->
        <prescribed_function />
        <!--Flag indicating whether or not the values of the coordinates should be prescribed according to
        the function above. It is ignored if the no prescribed function is specified.-->
        <prescribed>false</prescribed>
    </Coordinate>
    <Coordinate name="knee_tz_r">
        <!--Coordinate can describe rotational, translational, or coupled motion. Defaults to rotational.-->
        <motion_type>translational</motion_type>
        <!--The value of this coordinate before any value has been set. Rotational coordinate value is in
        radians and Translational in meters.-->
        <default_value>0</default_value>
        <!--The speed value of this coordinate before any value has been set. Rotational coordinate value is in
        rad/s and Translational in m/s.-->
        <default_speed_value>0</default_speed_value>
        <!--The minimum and maximum values that the coordinate can range between. Rotational coordinate
        range in radians and Translational in meters.-->
        <range>-0.1 0.1</range>
        <!--Flag indicating whether or not the values of the coordinates should be limited to the range, above.-
        ->
        <clamped>true</clamped>
        <!--Flag indicating whether or not the values of the coordinates should be constrained to the current
        (e.g. default) value, above.-->
        <locked>false</locked>
```

```
          <!--If specified, the coordinate can be prescribed by a function of time. It can be any OpenSim
          Function with valid second order derivatives.-->
          <prescribed_function />
          <!--Flag indicating whether or not the values of the coordinates should be prescribed according to the
          function above. It is ignored if the no prescribed function is specified.-->
          <prescribed>false</prescribed>
        </Coordinate>
      </objects>
      <groups />
    </CoordinateSet>
    <!--Whether the joint transform defines parent->child or child->parent.-->
    <reverse>false</reverse>
    <!--Defines how the child body moves with respect to the parent as a function of the generalized
    coordinates.-->
    <SpatialTransform>
      <!--3 Axes for rotations are listed first.-->
      <TransformAxis name="rotation1">
        <!--Names of the coordinates that serve as the independent variables     of the transform function.-->
        <coordinates>knee_extend_r</coordinates>
        <!--Rotation or translation axis for the transform.-->
        <axis>0 0 1</axis>
        <!--Transform function of the generalized coordinates used to     represent the amount of
        transformation along a specified axis.-->
        <function>
          <LinearFunction>
            <coefficients> 1 0</coefficients>
          </LinearFunction>
        </function>
      </TransformAxis>
      <TransformAxis name="rotation2">
        <!--Names of the coordinates that serve as the independent variables     of the transform function.-->
        <coordinates>knee_rotation_r</coordinates>
        <!--Rotation or translation axis for the transform.-->
        <axis>0 1 0</axis>
        <!--Transform function of the generalized coordinates used to     represent the amount of
        transformation along a specified axis.-->
        <function>
          <LinearFunction>
            <coefficients> 1 0</coefficients>
          </LinearFunction>
        </function>
      </TransformAxis>
      <TransformAxis name="rotation3">
        <!--Names of the coordinates that serve as the independent variables     of the transform function.-->
        <coordinates>knee_adduction_r</coordinates>
```

```
        <!--Rotation or translation axis for the transform.-->
        <axis>1 0 0</axis>
        <!--Transform function of the generalized coordinates used to       represent the amount of
        transformation along a specified axis.-->
        <function>
            <LinearFunction>
                <coefficients> 1 0</coefficients>
            </LinearFunction>
        </function>
    </TransformAxis>
    <!--3 Axes for translations are listed next.-->
    <TransformAxis name="translation1">
        <!--Names of the coordinates that serve as the independent variables       of the transform function.-->
        <coordinates>knee_tx_r</coordinates>
        <!--Rotation or translation axis for the transform.-->
        <axis>1 0 0</axis>
        <!--Transform function of the generalized coordinates used to       represent the amount of
        transformation along a specified axis.-->
        <function>
            <LinearFunction>
                <coefficients> 1 0</coefficients>
            </LinearFunction>
        </function>
    </TransformAxis>
    <TransformAxis name="translation2">
        <!--Names of the coordinates that serve as the independent variables       of the transform function.-->
        <coordinates>knee_extend_r</coordinates>
        <!--Rotation or translation axis for the transform.-->
        <axis>0 1 0</axis>
        <!--Transform function of the generalized coordinates used to       represent the amount of
        transformation along a specified axis.-->
        <function>
            <SimmSpline>
                <x> -2.0944 -1.2217 -0.5236 -0.34907 -0.17453 0.15915 2.0944</x>
                <y> -0.4226 -0.4082 -0.399 -0.3976 -0.3966 -0.39526 -0.396</y>
            </SimmSpline>
        </function>
    </TransformAxis>
    <TransformAxis name="translation3">
        <!--Names of the coordinates that serve as the independent variables       of the transform function.-->
        <coordinates>knee_tz_r</coordinates>
        <!--Rotation or translation axis for the transform.-->
        <axis>0 0 1</axis>
        <!--Transform function of the generalized coordinates used to       represent the amount of
```

```
            transformation along a specified axis.-->
            <function>
                <LinearFunction>
                    <coefficients> 1 0</coefficients>
                </LinearFunction>
            </function>
        </TransformAxis>
    </SpatialTransform>
</CustomJoint>
```

Appendices A3: Inverse Kinematics Methodology in OpenSim

The following information is copied from
http://simtk-confluence.stanford.edu:8080/display/OpenSim/How+Inverse+Kinematics+Works,
Last visited on December 2015

How Inverse Kinematics Works

The IK tool goes through each time step (frame) of motion and computes generalized coordinate values which positions the model in a pose that "best matches" experimental marker and coordinate values for that time step. Mathematically, the "best match" is expressed as a weighted least squares problem, whose solution aims to minimize both marker and coordinate errors. The topics covered in this section include:

Marker Errors
Coordinate Errors
Weighted Least Squares Equation
Important Note about Units

Marker Errors

A ***marker error*** is the distance between an experimental marker and the corresponding marker on the model when it is positioned using the generalized coordinates computed by the IK solver. Each marker has a weight associated with it, specifying how strongly that marker's error term should be minimized.

Coordinate Errors

A ***coordinate error*** is the difference between an experimental coordinate value and the coordinate value computed by IK.
What are "experimental coordinate values?" These can be joint angles obtained directly from a motion capture system (i.e., built-in mocap inverse kinematics capabilities), or may be computed from experimental data by various specialized algorithms (e.g., defining anatomical coordinate frames and using them to specify joint frames that, in turn, describe joint angles) or by other measurement techniques that involve other measurement devices (e.g., a goniometer). A fixed desired value for a coordinate can also be specified (e.g., if you know a specific joint's angle should stay at 0˚). The inclusion of experimental coordinate values is optional; the IK tool can solve for the motion trajectories using marker matching alone.
A distinction should be made between ***prescribed*** and ***unprescribed coordinates***. A prescribed coordinate (also referred to as a ***locked coordinate***) is a generalized coordinate whose trajectory is known and which will not be computed using IK. It will get set to its exact trajectory value instead. This can be useful when you have enough confidence in some generalized coordinate value that you don't want the IK solver to change it.
An ***unprescribed coordinate*** is a coordinate which is not prescribed, and whose value is computed using IK.
Using these definitions, only ***unprescribed coordinates*** can vary and so only they appear in

the least squares equation solved by IK. Each unprescribed coordinate being compared to an experimental coordinate must have a weight associated with it, specifying how strongly that coordinate's error should be minimized.

Weighted Least Squares Equation

The weighted least squares problem solved by IK is

$$\min_{\mathbf{q}}\left[\sum_{i\in \text{markers}} w_i \left\|\mathbf{x}_i^{\text{exp}} - \mathbf{x}_i(\mathbf{q})\right\|^2 + \sum_{j\in \text{unprescribed coords}} \omega_j \left(q_j^{\text{exp}} - q_j\right)^2\right]$$

$$q_j = q_j^{\text{exp}} \text{ for all prescribed coordinates } j$$

where $\mathbf{q}$ is the vector of generalized coordinates being solved for, $\mathbf{x}_i^{\text{exp}}$ is the experimental position of marker i, $\mathbf{x}_i(\mathbf{q})$ is the position of the corresponding marker on the model (which depends on the coordinate values), q_j^{exp} is the experimental value for coordinate j. Prescribed coordinates are set to their experimental values. For instance, in the gait2354 and gait2392 examples, the subtalar and metatarsophalangeal (mtp) joints are locked and during IK they are assigned the prescribed value of 0˚.

The marker weights (w_i's) and coordinate weights (ω_j's) are specified in the <IKMarkerTask> and <IKCoordinateTask> tags, respectively. These are all specified within a single <IKTaskSet> tag, as will be outlined in How to Use the IK Tool. This least squares problem is solved using a general quadratic programming solver, with a convergence criterion of 0.0001 and a limit of 1000 iterations. These are currently fixed values that cannot be changed in the XML files.

Appendices A4: Sagittal Plane Torque Error with Each Cost Function

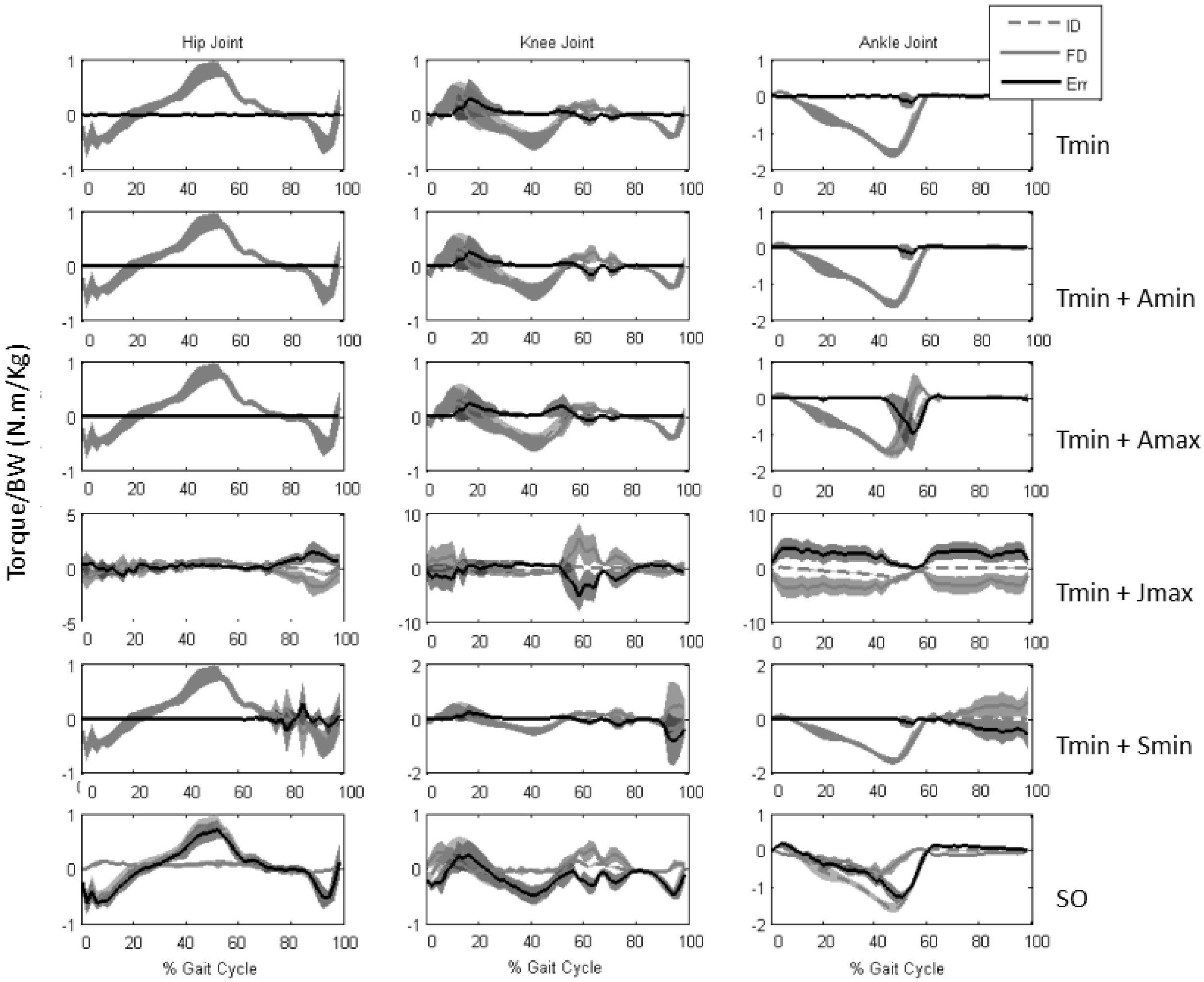

Figure A4.1: Cross-subject average +/- standard deviation cloud of sagittal plane torque normalized to bodyweight (Kg) from inverse (ID – dashed grey line) and forward (FD – solid grey line) dynamics and the error (solid black line) between them for each objective function at the hip, knee and ankle joints. Objective functions are Tmin: Minimization of torque error only. Tmin+Amin: Addition of minimization of total muscle activation. Tmin+Amax: Addition of maximizing total muscle activation. Tmin+Jmax: Addition of maximizing axial knee compression. Tmin+Smin: Addition of minimizing shear forces at the knee. SO: OpenSim static optimization results obtained from inverse dynamics only.

Appendices A5: Conference Poster Presentation

A poster showing the research on the effect of changing the objective function in the hybrid simulation framework was presented at the International Society of Biomechanics (ISB) conference in Glasgow in July 2015. The following is its published abstract.

PO-0216

uOttawa

Comparison of Knee Joint Muscle Activation Predictions of Hybrid Forward-Inverse Dynamics Simulations with Static Optimization and Experimental EMG

Brigitte M. Potvin (M.A.Sc Candidate)[2], Mohammad S. Shourijeh (Ph.D.)[1,3],
Kenneth B. Smale (Ph.D. Candidate)[2], Daniel L. Benoit (Ph.D.)[1,2,3]
Contact: dbenoit@uottawa.ca

INTRODUCTION

Musculoskeletal modeling and computer simulations are becoming increasingly popular to improve our understanding of the musculoskeletal system and in implementing evidence based medical decisions in clinical settings [1,2]. However, the exact way in which muscles contribute to movement and joint stability is not yet fully understood and as a result, these models and simulation frameworks do not yet provide results able to be reliably applied in clinical settings [2-4].

The knee joint is a high load bearing joint and is stabilized in large part by active and passive soft tissues (muscles and ligaments respectively) [5]. It is important to determine healthy muscle activation patterns and how they contribute to smooth and stable joint motion and loading in order to identify pathological ones and the serious consequences they may create.

A hybrid forward-inverse dynamics simulation framework was recently developed that combines the advantages of both inverse and forward dynamics based modeling frameworks, offering the possibility of modifying muscle parameters while remaining computationally economical[6]. In addition, this framework does not require extensive customization, medical imaging or parameter tuning between each subject and trial as is the case of others making it much more accessible to researchers without extensive modeling backgrounds.

Furthermore, as there are many muscles to consider and too few equations of motion resulting from the inverse or forward dynamics processes, optimization methods are required to solve for individual muscle activations, forces and joint loading [7]. The choice of objective function to be reached by the optimization protocol has been shown to be important in obtaining physiologically realistic results [8].

The purpose of this study was to evaluate this new hybrid framework and to study the effect of adding a physiologically based objective function within it, by comparing the muscle activation results to those of OpenSim's integrated static optimization (SO) protocol (*http://opensim.stanford.edu*) and to experimental electromyography data (EMG).

METHOD

Data Collection

Motion capture, ground reaction force and electromyography data were collected for gait trials of five healthy young adult males (mean age, body weight and height were 24±1.9yrs, 80.8±9.1kg and 177.3±8.1cm respectively). Marker trajectories were collected at 200Hz and force plate data at 1000Hz, then filtered with a 4th order dual pass Butterworth filter with 10Hz cutoff. EMG data of the gluteus maximus (GLTMAX), gluteus medius (GLTMED), tensor fascia latae (TFL), rectus femoris (RFEM), vastus medials (VMED), vastus lateralis (VLAT), biceps femoris (BFEM), semitendinosus (STEN), tibialis anterior (TA), medial gastrocnemius (MGAS), lateral gastrocnemius (LGAS) and soleus (SOL) were collected at 1000Hz and filtered with a 4th order dual pass Butterworth filter with a cutoff of 8Hz and normalized to maximum voluntary isometric contraction levels.

Musculoskeletal Model Definition

We implemented a modified version of the musculoskeletal model created by Xu et al. [8], available in the OpenSim model repository *simtk.org*, which has 29 DoFs, 56 muscles and 8 ligaments. The knee has 4DoFs (3 rotations and medio-lateral translation) with 2 prescribed DoFs. The patella is also included to better visualize and control the moment arm created by the patellar tendon and quadriceps muscles. Ligaments were removed from the model; the muscle model was updated to the Millard (2012) Equilibrium Model and the patella's definition was changed to follow the distal femur rather than the tibia's position and orientation. The model is illustrated in Fig 1.

Fig 1: Modified Xu et al. musculoskeletal model

Hybrid Forward-Inverse Dynamics Simulation Framework

The hybrid method initially calculates knee joint torques by first scaling a generic sized model to subject specific marker placement using the MatLab-OpenSim API (MatLab 2014a, The Mathworks, USA and OpenSim 3.2 , simtk.org, Simbios, National NIH Center for Biomedical Computing, USA), followed by inverse kinematics and dynamics calculations (shown in the right hand side of Fig 2). The static optimization (SO) protocol built into OpenSim 3.2 that minimizes overall muscle activations was run to obtain initial muscle activation approximations.

Following this, forward dynamics with prescribed motion using the inverse kinematics data are run to estimate muscle excitations (u), activations (a) and forces (f) that yield knee joint torques as close to those described by the inverse dynamics method (left hand side of Fig 2).

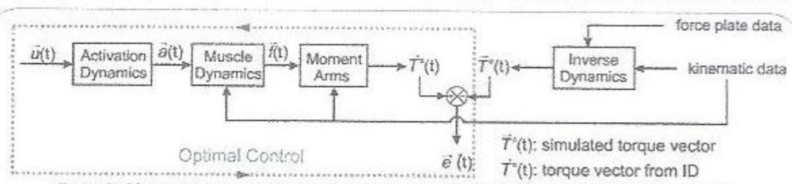

Fig 2: Hybrid forward-inverse dynamics simulation framework minimizing joint torque prediction differences e(t). Other variables are as follows: u(t)=muscle excitation, a(t)=muscle activation, f(t)=muscle forces

Simulation Optimization Objective Functions

To minimize the difference in joint torque predictions, an optimization protocol was run to find the ideal muscle activation combination. The hybrid framework's basic objective function (J) minimizes the normalized torque error (TE) divided by absolute values of torque determined from inverse dynamics (ID_Torques), and rejects combinations of values where muscle activations (a) are outside the range of [0,1], by assigning a large penalty to them. The simulation attempts to obtain the solution with the smallest value of the objective function J_{Tmin}.

$$J_{Tmin} = \min\{\Sigma(|TE| \,/\, |ID\_Torques|) + 1e6 * (a<0) + 1e6 * (a>1)\}$$

A physiological objective function was added to the basic cost function to minimize the sum of muscle activations to see what impact if had on final muscle activation outputs.

$$J_{phys} = \min \Sigma\, (a_{min})^2$$

Each subjects' results from these simulations were graphically compared with their respective SO muscle activation results and experimental EMG data.

RESULTS

The average results of the hybrid and SO activation predictions for each muscle with EMG data are shown in Fig 3. It can be seen that the hybrid simulations with the objective function of minimization of muscle activation (*Tmin+Amin*) predicted the TA, MGAS and SOL muscle activations in a manner consistent with experimental EMG. The torque error minimization (*Tmin*) testing condition also resulted in muscle activation patterns similar to the EMG of the MGAS and SOL muscles.

Static optimization (SO) muscle activation results calculated within OpenSim showed weak muscle activation levels overall for all subjects compared to hybrid results. Curve shapes for these predictions, however, follow those of experimental EMG for the MGAS and SOL muscles in all participants.

A slight shift between EMG and muscle activation peaks can be most notably observed in the MGAS and SOL muscles, which is consistent with the electromechanical delay between muscle excitation and actual force production as well as from electrode placement effects [10,11]. Among the participants, this shift was on the order of approximately 50ms.

Individually, some subjects showed similar patterns between EMG and hybrid outputs for the RFEM muscle but this was not consistent. Looking at Fig 3, it could be construed that hybrid muscle activation predictions, on average, increase following EMG peaks and thus follows principles of electromechanical delay.

Average BFEM prediction patterns also suggests this trend where activations drop following a decrease in EMG magnitude. This it is not clear, however, when looking at only one gait cycle given the relatively large standard deviations. Note also that for both RFEM and BFEM muscle EMG showed relatively low activation levels experimentally which was not the case using *Tmin* or *Tmin+Amin*. This could be a function of EMG normalisation or an overestimation with the simulation.

The TFL showed similarities to experimental EMG for only one subject with both *Tmin* and *Tmin+Amin* conditions, whereas GLTMAX and GLTMED hybrid results did not show particular relationships with experimental EMG for any subjects.

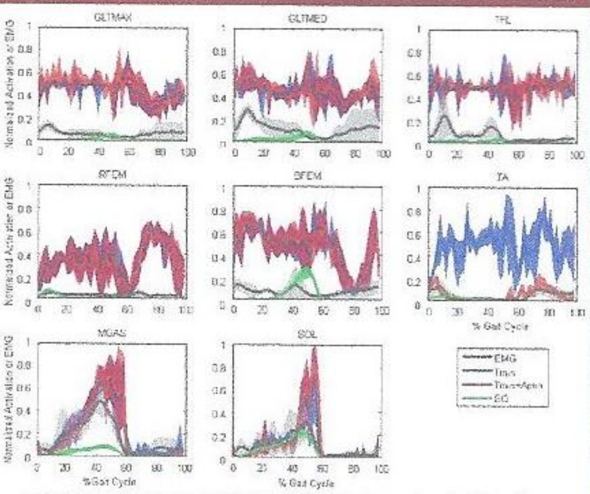

Fig 3: Hybrid simulation muscle activation results as an average of each subject with standard deviation cloud with cost functions of torque error minimization (*Tmin*) and torque error minimization + minimization of muscle activations (*Tmin+Amin*) compared to experimental EMG data and to static optimization results (SO) from OpenSim 3.2. Gait cycle is normalized from right heel strike to right heel strike. Only muscles obtained for both EMG and from the model are presented here.

DISCUSSION AND CONCLUSIONS

Results obtained using the hybrid forward-inverse dynamics simulation framework show improved similarities with experimental EMG data for some muscles compared to SO. In particular, SO had a tendency to 'turn off' muscles for extended periods, despite physiological fluctuations of EMG-based muscle activations. The addition of a physiologically based objective function improved the muscle activation pattern and magnitude prediction for the TA muscle in particular. This is because the *Tmin* condition only finds a mathematically appropriate result without considering any physiological criteria. Therefore, many muscle activation combinations could have resulted from the *Tmin* simulation optimization.

As expected, muscle activation levels in the *Tmin* hybrid condition are greater or equal to those from the *Tmin+Amin* condition. This suggests that the addition of a physiological cost function as an optimization criterion is important when running musculoskeletal simulations to find physiologically appropriate muscle activation profiles. In this case of gait at a self-selected pace, minimization of total muscle activation seems to provide adequate results in muscle activation predictions, notably for the TA, MGAS and SOL muscles. To improve predictions on more muscles, it may be beneficial to run simulations with more physiologically appropriate goals to the optimization protocol depending on the studied motion.

Various sources of inaccuracies and errors may further explain the poor relation between hybrid results and experimental EMG for the GLTMAX, GLTMED and TFL muscles. These include musculoskeletal model limitations in the accuracy of muscle properties and geometrical definitions, joint degrees of freedom (DoF) definitions as well as the quantity of muscles used to actuate each joint in all directions. Experimental limitations of EMG are also a factor, in particular with respect to normalisation and electrode placement during dynamic tasks. Furthermore, simulations were run to minimize error in torque calculations using only the flexion/extension DoFs, thus neglecting rotation and ab/adduction. The upper body and non-dominant leg during the optimization processes were also omitted. Although a more complex musculoskeletal model may improve simulation outputs, we believe a more physiologically representative knee joint would also improve simulations without the additional computational costs, making it more practical for clinical use.

ACKNOWLEDGMENTS

This research was supported by the Ontario Graduate Scholarship (OGS) and by the National Science and Engineering Research Council (NSERC) CGS-M scholarship and Discovery Program.

CONFLICT OF INTEREST

The authors declare that here were no conflicts of interest of financial or personal natures that may have compromised this research project or the writing of this poster

REFERENCES

[1] Mansouri et al., J. Biomech.,2012
[2] Fregly et al., J. Orthop. Res., 2011.
[3] Vanheule et al., XXIV ISB Congress, 2013
[4] Manal et al., J. Biomech. Eng., 2013
[5] McLean et al., Transac. ASME, 2003
[6] Sjourijeh & Benoit, ISB2015 AS-0295
[7] Buchanan et al., J. Biomech. Eng., 1996
[8] Sanford et al., Op. J. Biophys, 2013
[9] H. Xu et al., *Comput. Meth. Biomech. Biomed. Engin.*, 2014.
[10] De Luca, J. App. Biomech, 1997
[11] Hug et al., J. Orthop. Sports Phys. Ther. 2015

Neuromuscular Rehabilitation Research Unit

1.School of Rehabilitation Sciences– University of Ottawa, Canada,
2.School of Human Kinetics– University of Ottawa, Canada
3.School of Engineering – University of Ottawa, Canada

25th congress of the International Society of Biomechanics
July 12th-16th 2015
Glasgow, UK